

AD-A102 262

MASSACHUSETTS UNIV AMHERST ASTRONOMY RESEARCH FACILITY
SCRIBE I DATA ANALYSIS, (U)

F/6 7/4

APR 81 H SAKAI

F19628-79-C-0062

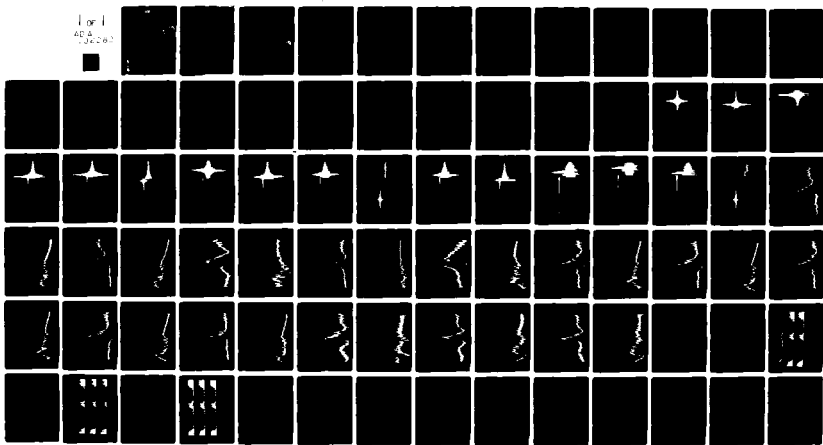
UNCLASSIFIED

UMASS-ARF-81-315

AFGL-TR-81-0129

NL

1 of 1
4D-A
132262



END
DATE FILMED
9-81
DTIC

ADA102262

AFGL-TR-81-0129

LEVEL II

(12) 72

SCRIBE I DATA ANALYSIS

Hajime Sakai

Astronomy Research Facility
University of Massachusetts
Amherst MA 01003



Approved for public release; distribution unlimited.

April 1981

Scientific Report No. 1

AIR FORCE GEOPHYSICS LABORATORY
AIR FORCE SYSTEMS COMMAND
UNITED STATES AIR FORCE
HANSCOM AFB, MASSACHUSETTS 01731

81 7 31 108

**Qualified requestors may obtain additional copies from the
Defense Technical Information Center. All others should
apply to the National Technical Information Service.**

UNCLASSIFIED

SECURITY CLASSIFICATION OF THIS PAGE (When Data Entered)

17 REPORT DOCUMENTATION PAGE		READ INSTRUCTIONS BEFORE COMPLETING FORM
1. REPORT NUMBER AFGL-TR-81-0129	2. GOVT ACCESSION NO. AD-A102262	3. RECIPIENT'S CATALOG NUMBER
4. TITLE (and Subtitle) SCRIBE I DATA ANALYSIS	5. TYPE OF REPORT & PERIOD COVERED Scientific Report No. 1	
7. AUTHOR(s) Hajime Sakai	6. PERFORMING ORG. REPORT NUMBER UMASS-ARF-81-315 SCIENTIFIC	
9. PERFORMING ORGANIZATION NAME AND ADDRESS Astronomy Research Facility University of Massachusetts Amherst MA 01003	8. CONTRACTOR OR GRANT NUMBER F19628-79-C-0062 NC	
11. CONTROLLING OFFICE NAME AND ADDRESS Air Force Geophysics Laboratory Hanscom AFB, Massachusetts 01731 Monitor/George Vanasse/OPI	10. PROGRAM ELEMENT, PROJECT, TASK AREA & WORK UNIT NUMBERS 61102F 23101AL 17A-1	
14. MONITORING AGENCY NAME & ADDRESS (if different from Controlling Office)	12. REPORT DATE April 1981	
	13. NUMBER OF PAGES 81 12 83	
16. DISTRIBUTION STATEMENT (of this Report)	15. SECURITY CLASS. (of this report) Unclassified	
Approved for public release; distribution unlimited.	15a. DECLASSIFICATION/DOWNGRADING SCHEDULE	
17. DISTRIBUTION STATEMENT (of the abstract entered in Block 20, if different from Report)	DTIC ELECTED JUL 3 1981 C	
18. SUPPLEMENTARY NOTES		
19. KEY WORDS (Continue on reverse side if necessary and identify by block number)		
Atmospheric emission	H_2O	
Cryogenic interferometer	CO_2	
Fourier spectroscopy	O_3	
20. ABSTRACT (Continue on reverse side if necessary and identify by block number)		
The data collected by the SCRIBE October 1980 flight were analyzed. The obtained results are reported in this report, together with the hardware and the software developed.		

400-989

SCRIBE* I Data Analysis

Introduction

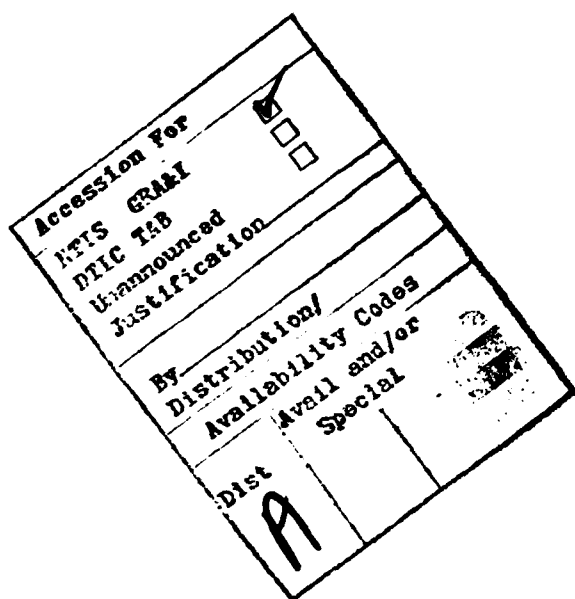
>A LiN₂ cooled cat's eye interferometer was flown on October 8, 1980, at Holloman AFB under the SCRIBE program. We at the University of Massachusetts took a responsibility for the post-flight data analysis which can be divided into three major functions: (1) extraction of the interferogram data from the PCM telemetry record; (2) recovery of the spectral data from the extracted interferograms; and (3) analysis of the spectral data in terms of the atmospheric molecular parameters. The experiment was successful only during the first 20 minutes of flight. The balloon-borne instrument failed to produce the interferogram data after the balloon reached an altitude of 6 km.

Our major effort up to the present can be summarized in the following four major categories: (1) to assemble the electronics interface to receive the output data of the PCM decommutator and to modify them in a proper format for the PDP11/20 computer; (2) to implement a scheme for recording the interferogram data extracted from the PCM record onto a digital magnetic recording tape; (3) to develop a scheme for processing the produced interferogram data recorded on a magnetic tape; and (4) to improve the analysis scheme on the recovered spectral data. Our efforts in all of these activities were successful in that we were able to obtain the atmospheric emission spectra from the telemetry record. Unfortunately, the flight data did not provide

*Stratospheric Cryogenic Interferometer Balloon Experiment. The technical detail of the program and of the October 8, 1980, flight is given in G. Vanasse, AFGL Report (1981).

a full test of our developed scheme. The quality of the flight data did not reach the expected level due to the interferometer scanning problem. In addition, mere 16 interferogram data extracted from the telemetry record were not sufficient to provide a solid basis for studying the infrared atmospheric emission as a function of the altitude.

The present scientific report summarizes our effort which was carried out for processing of the October 1980 data. Included in the report are a description of the interferogram electronics hardware constructed for our decommutation scheme, the PDP11 software employed in conjunction with our decommutation scheme, and the CDC software written for the spectral recovery from the interferogram data recorded on a PDP11/RT11 format magnetic tape.



Decommunication of the Telemetry Data

The data obtained during the flight were sent to the ground station through a telemetry radio link. The scheme used for the telemetry is shown in a block diagram of Fig. 1. The digitized interferogram data together with other signals were fed into the PCM encoder, which produced the PCM telemetry signal in a proper bit sequence. The telemetry signal transmitter in the balloon-borne package and the receiver in the ground station formed a radio link between the data obtained by the balloon-borne instruments and the ground station recording device. The SABRE IV magnetic tape recorder was used to record the telemetry signal on a 1/2" analog tape in a direct recording mode. The recording was done at 800 K BPS at 60 IPS.

The telemetry signal was formatted in a 72 bit per frame, which consisted of a 20-bit synchronization word, a 4-bit frame-identification word, a 16-bit interferogram data word, and four 8-bit words for other data. The synchronization-word bit pattern is given in Table I. The interferogram data were made of a 12-bit word representing the A/D converter output and a 4-bit control status word, as shown in Table I. The interferometer was scanned at an approximate rate of .3 cm OPD/sec. The interferogram data were sampled at twice the HeNe laser line wavelength of 6329 Å (in vacuum). The telemetry rate of 11, 1 K frame-per-second was considerably higher than the interferogram data sampling rate which was less than 2 K word-per-second. This scheme was designed to accommodate fluctuating interferogram sampling intervals by making the telemetry signal transmission deliberately faster than the interferogram sampling rate. It was devised in such a way that the data transmission was never caught up by the data sampling. Within the interferometer scanning

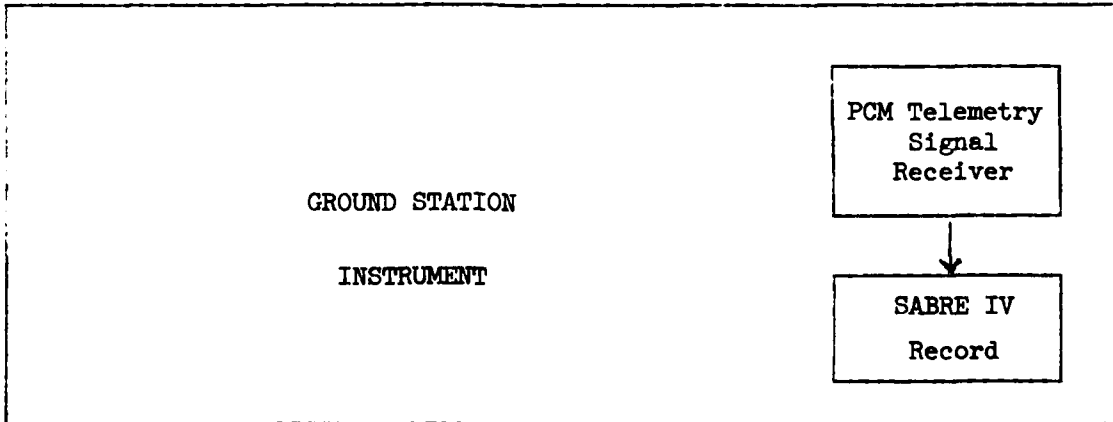
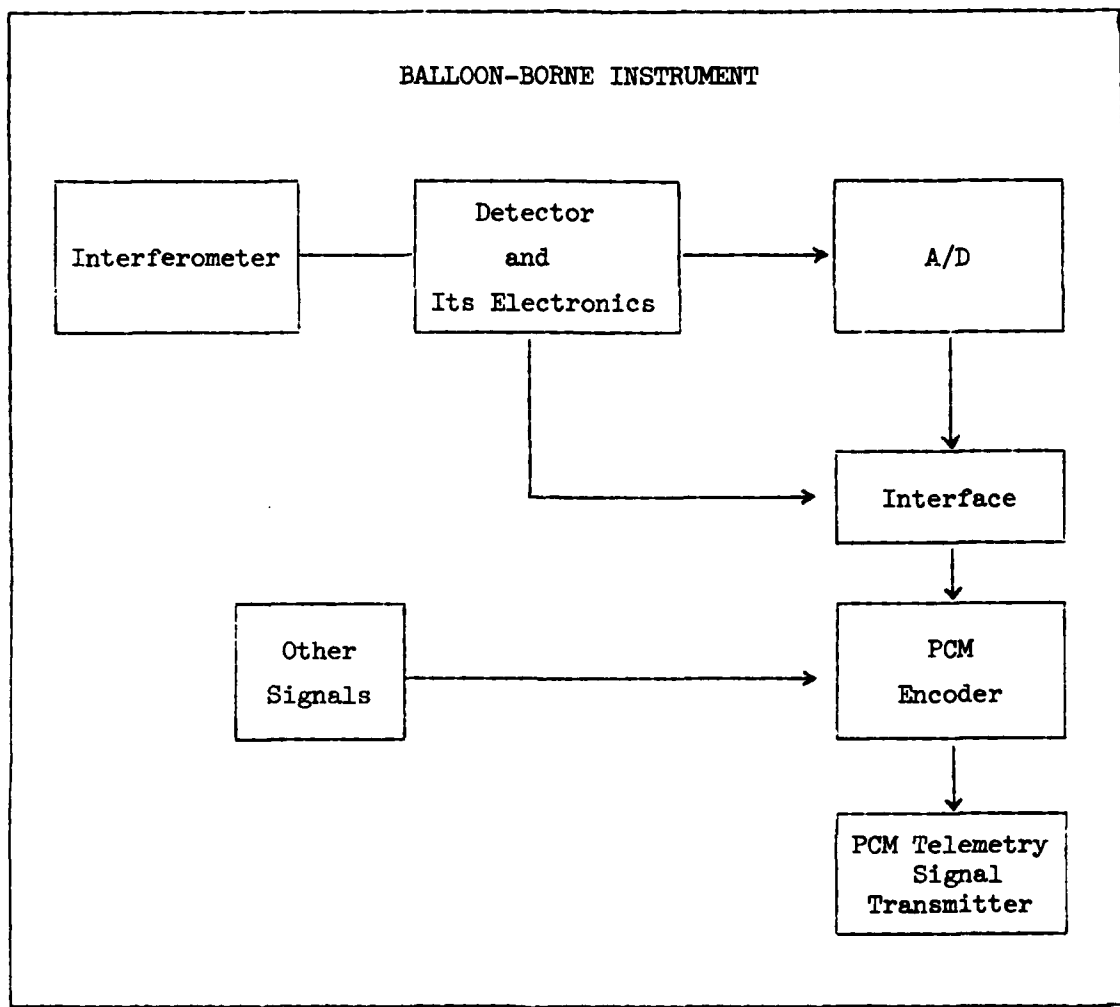
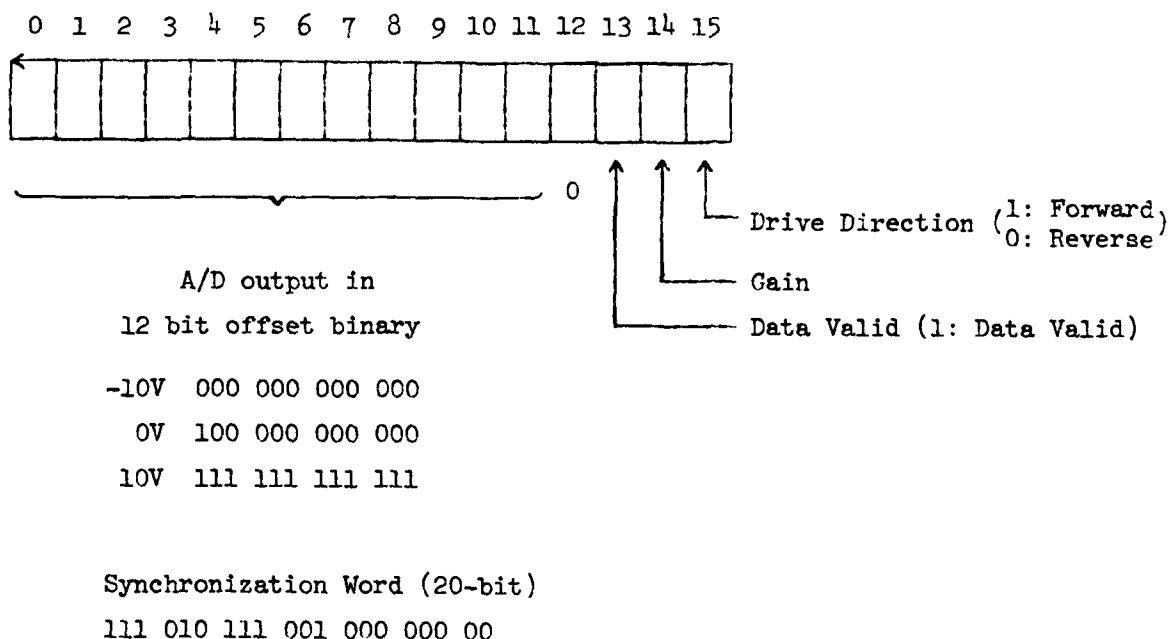


Figure 1

Table I
Interferogram Data Bit Format



tolerance, no interferogram data should be lost in the transmission. The on-board electronics produced a sequence of zero-word data after the sampled interferogram signal was transmitted until the next sampled interferogram signal became ready for the transmission. The data status was coded in a 4-bit word shown in Table I.

Fig. 2 shows an overall scheme for our data extraction electronics. The PCM decommutator manufactured originally by the Monitor System provides two functions: it finds a clock-rate of the telemetry signal which is play-backed by SABRE IV, and it generates a clock-pulse stream synchronized with the telemetry signal. The unit was modified by us to accept a bit rate of 800 K BPS. The produced output was a serial 72-bit string together with the synchronization clock pulse, if the unit succeeds to detect a bit pattern of the synchronization word. When a detection failure occurs, the clock pulse stops and the error flag is raised. The error status continues until the reset switch is manually intervened.

The interface electronics provides two major functions: (1) an extraction of a proper 16-bit word from a serial 72-bit string of the telemetry; and (2) a parallel 16-bit output to DR11B parallel I/O interface of PDP11/20. The unit accepts three signals provided by the PCM decommutator: (1) PCMIN signal of a serial 72-bit data word; (2) a clock signal synchronized with PCMIN, and (3) FTO signal indicating a completion of each PCMIN signal transmission. The logic used in our scheme is shown in a block diagram of Fig. 3. The WORD SELECT logic accepts either a command from a manual switch on the front panel, or an external control signal provided by the PDP11. The HAND SHAKE circuit provides an ordinary flag logic for indicating that the data are ready for transfer to the CPU. Figs. 4 through 8 show the component circuits

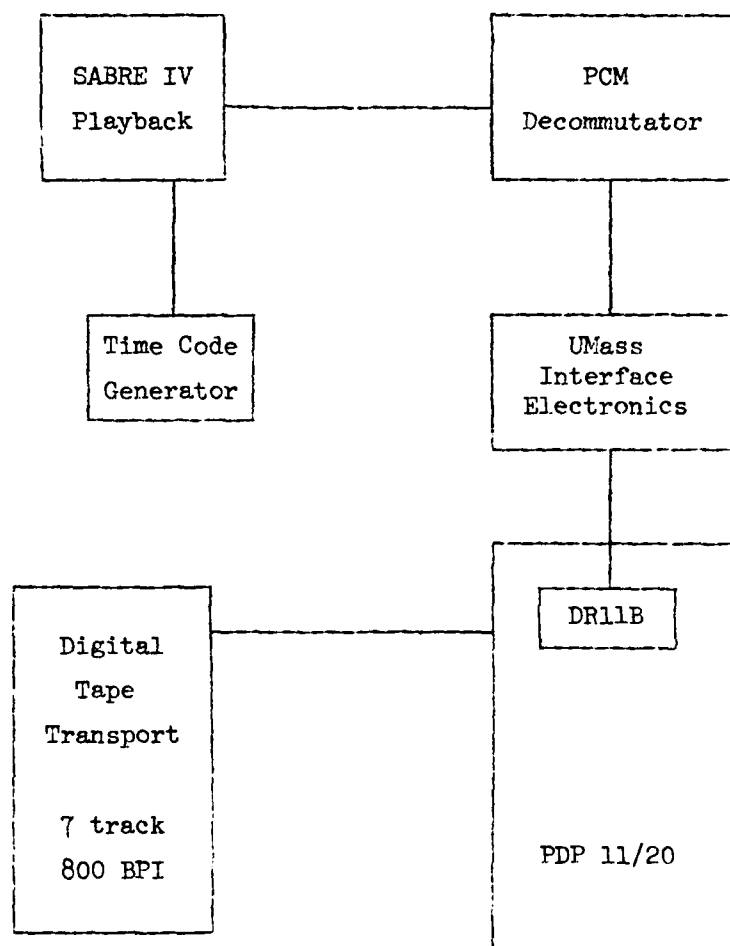
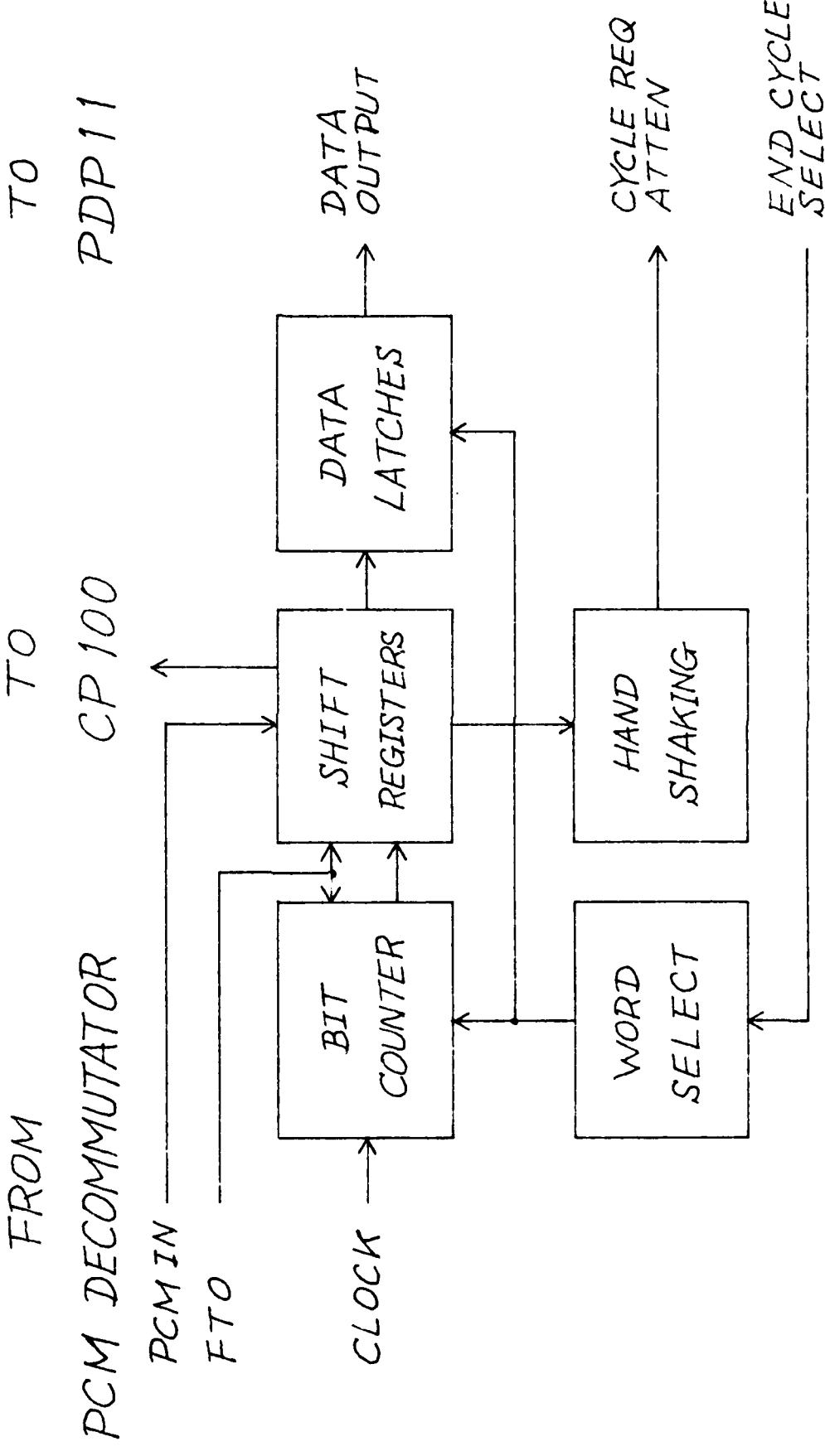


Figure 2

in detail.

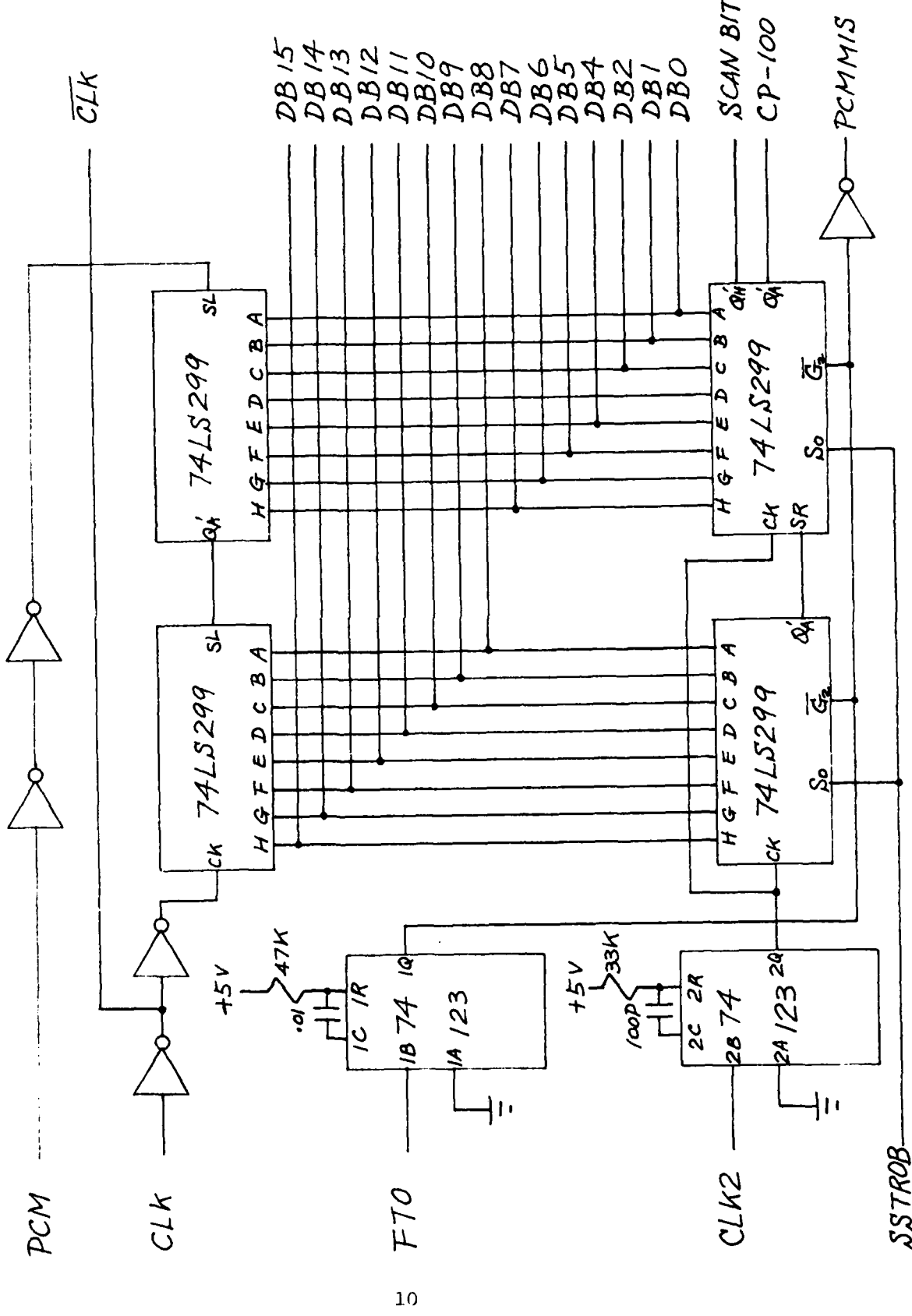
The PDP11/20 mainframe accepts the parallel 16-bit data via DR11B parallel I/O Interface. The first program disregards the bit pattern of the control status word, and transfers the entire 16-bit word to RK1 disk memory without discriminating the zero words interspersed in the interferogram signal. The second program examines the data stored on RK1 for their validation. Only the proper data are selected to transfer to DTO. The generated data files on DTO are recorded with the standard RT11 format. The data transfer from DTO to MT is done using the standard RT11 peripheral interchange software PIP. The final data recorded on MT are formatted on 800 BPI, 7 track, odd parity magnetic tape blocked by 256 16-bit words, which are composed by 4 6-bit bytes with a parity bit accompanying to each byte. The software programs loaded on PDP11/20 for these operations are listed in APPENDIX.

DATA ACQUISITION INTERFACE

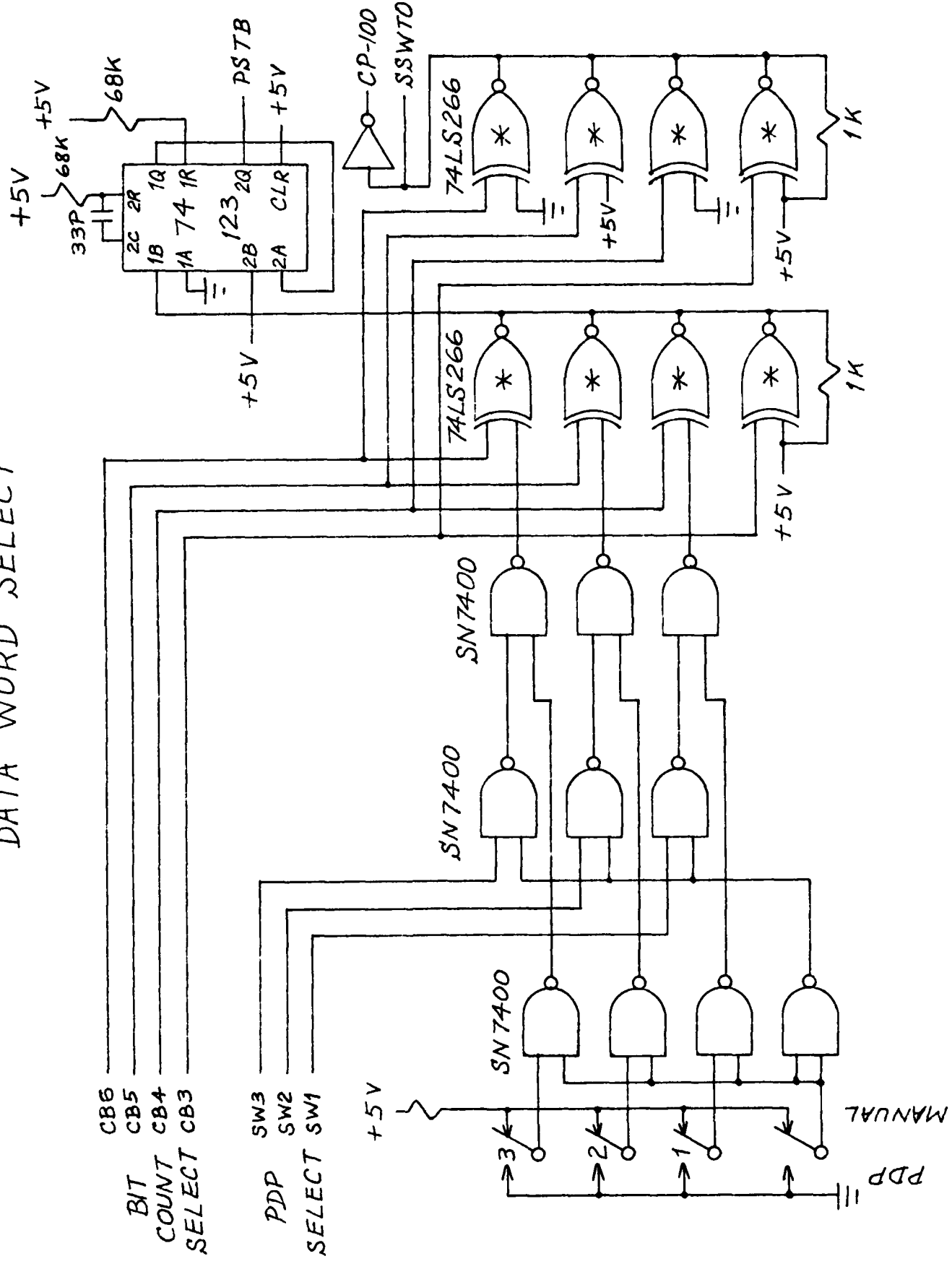


SHIFT/STORAGE REGISTERS

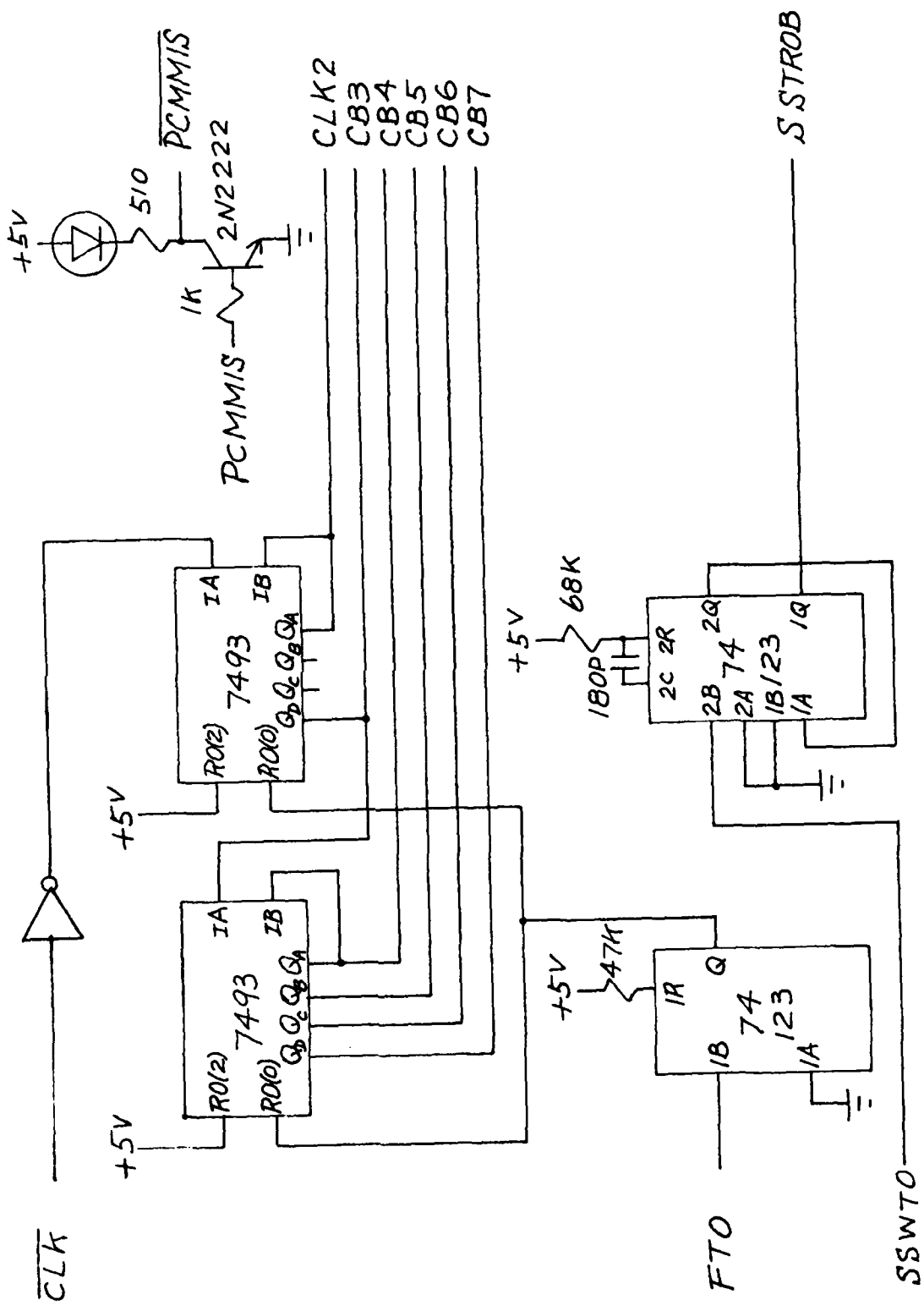
PCM



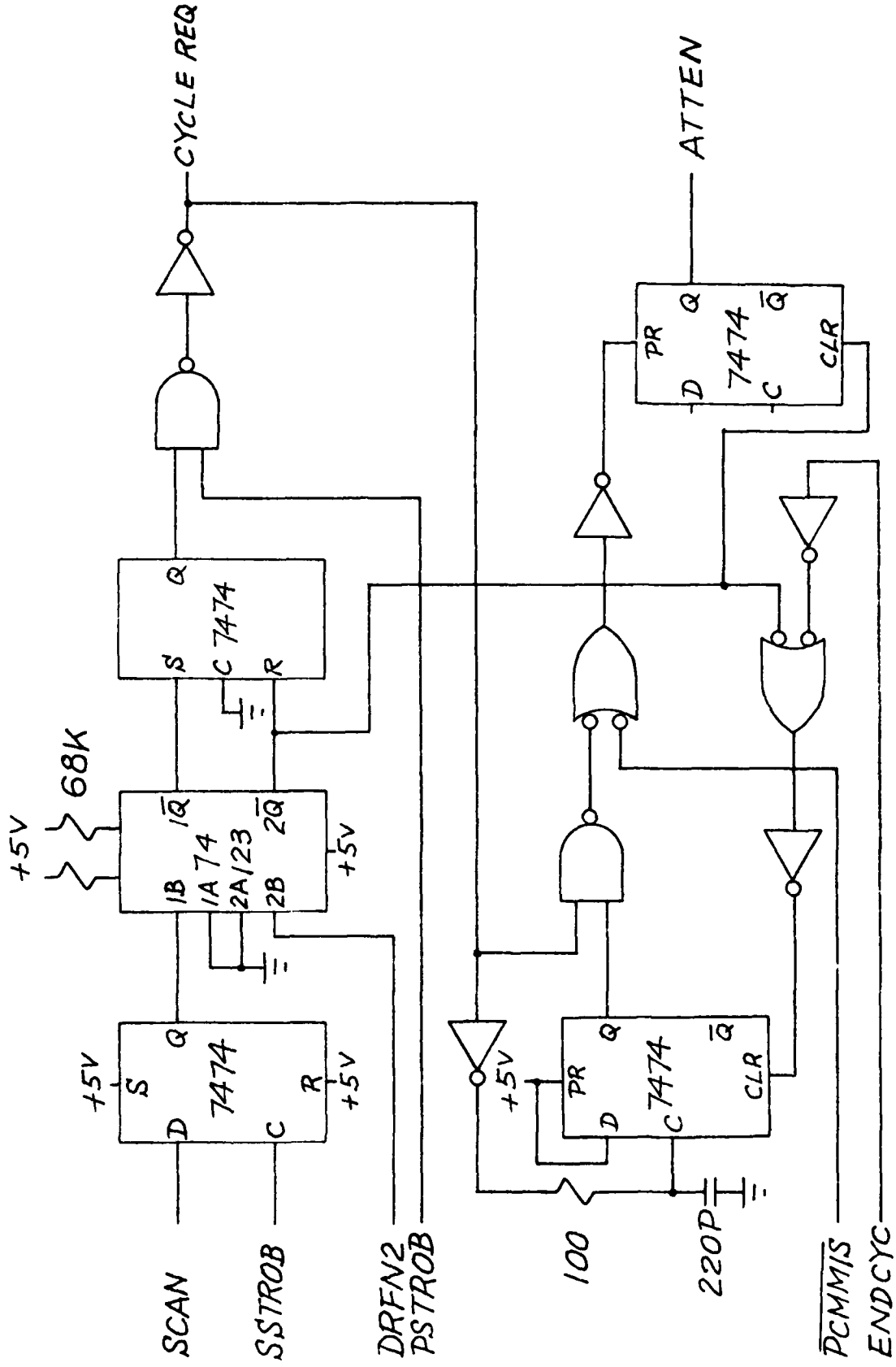
DATA WORD SELECT



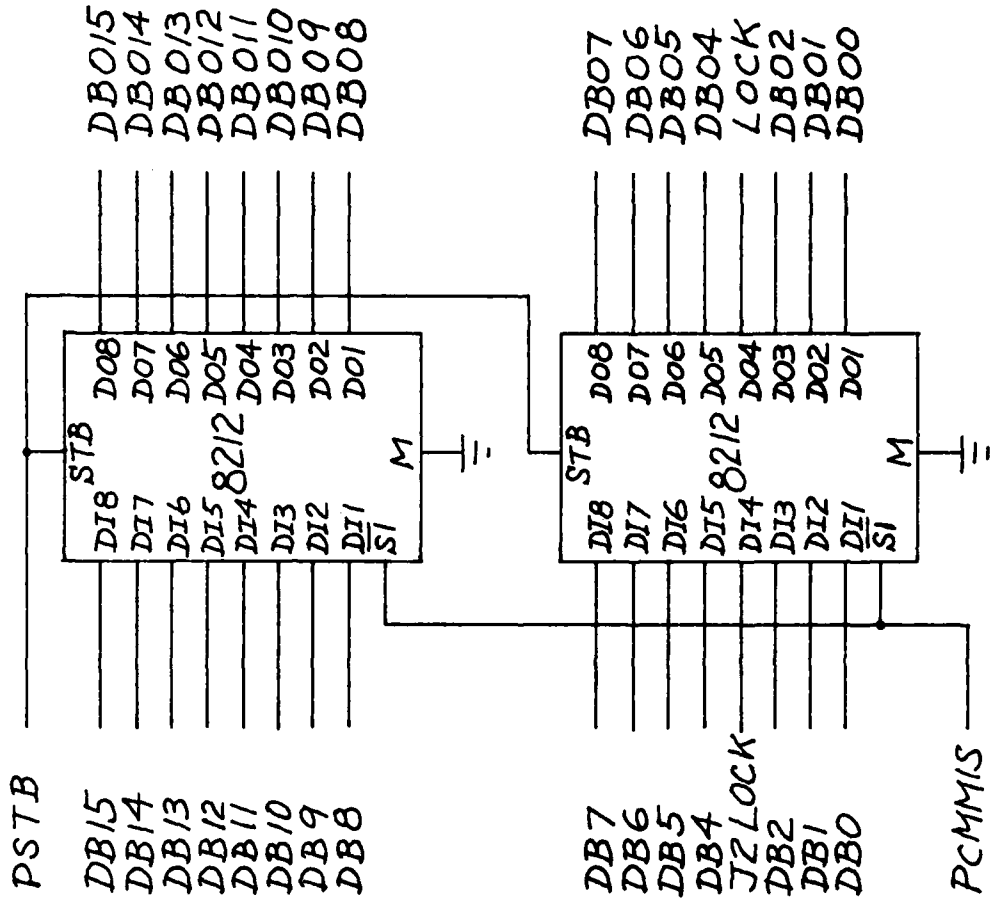
BIT COUNTERS



DR//B HAND SHAKING



BUFFERED DATA LATCHES



Spectral Recovery Process on CDC Cyber

The interferogram data on a 7-track, 800 BPI magnetic tape are recorded under control of the PDP/RT11 operating system. The general scheme for spectral recovery shown in a block diagram of Fig. 9 has consequently an extra step required for a conversion of the RT11 format word to the CDC internal format. The CDC's COPYBF command under the NOS operating system provides a satisfactory data transfer to the CDC disk memory for our data generated by the PDP/RT11 system. The conversion of the data to the CDC Cyber format is carried out by SXREAD listed in APPENDIX. The gain change in the interferogram data is adjusted by SKXREAD, also listed in APPENDIX. These two programs were developed by us for this operation. The rest of the numerical computation process is our standard routine used for general purpose spectral recovery in our Fourier spectroscopy effort. The Appendices provide a listing of the entire software package. The final outputs are generally produced with (16I5) format with the highest peak value of the recovered spectrum normalized to 1000.

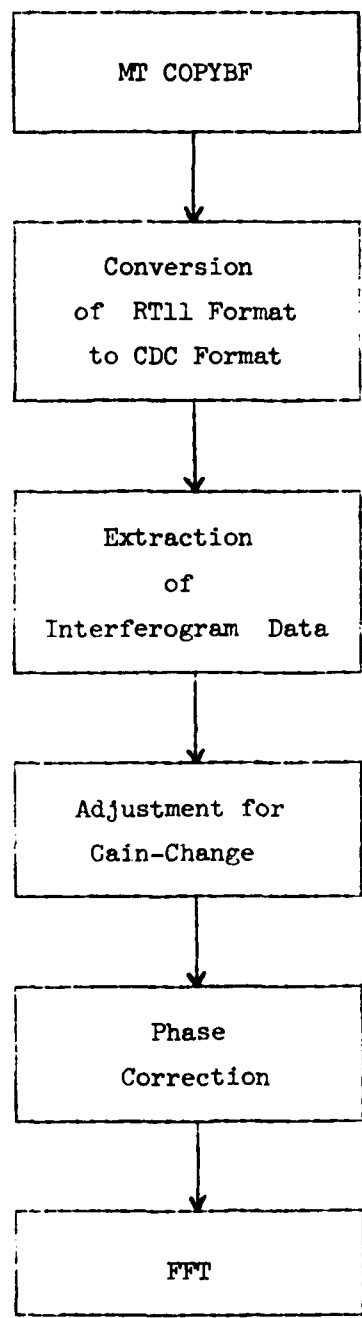


Figure 9

Interferogram Data

The interferogram data extracted from the telemetry record are summarized in Table II. The time-code generator failed to function at the time of our data extraction effort. The extracted interferogram data were identified by reading the SABRE IV footage counter. Included in the Table are the approximate balloon altitudes. We found two major trouble spots in the telemetry record, where the PCM decommutator failed to establish a lock-in, (1) between 1600 ft. and 2300 ft., and (2) between 4150 ft. and 4340 ft. The telemetry record beyond 4340 ft. produced the interferogram data not extending to the full optical path difference. The PCM decommutator was able to lock-in to the synchronization word for those data.

We observed that the interferogram data starting position varied considerably among these sixteen extracted from the telemetry record. The gain-change scheme was implemented under the basic design assumption that the interferometer would commence to take data without a narrow proximity centered at a pre-fixed position. The first several hundred data points would be measured with a low gain setting, since they would fall in a region of the central modulation. After these data points, the detector amplifier would be set at a high gain (a factor of 5.6 times the gain in the first region). The interferometer did not scan in accordance with this design during the flight. The gain-change scheme lost its function and a majority of the interferogram data were recorded with a single gain. In addition to the gain-switching scheme, the detector amplifier was designed to accommodate a gain-adjustment in accordance with the preceding interferogram modulation in the ZPD region. Because the gain-switching position did not provide a required

Table II

<u>Designation</u>	<u>SABRE IV Footage Reading</u>	<u>Balloon Altitude</u>
A	1100	2700 m
B	1200	2800
C	1340	2900
D	1480	3050
E	2300	3800
F	2400	3950
G	2560	4100
H	2700	4200
K	2840	4350
L	2980	4500
M	3110	4600
N	3400	4900
P	3510	5000
Q	3650	5150
R	3790	5250
S	3930	5400
T*	4340	5800
U*	4470	5900
V*	4600	6050
X*	4745	6150

*The PCM decommutator was able to lock-in, but the interferogram data were fragmentary.

synchronization with the interferogram ZPD position due to the trouble described above, a considerable gain fluctuation was resulted among the data. The central modulation of some data was found to be saturated.

A critical inspection of the data quality became necessary in our effort because of the difficulties in the interferometer scanning. We devised to observe the phase curve of the ZPD region for all the interferogram data extracted, and found it varying from one interferogram data to another in a substantial degree.

The S/N in the recovered spectra was found far below the figure expected. The interferogram data were not measured with a dynamic range originally planned because of the interferometer scanning problem. We believe that a correction of the interferogram scanning difficulty is essential for achieving overall improvement of the spectrometry.

The data were sampled at an interval of twice the HeNe laser line wavelength. We do not believe that the sampling scheme used for the October 1980 flight would add any advantages to the scheme which we planned originally. The resulted disadvantage was far greater than otherwise. We strongly recommend to adopt the originally planned sampling interval.

We found that the 4-bit status word for the interferogram data produced no consistency to what the data indicated. The gain-bit registered in the status word did not conform with the actual gain-setting of the detector amplifier. We judged the amplifier gain by inspecting the off-set bias voltage in the data, the scheme implemented by the University of Denver. A problem faced us with the U. Denver scheme was that we found it rather difficult to write a fail-safe software for accommodating the gain-adjustment. The software listed in APPENDIX

provided a service for a majority of the cases. We did not bother to rewrite it for broadening its coverage of the cases which fall outside of its applicability. We knew that its applicability was limited and that several cases could not be processed by using the scheme. The gain adjustment for those cases was implemented manually by inspecting the raw data. The procedure that we adopted for the present case cannot produce a sufficient efficiency for the case where the processing involves several hundred of the interferogram data. For future flights, we hope that the status word would furnish a true reflection of the interferogram data.

Figures 10 through 25 show the raw interferogram data extracted from the telemetry record. Figures 26 through 38 show the spectra recovered with a resolution of $.5 \text{ cm}^{-1}$. The data F, L and S had its central modulation recorded in the low gain setting. A dynamic range of their recording was extremely small, resulting in the recovered spectra of an exceptionally low S/N. They are not shown because of excessive noise content. The phase curves shown in Figure 39 are obtained with a spectral resolution of approximately 125 cm^{-1} . They are not stable principally because of the dynamic range saturation in the CM region. It was found that among these interferograms processed, the data N was free from these problems.



Fig. 10 Interferogram A

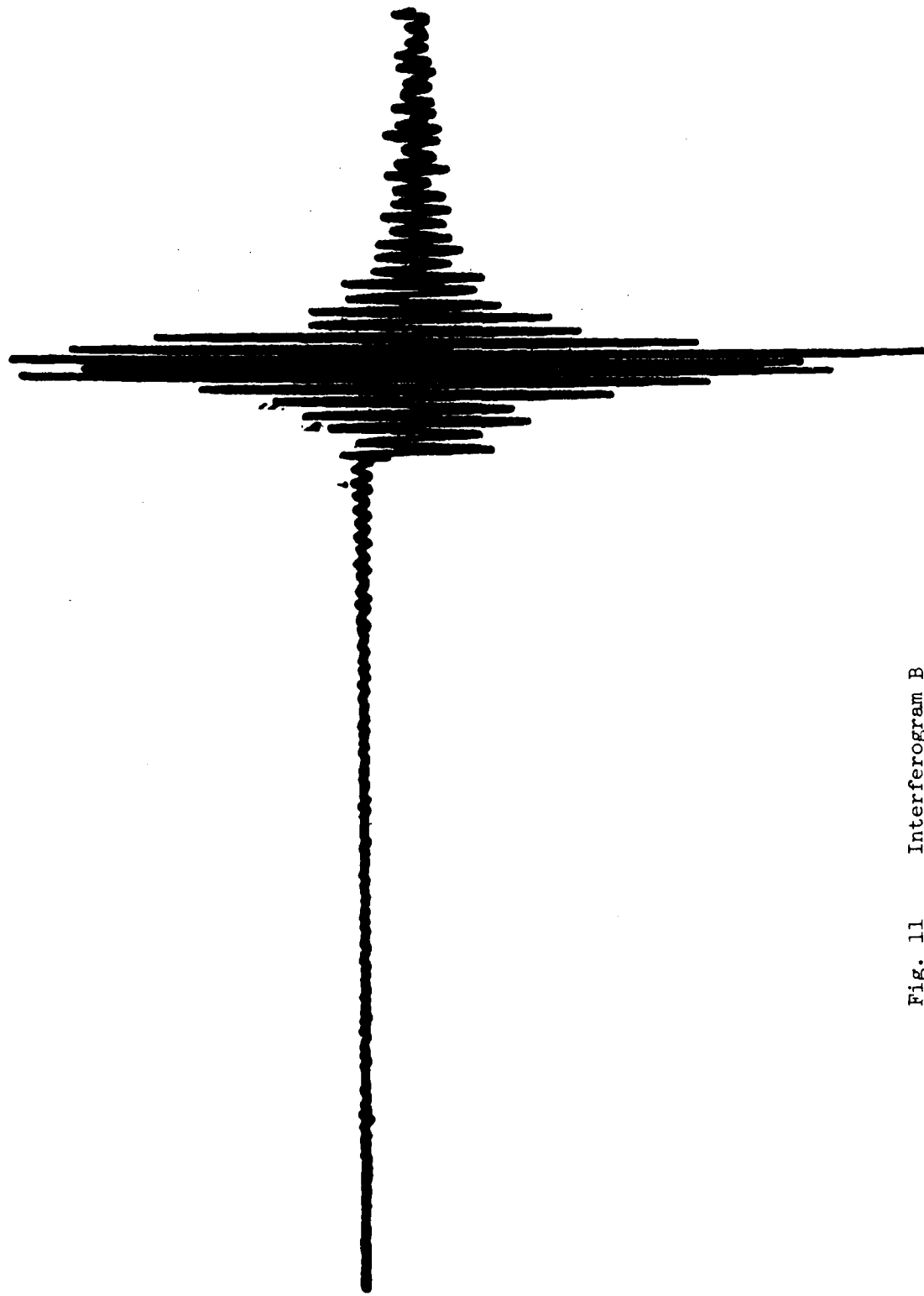


Fig. 11 Interferogram B

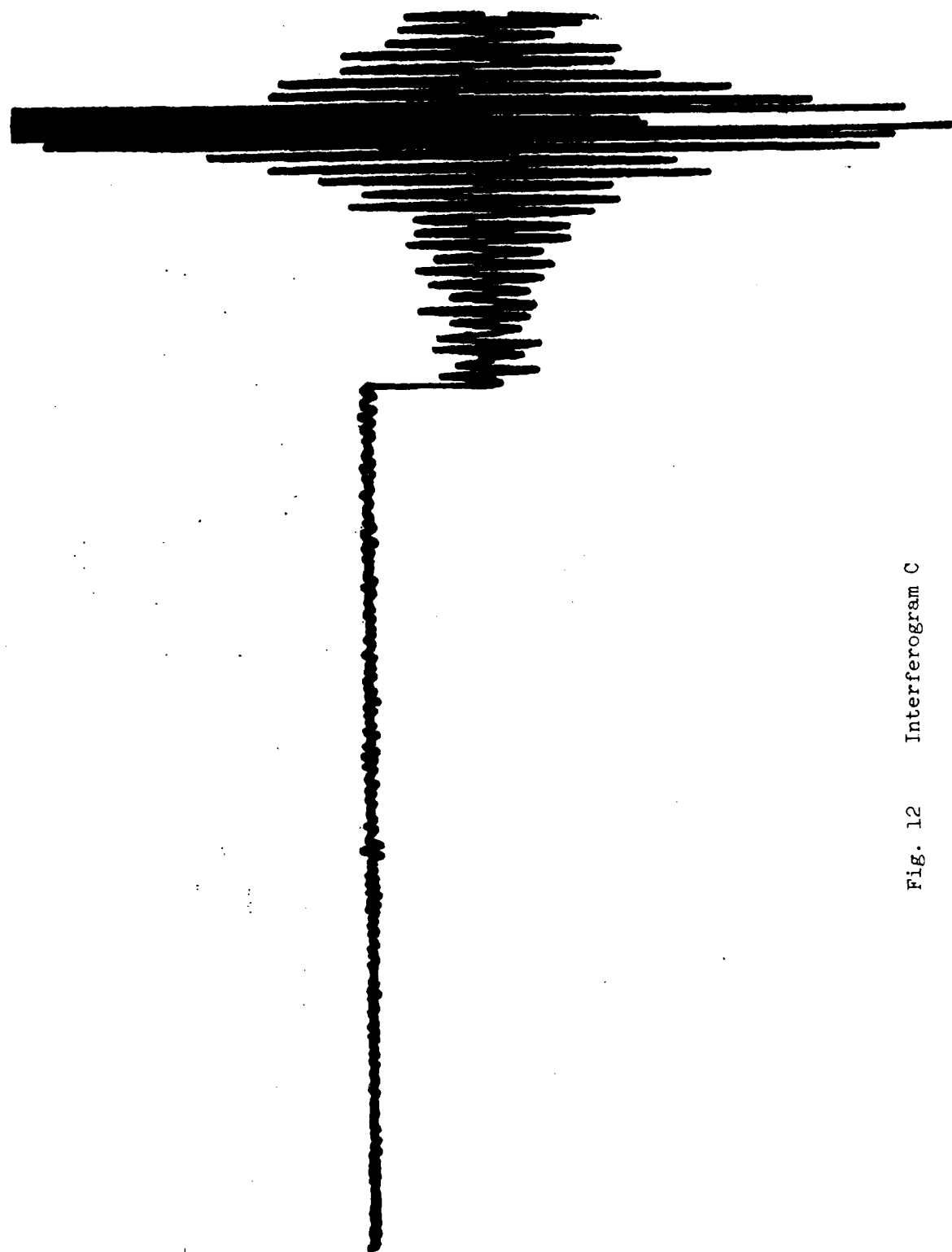


Fig. 12 Interferogram C

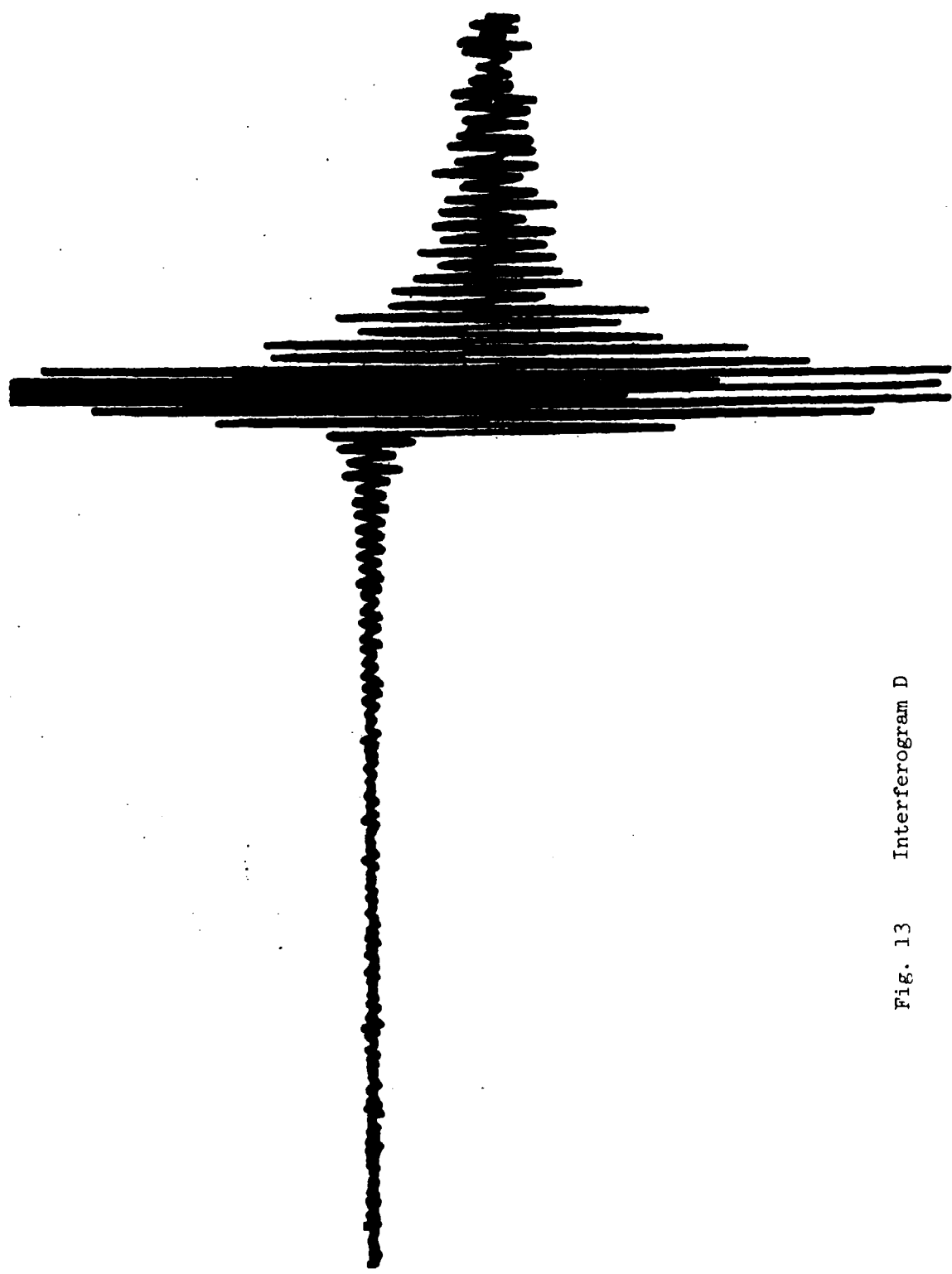


Fig. 13 Interferogram D

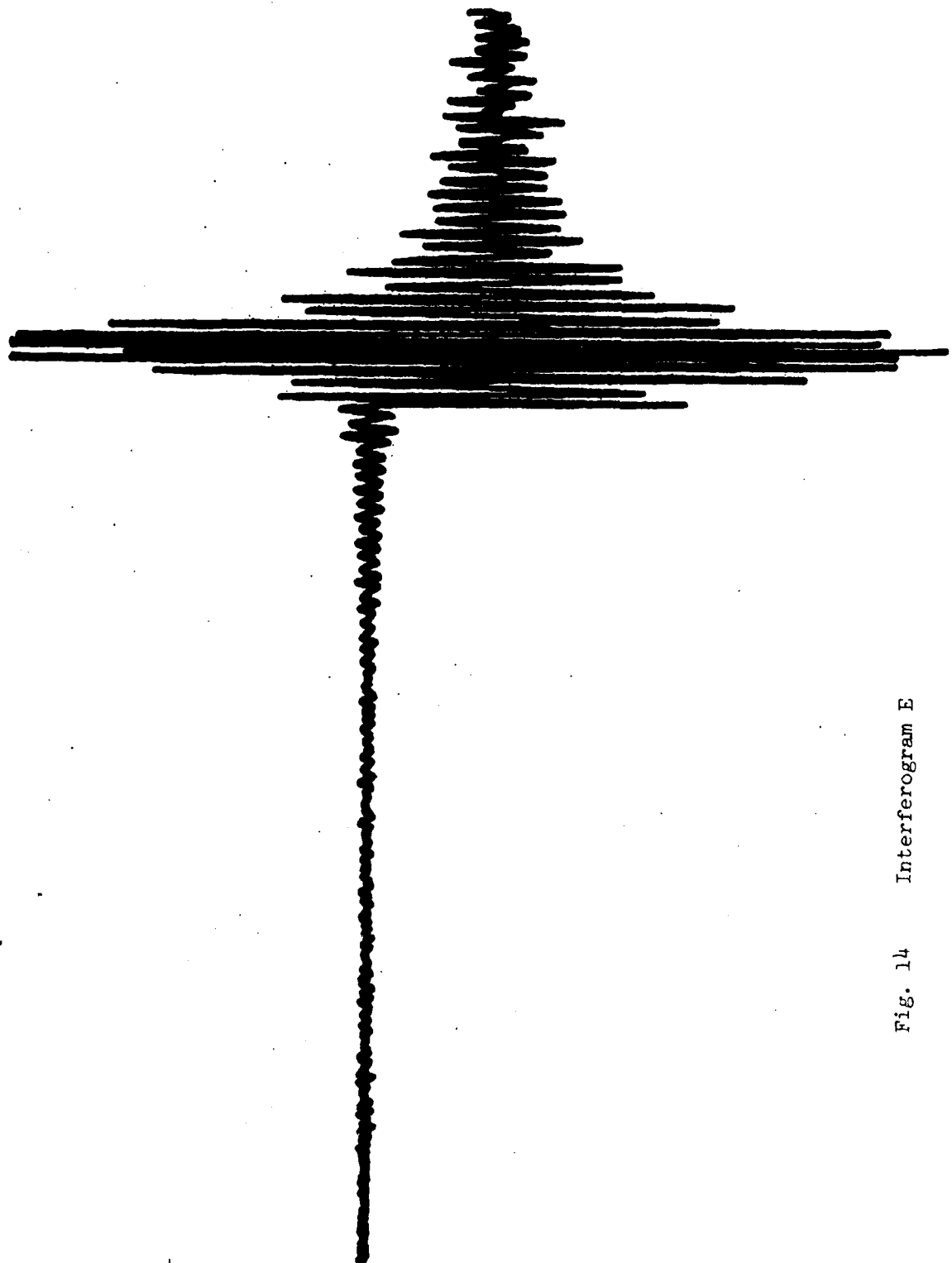


Fig. 14 Interferogram E

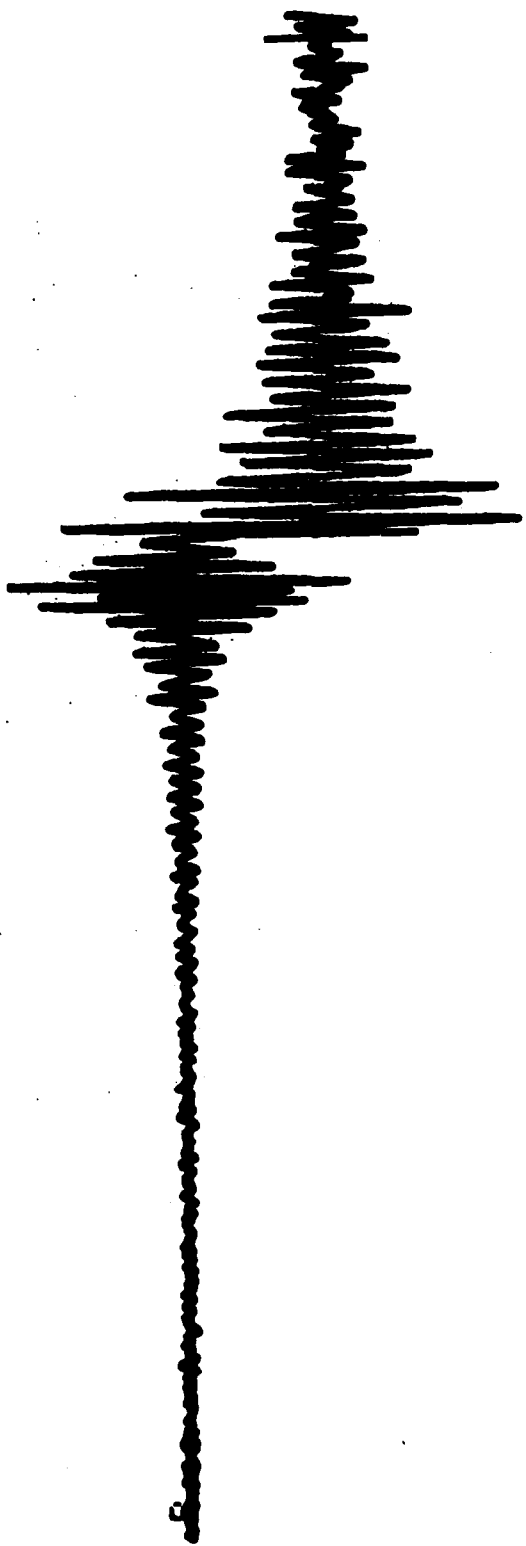


Fig. 15 Interferogram F

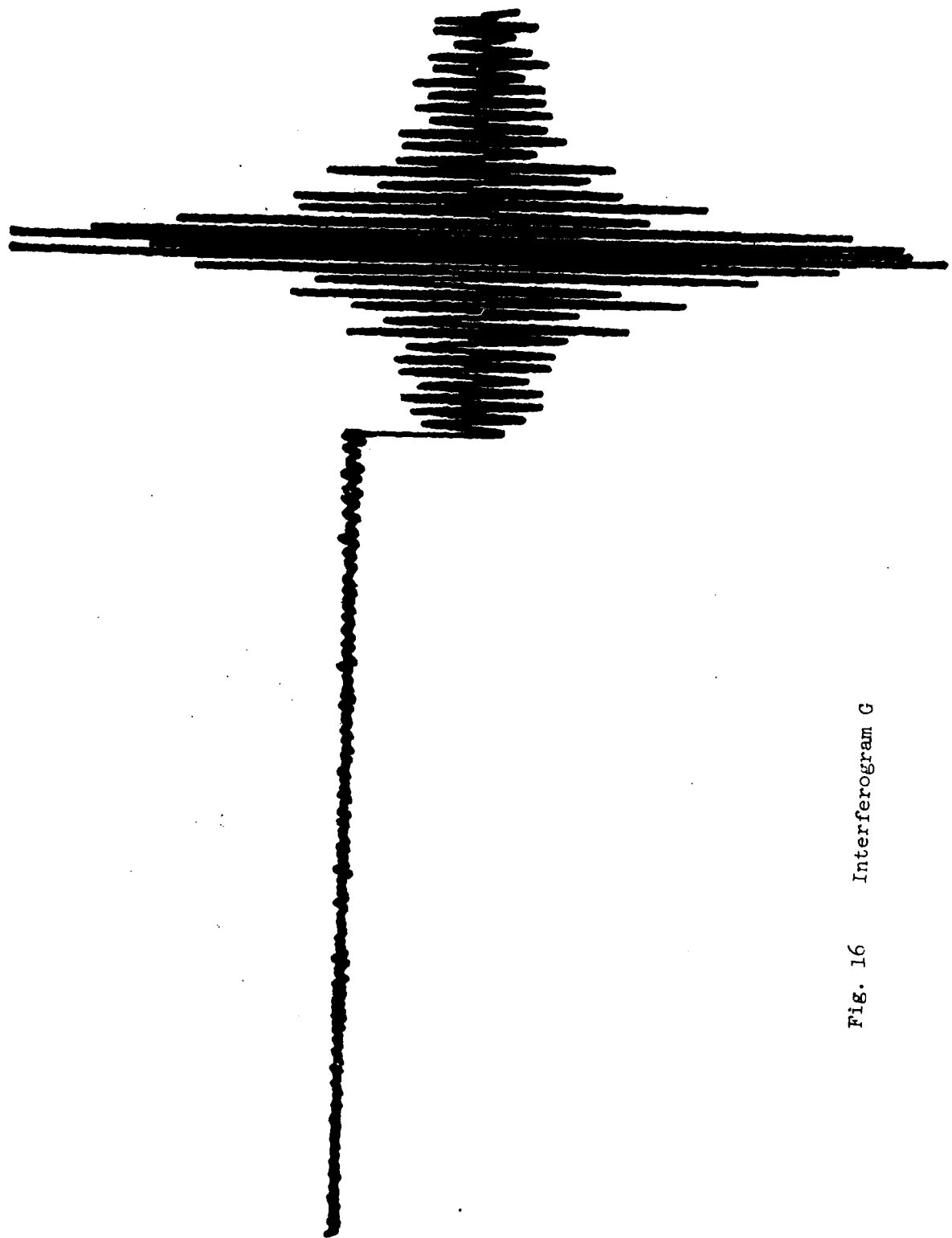


Fig. 16 Interferogram G

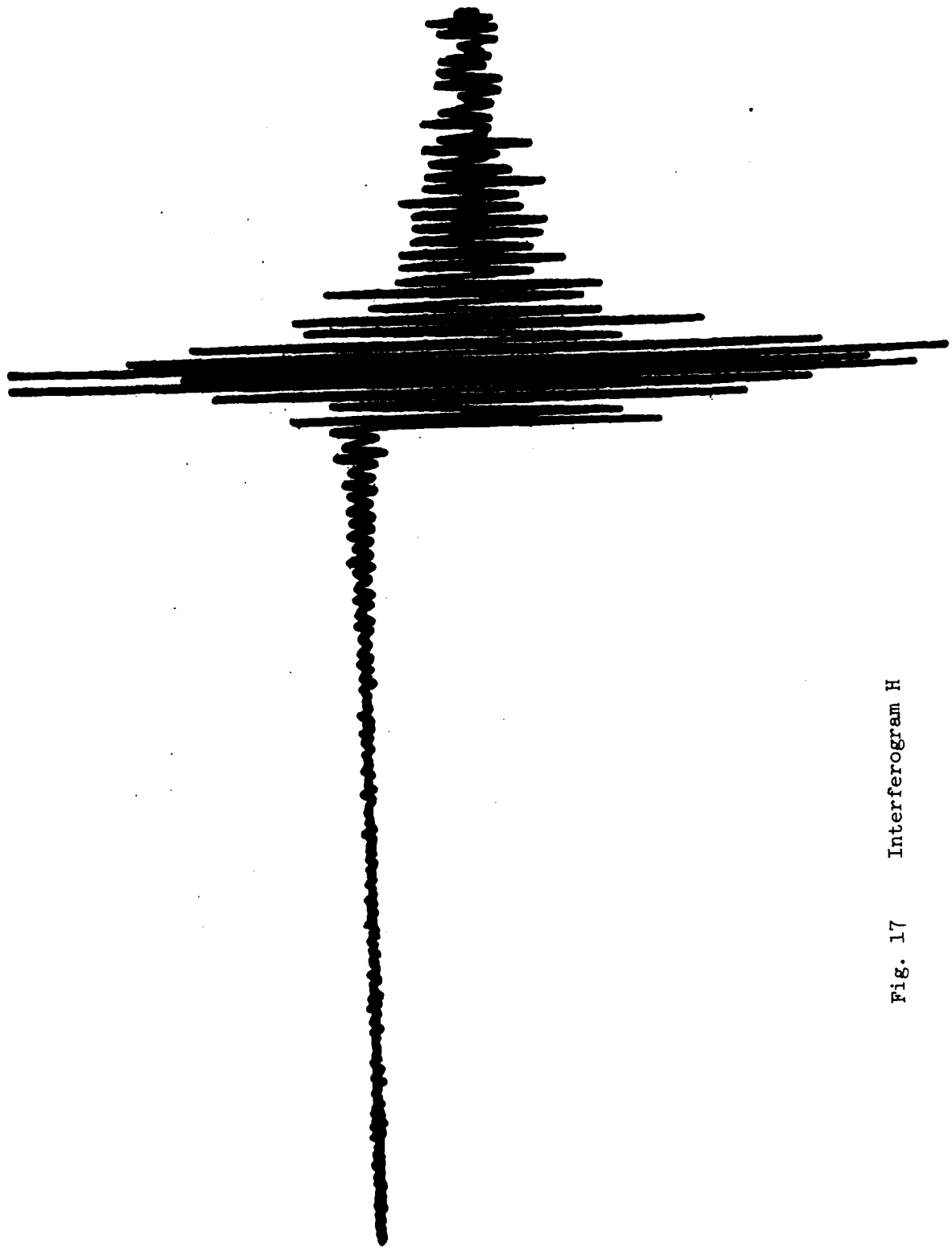


Fig. 17 Interferogram H

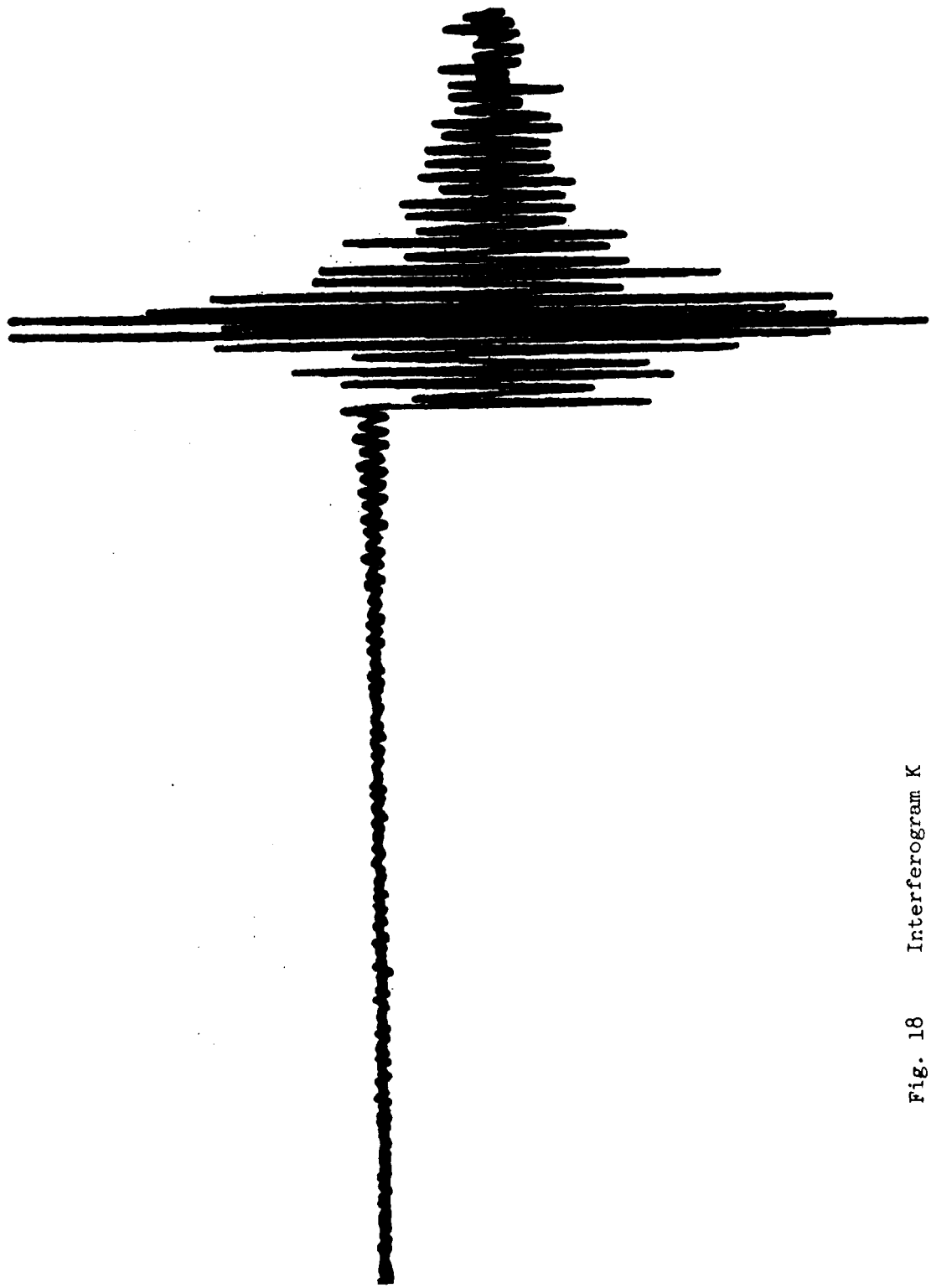


Fig. 18 Interferogram K

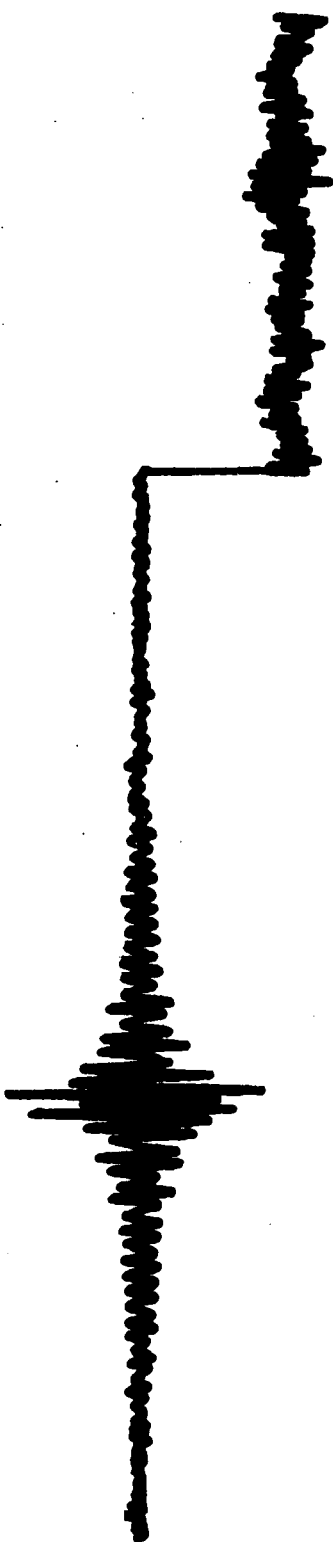


Fig. 19 Interferogram L

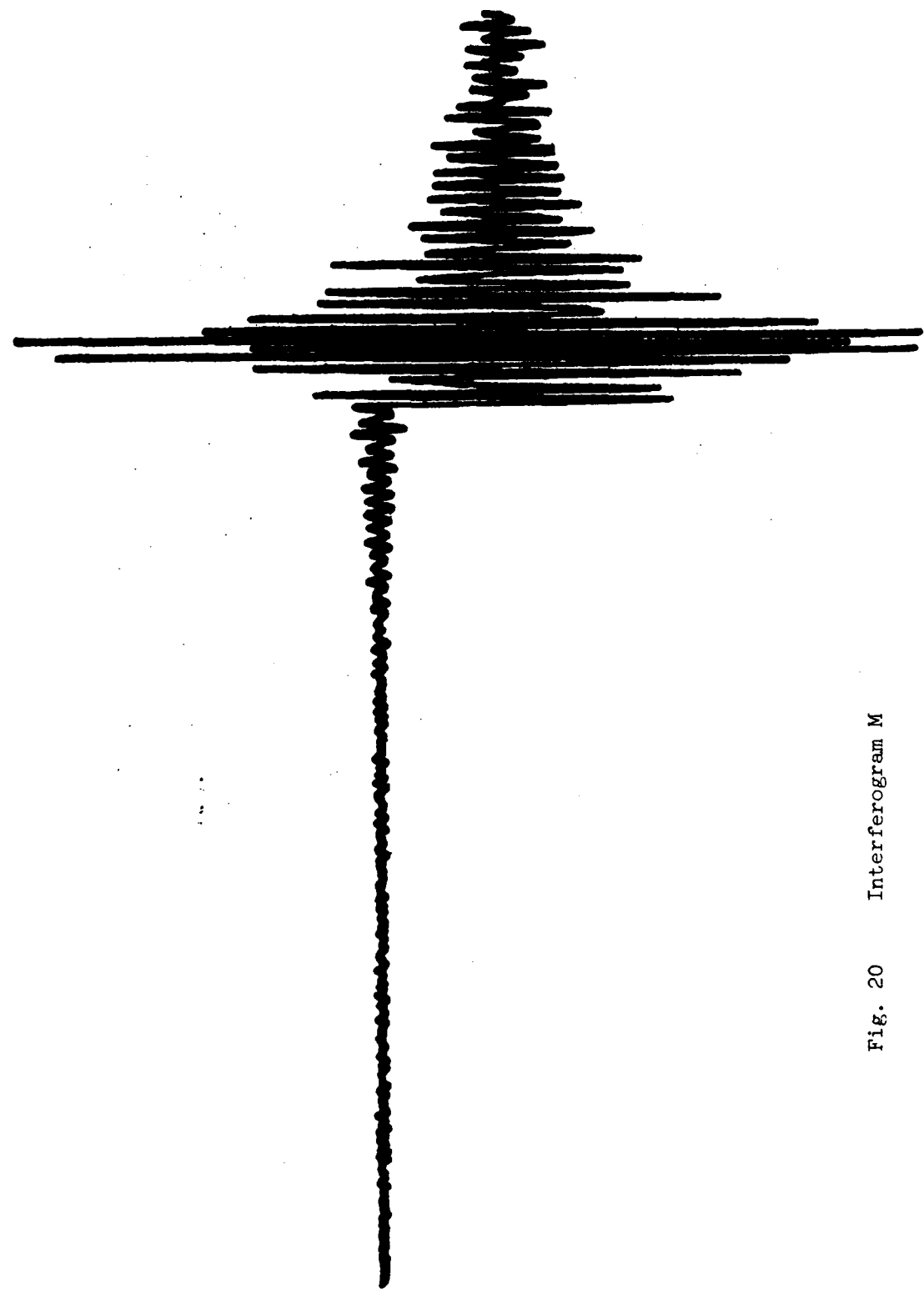


Fig. 20 Interferogram M

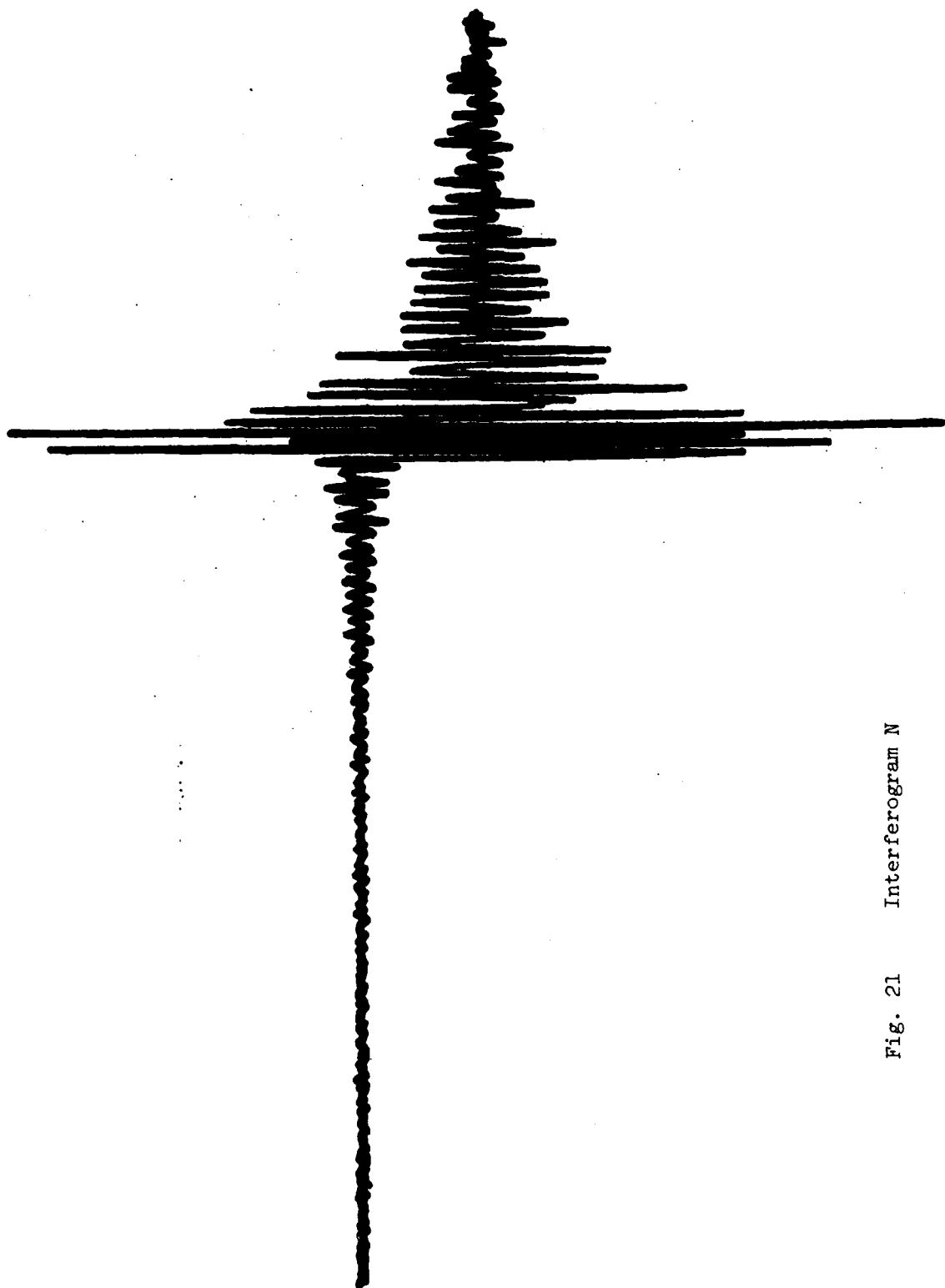


Fig. 21 Interferogram N

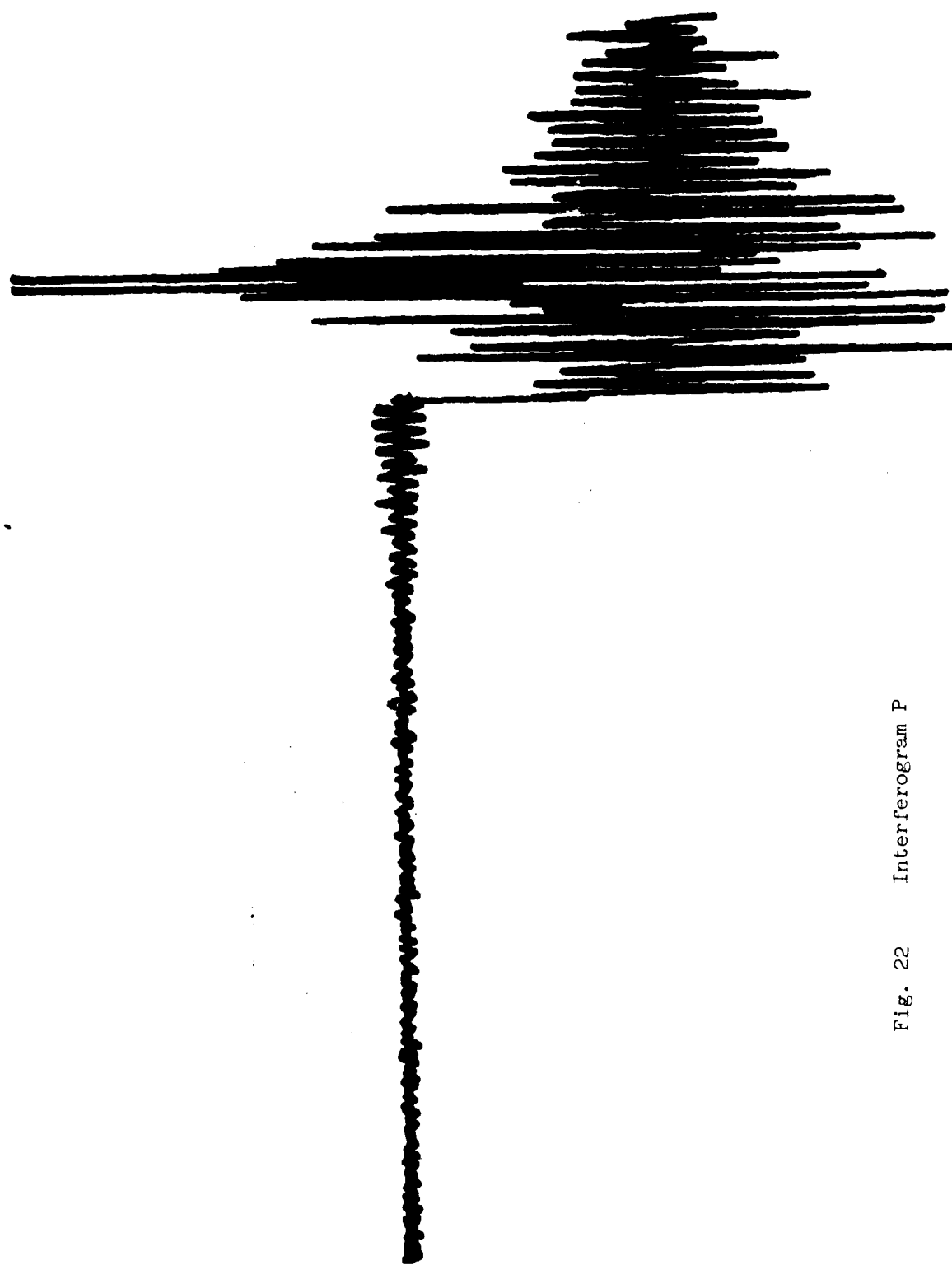


Fig. 22 Interferogram P

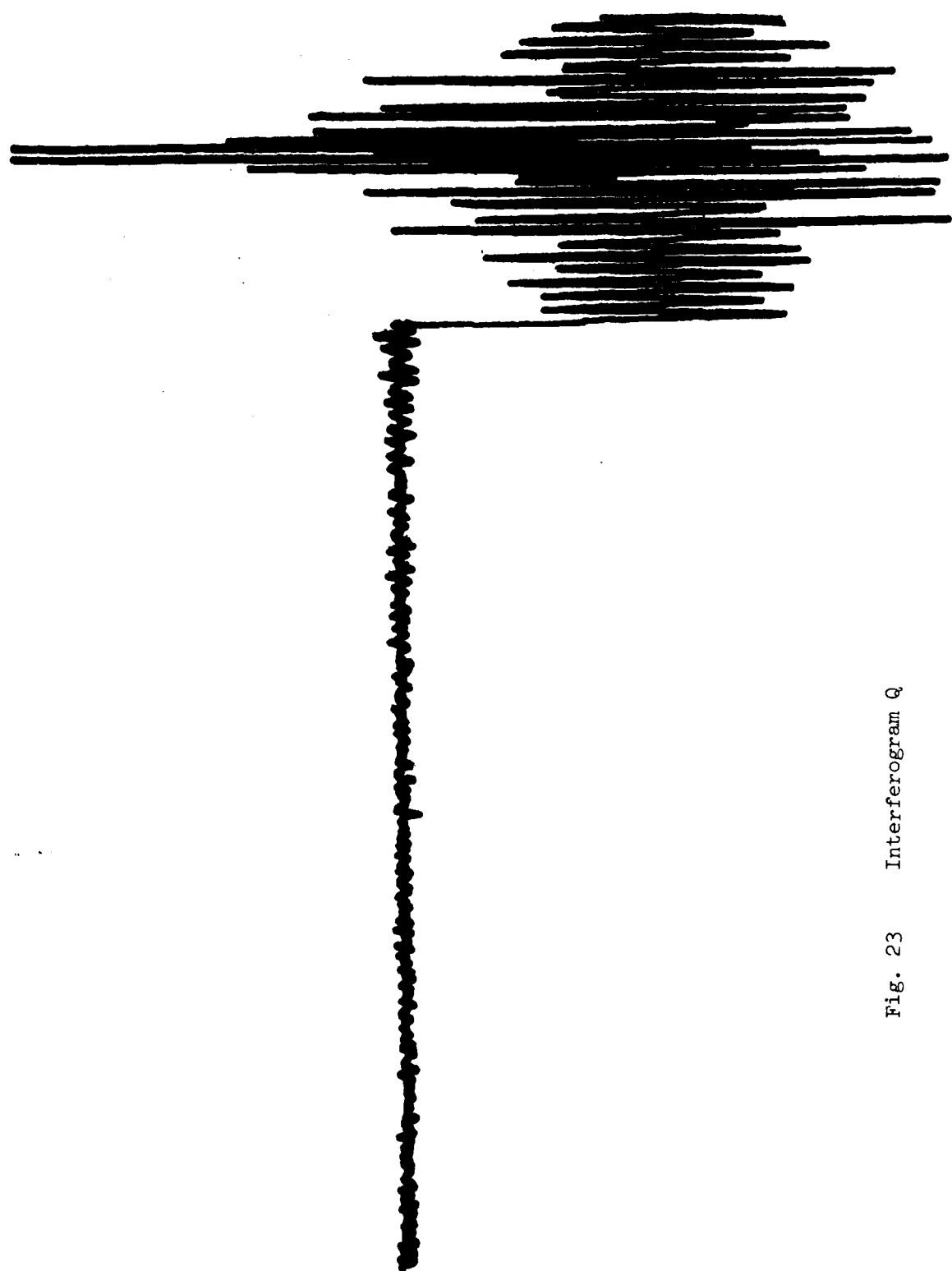


Fig. 23 Interferogram Q

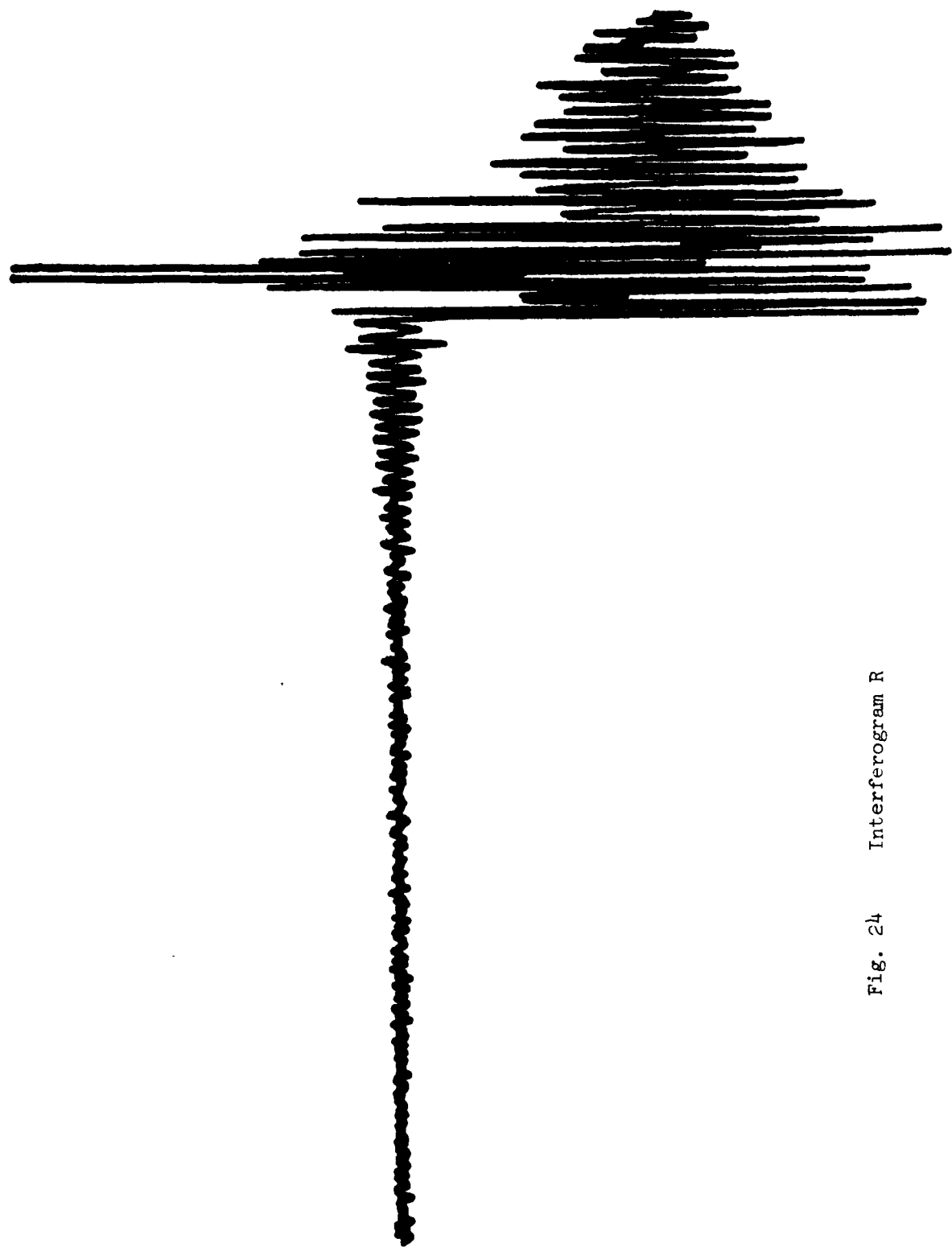


Fig. 24 Interferogram R

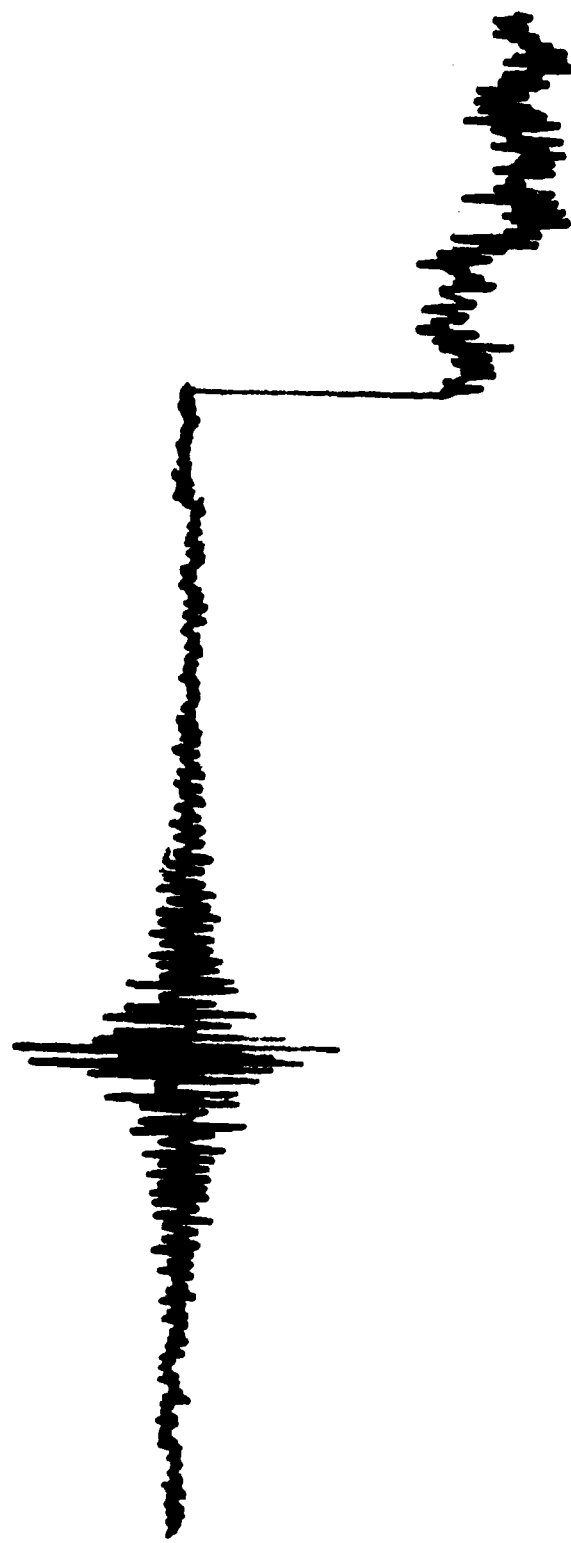


Fig. 25 Interferogram S

Fig. 26 (a) Spectrum A $500 \text{ cm}^{-1} \sim 1000 \text{ cm}^{-1}$

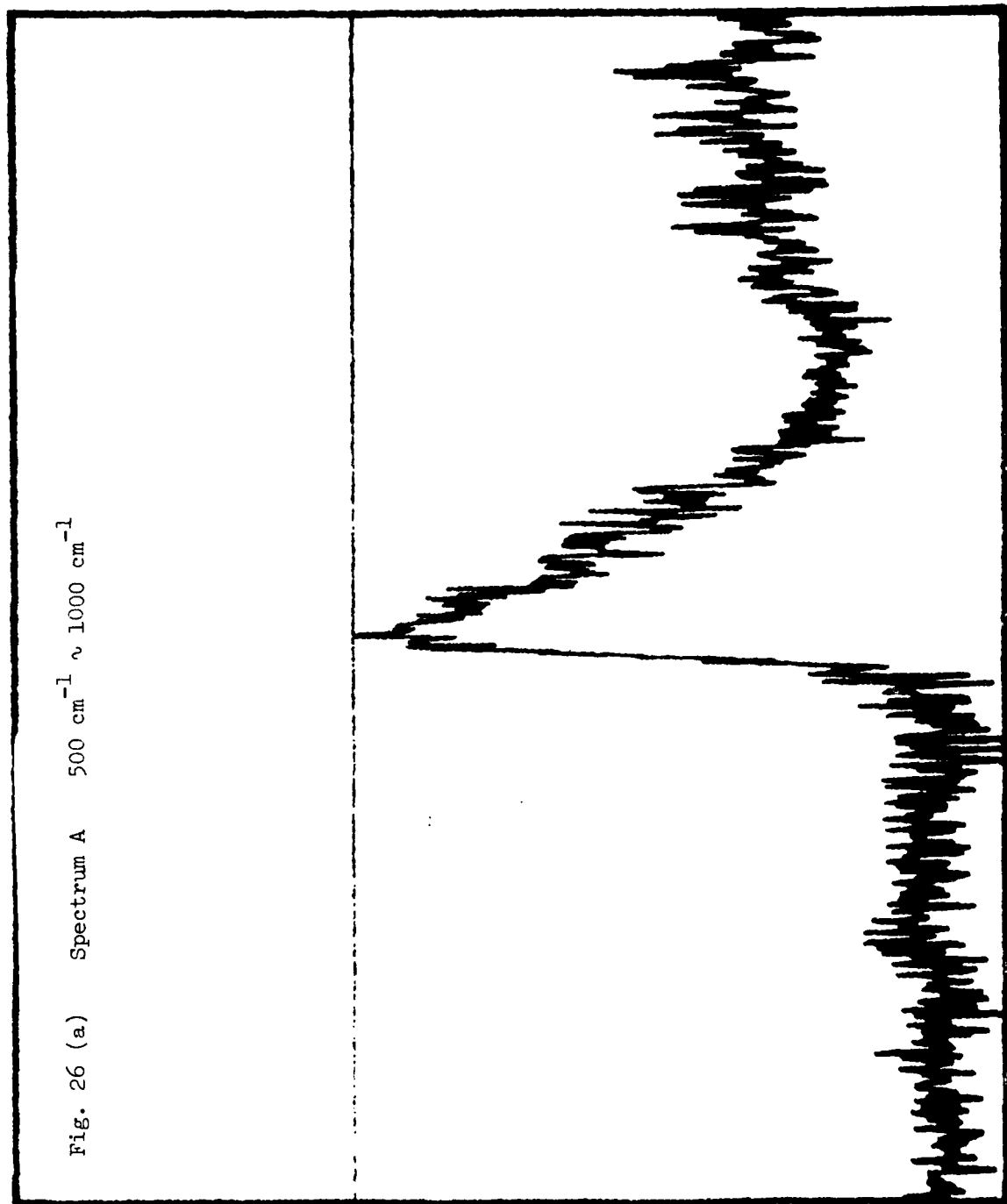


Fig. 26 (b) Spectrum A 1000 cm^{-1} ~ 1500 cm^{-1}

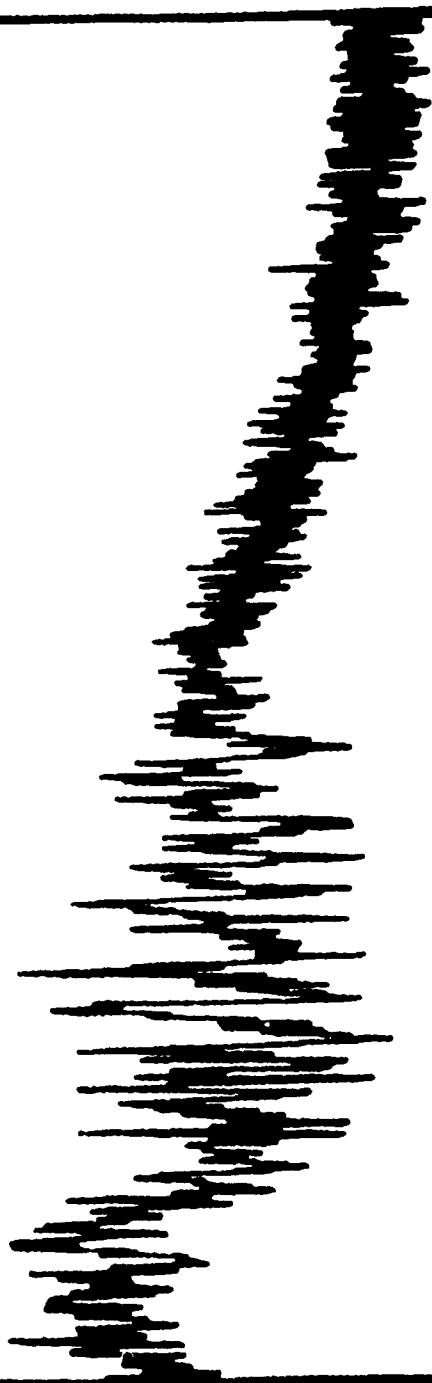


Fig. 27 (a) Spectrum B $500 \text{ cm}^{-1} \sim 1000 \text{ cm}^{-1}$

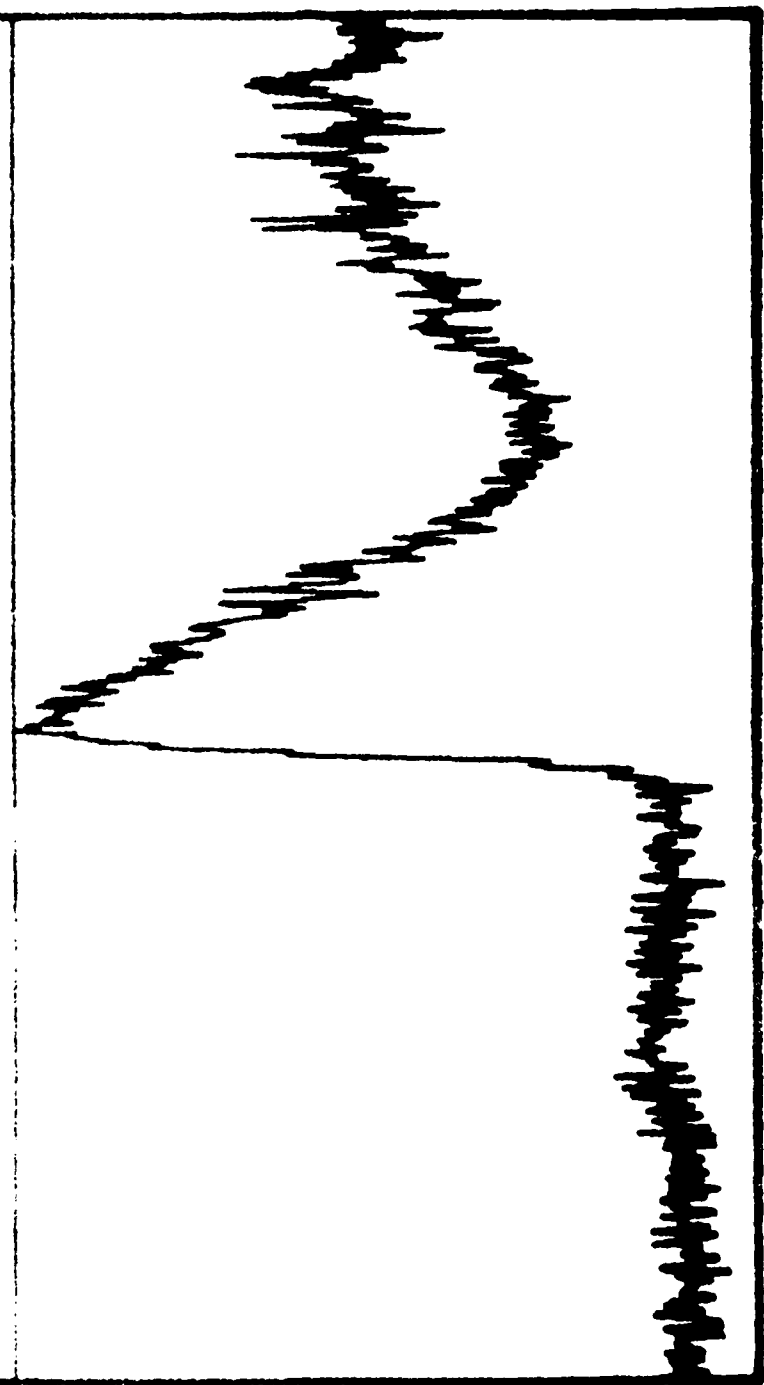


Fig. 27 (b) Spectrum B $1000 \text{ cm}^{-1} \sim 1500 \text{ cm}^{-1}$

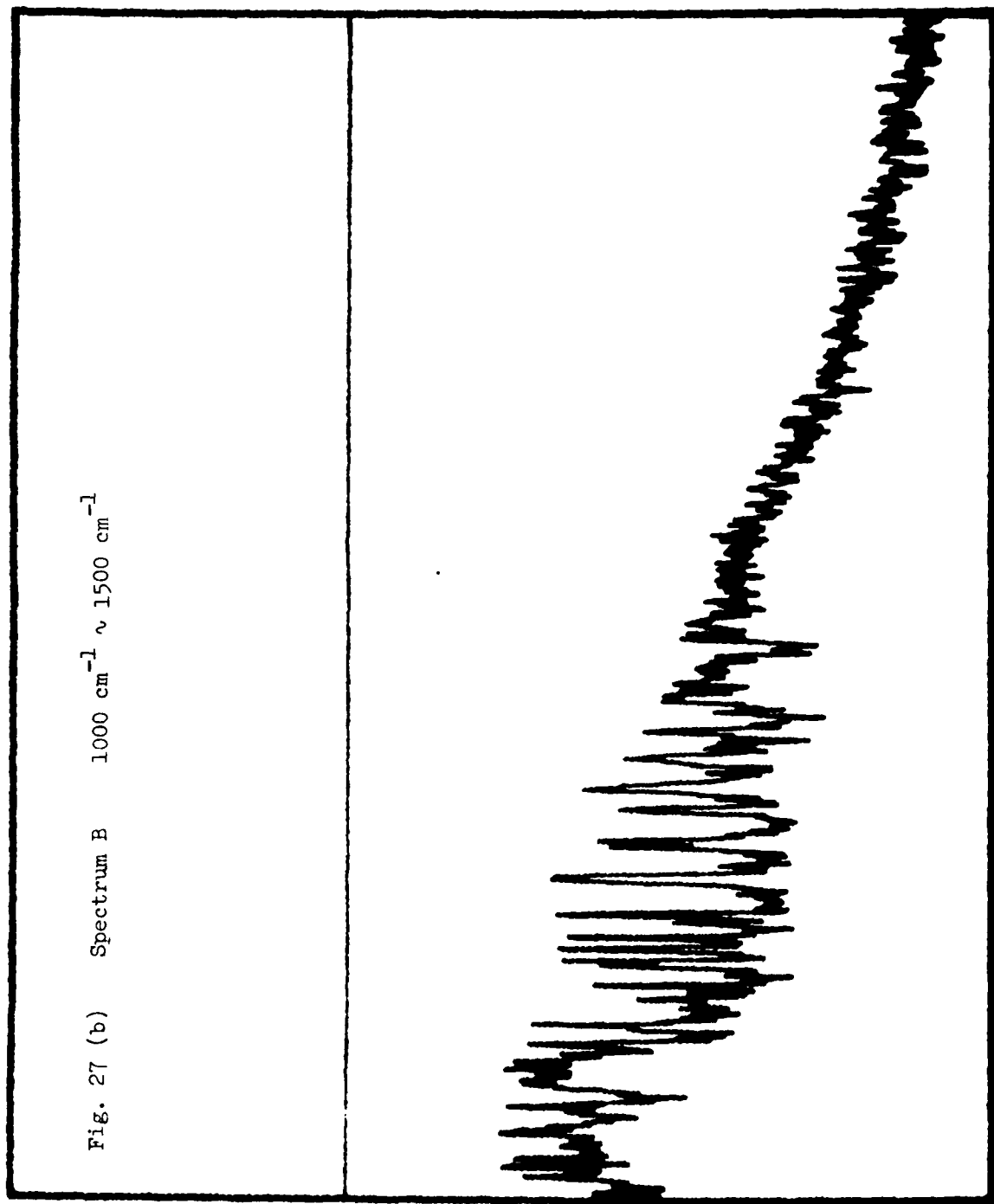


Fig. 28 (a) Spectrum C $500 \text{ cm}^{-1} \sim 1000 \text{ cm}^{-1}$

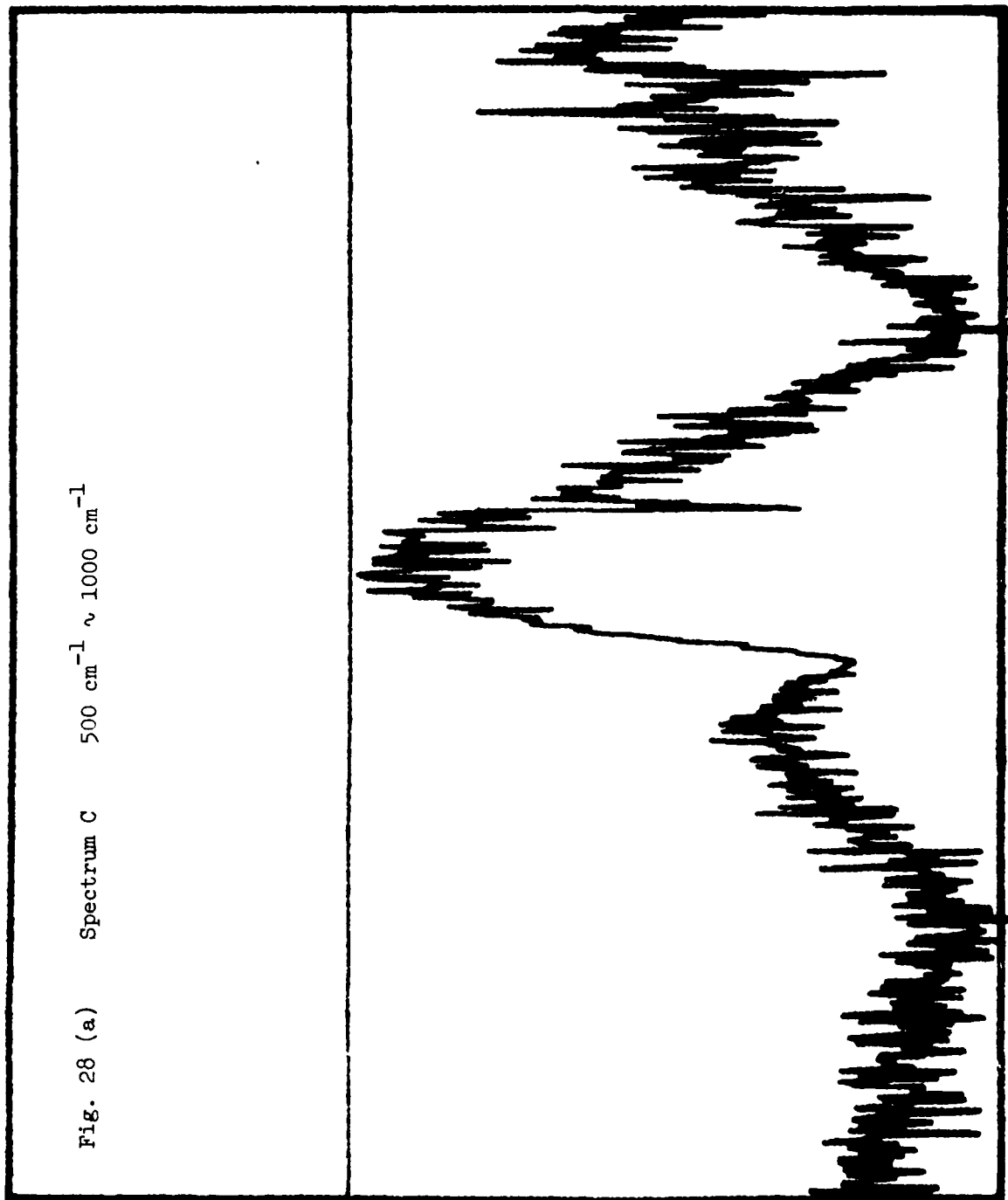


Fig. 28 (b) Spectrum C $1000 \text{ cm}^{-1} \sim 1500 \text{ cm}^{-1}$

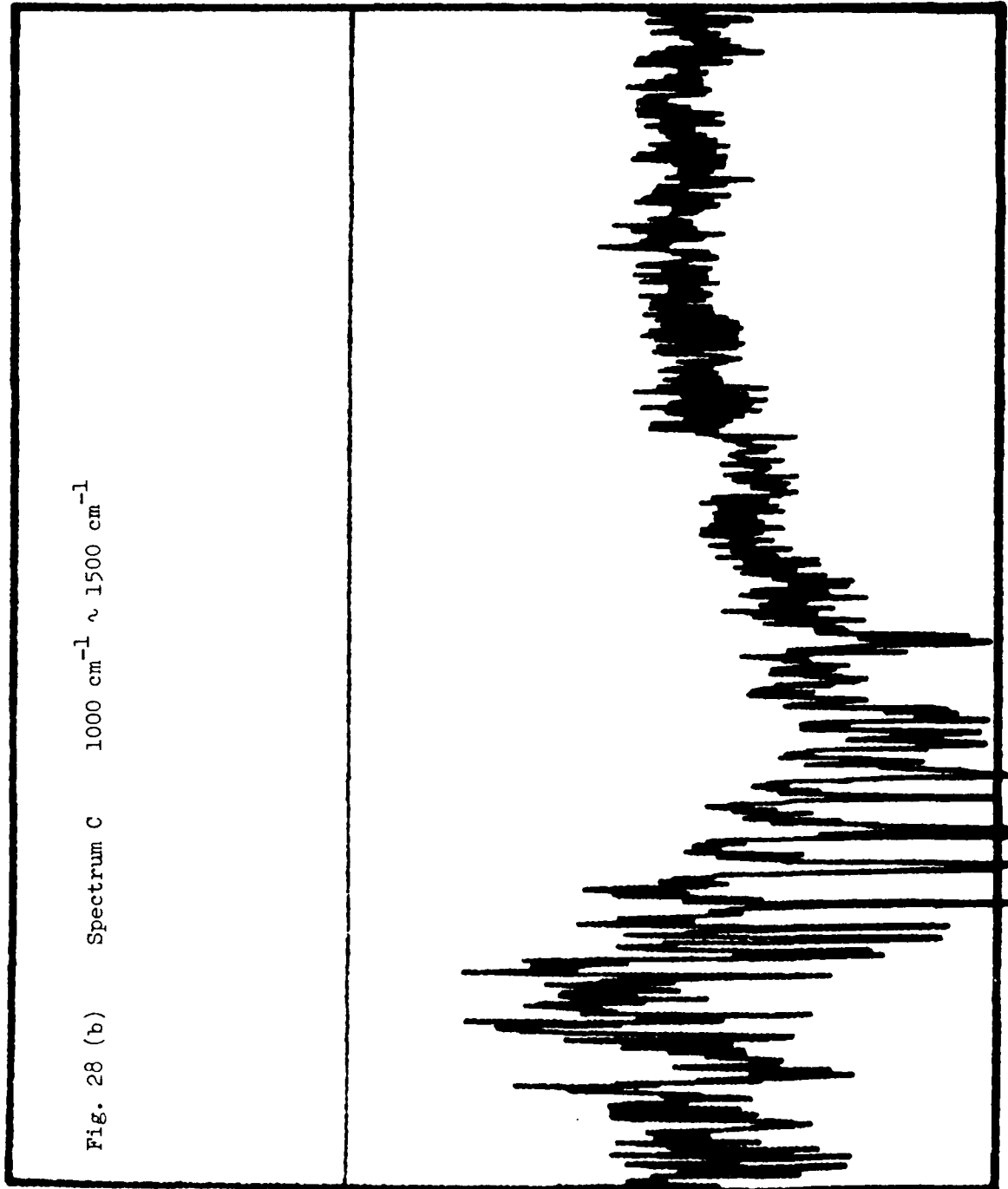


Fig. 29 (a) Spectrum D $500 \text{ cm}^{-1} \sim 1000 \text{ cm}^{-1}$

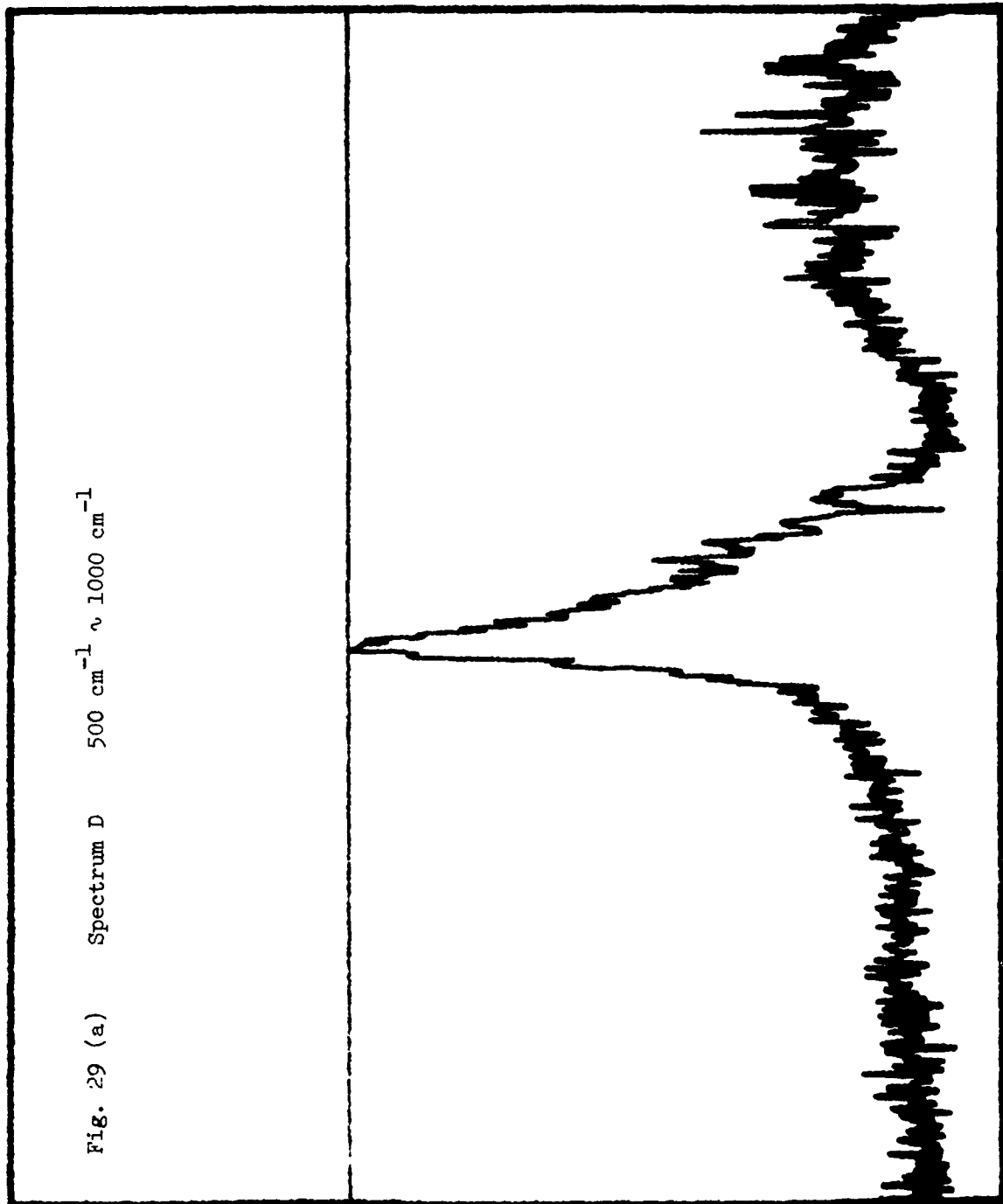


Fig. 29 (b) Spectrum D $1000 \text{ cm}^{-1} \sim 1500 \text{ cm}^{-1}$

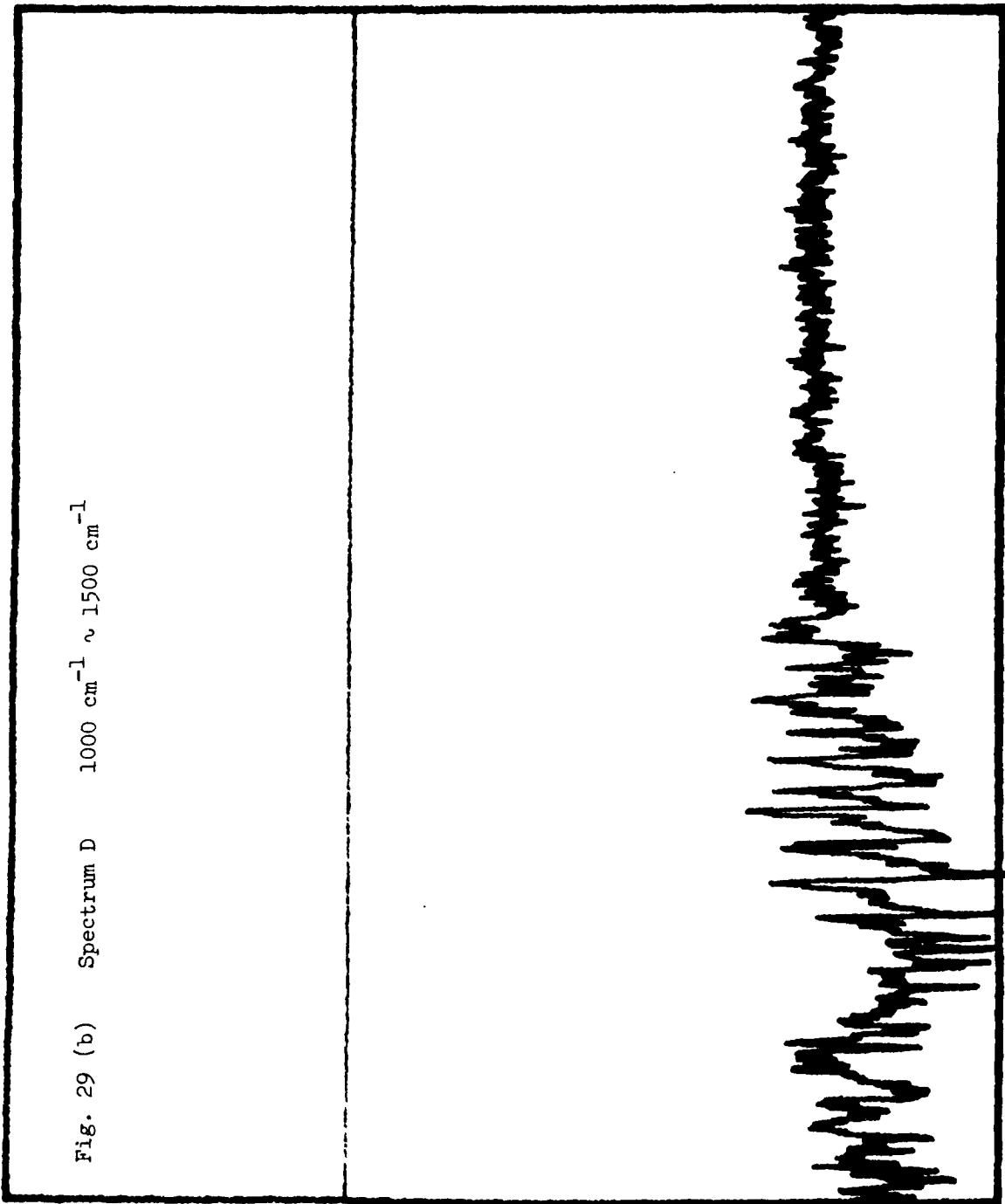


Fig. 30 (a) Spectrum E $500 \text{ cm}^{-1} \sim 1000 \text{ cm}^{-1}$

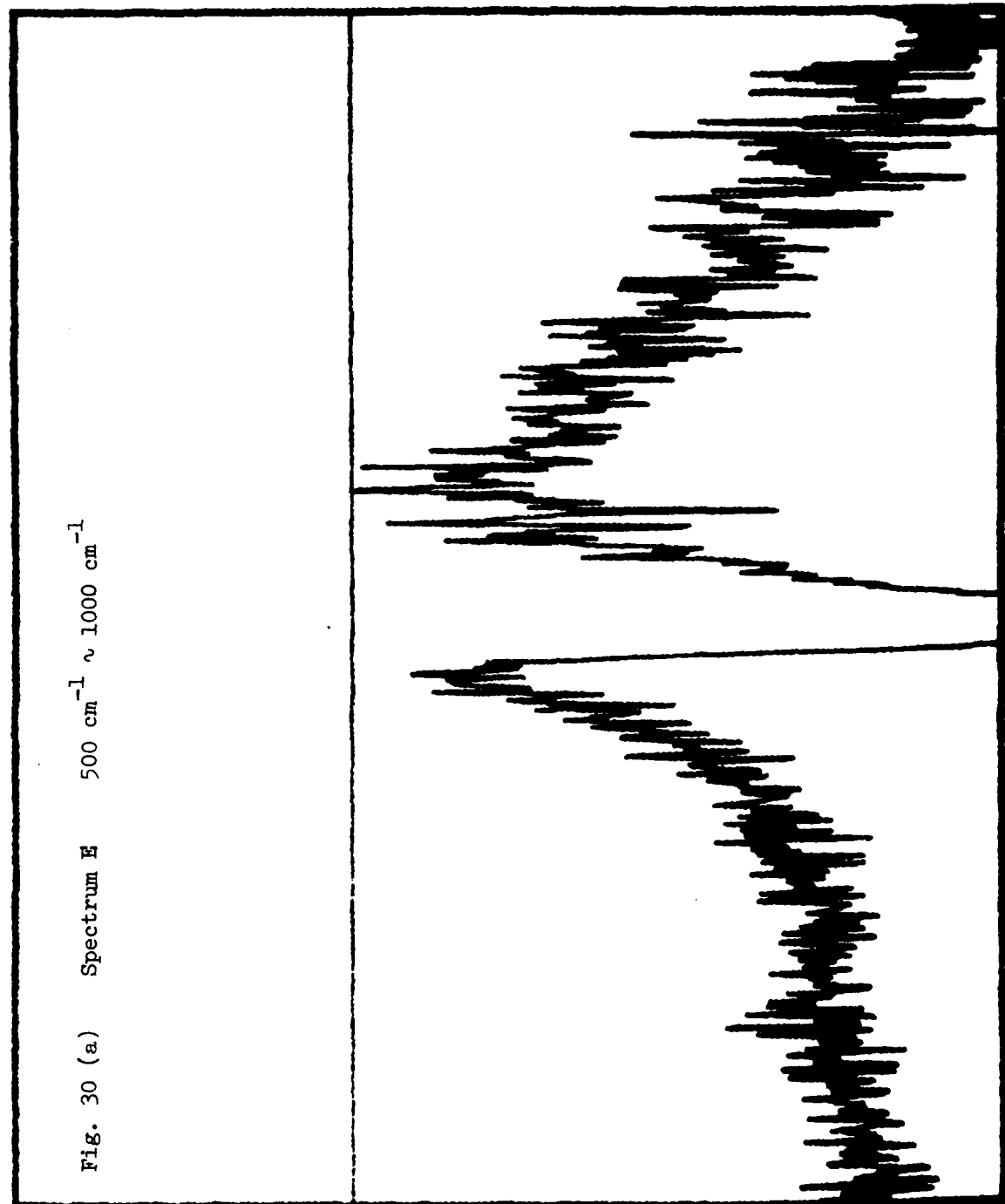


Fig. 30 (b) Spectrum E $1000 \text{ cm}^{-1} \sim 1500 \text{ cm}^{-1}$

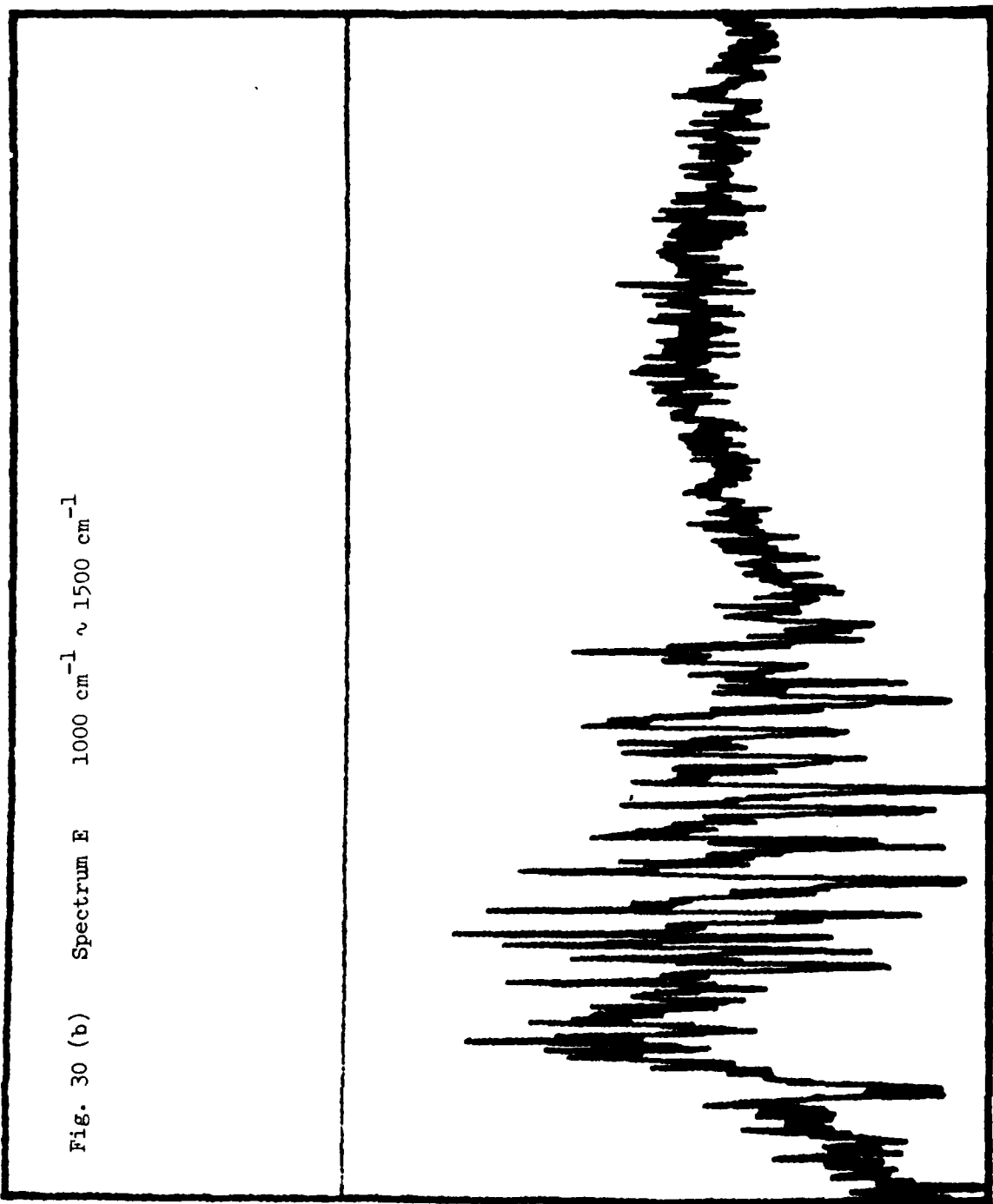


Fig. 31 (a) Spectrum G 500 cm^{-1} $\sim 1000 \text{ cm}^{-1}$

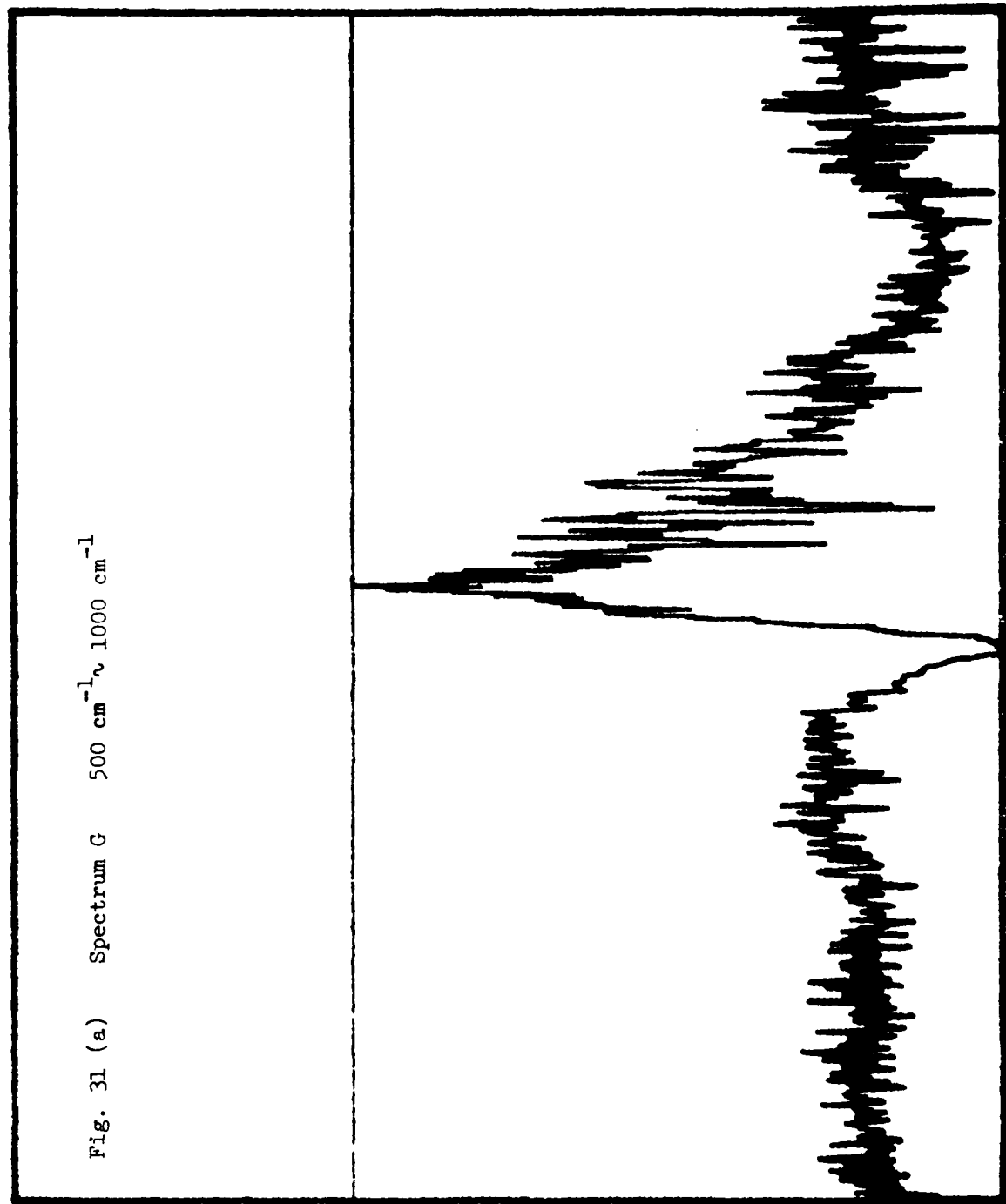


Fig. 31 (b) Spectrum G $1000 \text{ cm}^{-1} \sim 1500 \text{ cm}^{-1}$

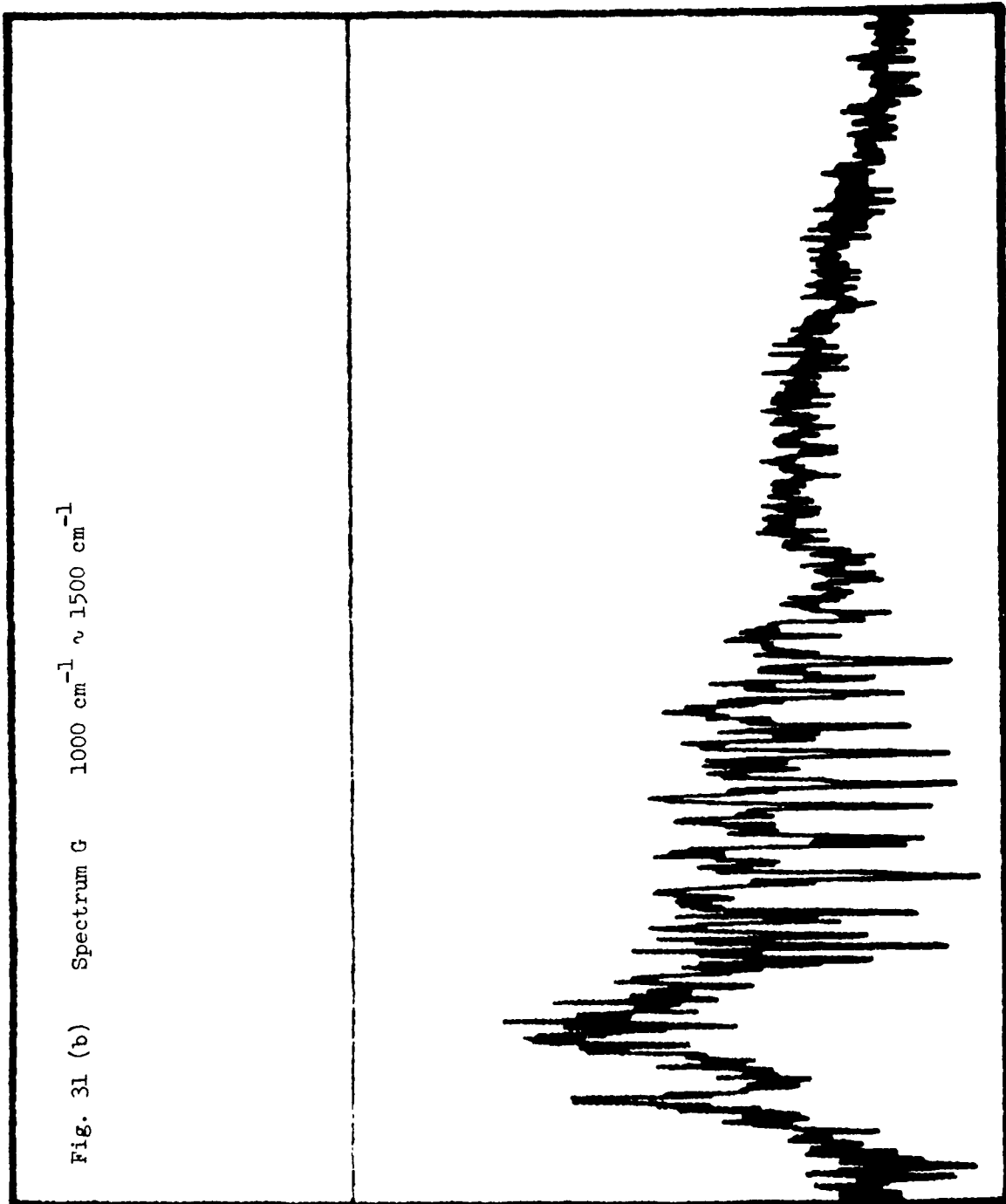


Fig. 32 (a) Spectrum H $500 \text{ cm}^{-1} \sim 1000 \text{ cm}^{-1}$

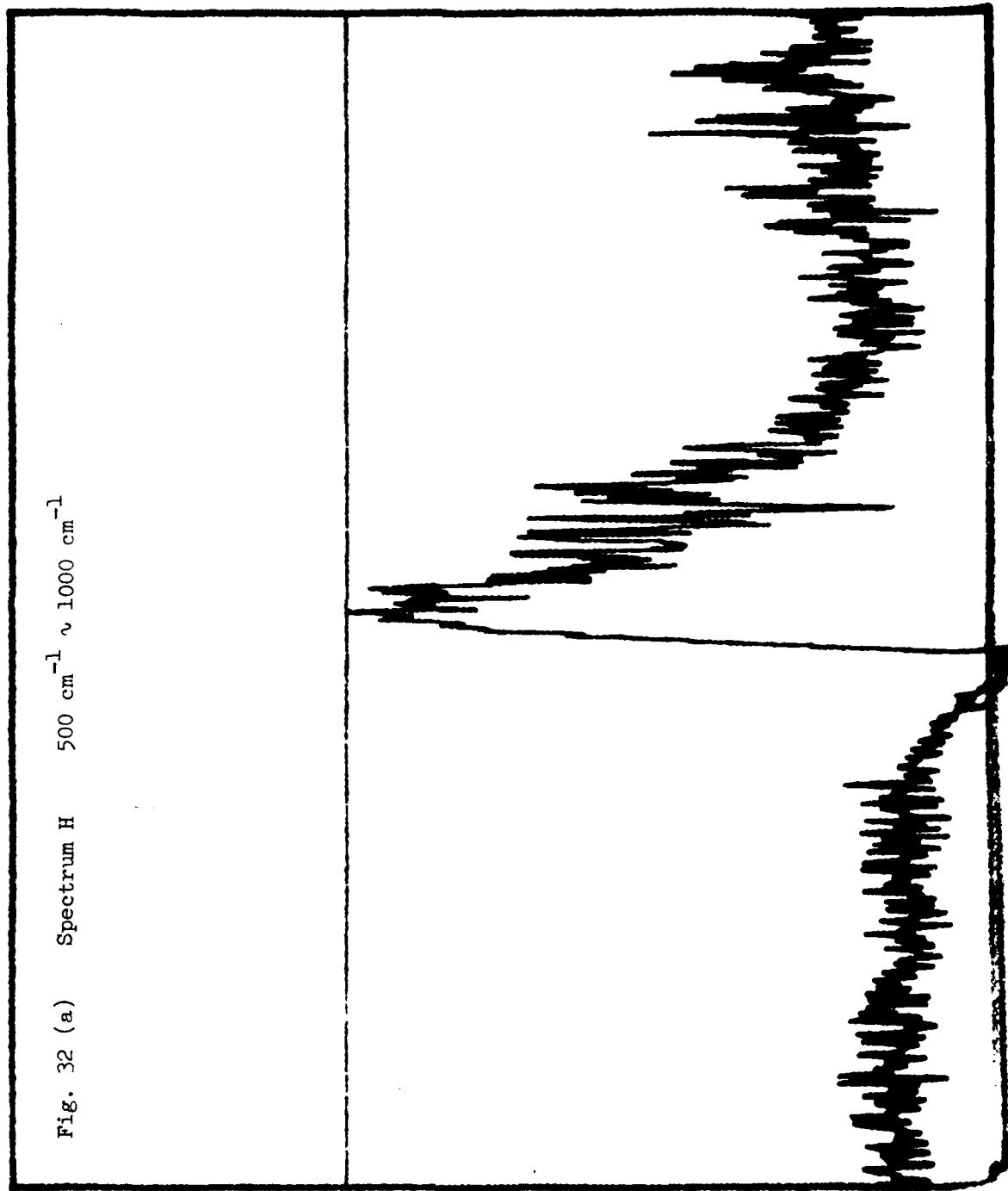


Fig. 32 (b) Spectrum H $1000 \text{ cm}^{-1} \sim 1500 \text{ cm}^{-1}$

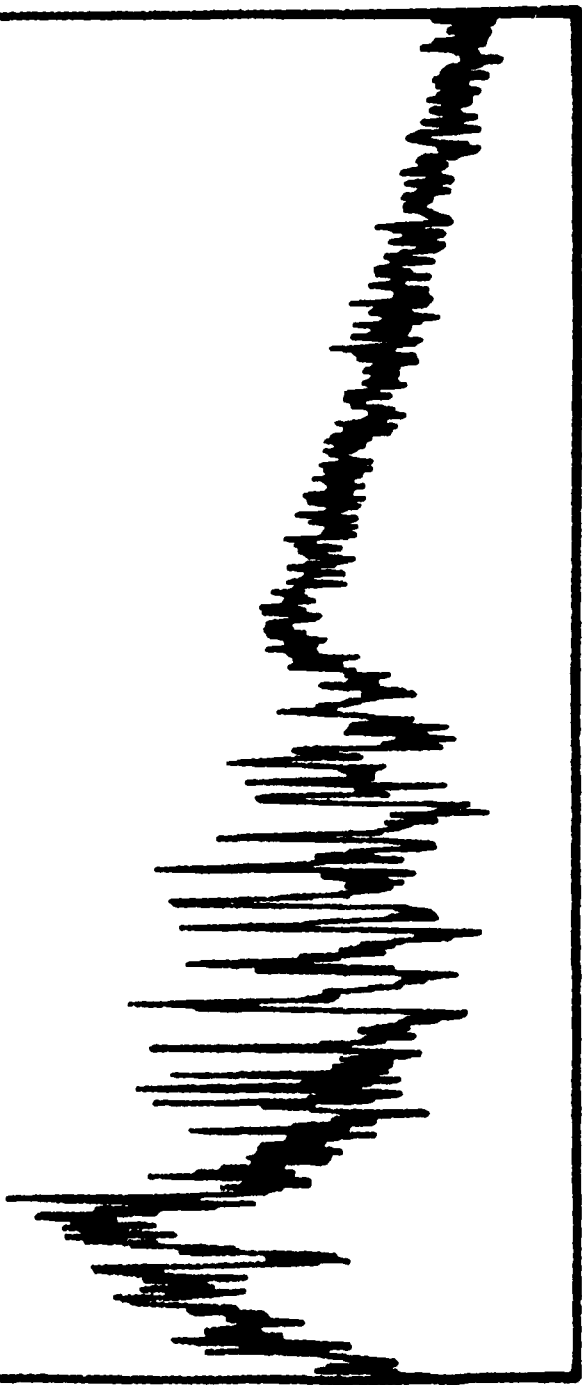


Fig. 33 (a) Spectrum K $500 \text{ cm}^{-1} \sim 1000 \text{ cm}^{-1}$

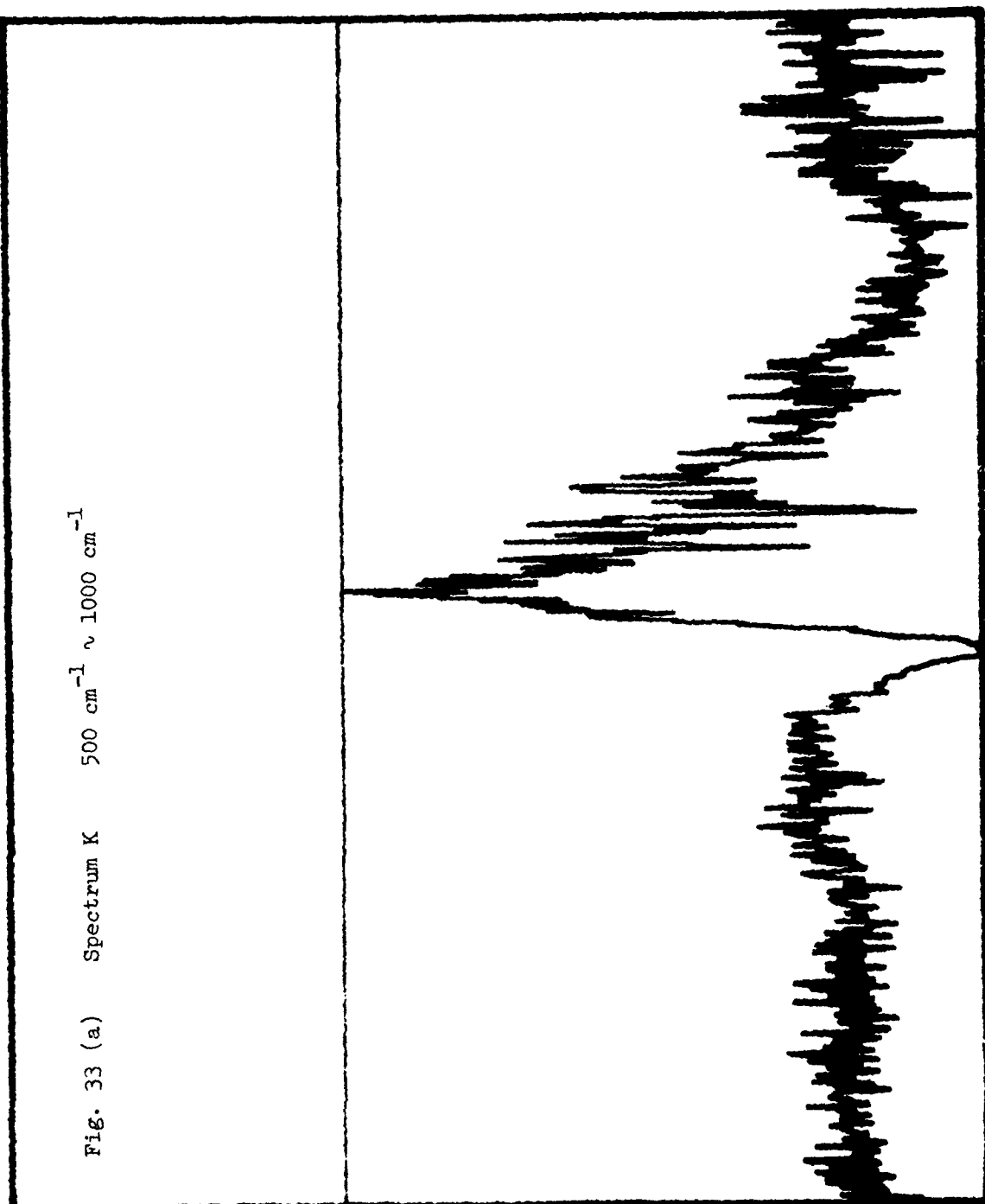


Fig. 33 (b) Spectrum K $1000 \text{ cm}^{-1} \sim 1500 \text{ cm}^{-1}$

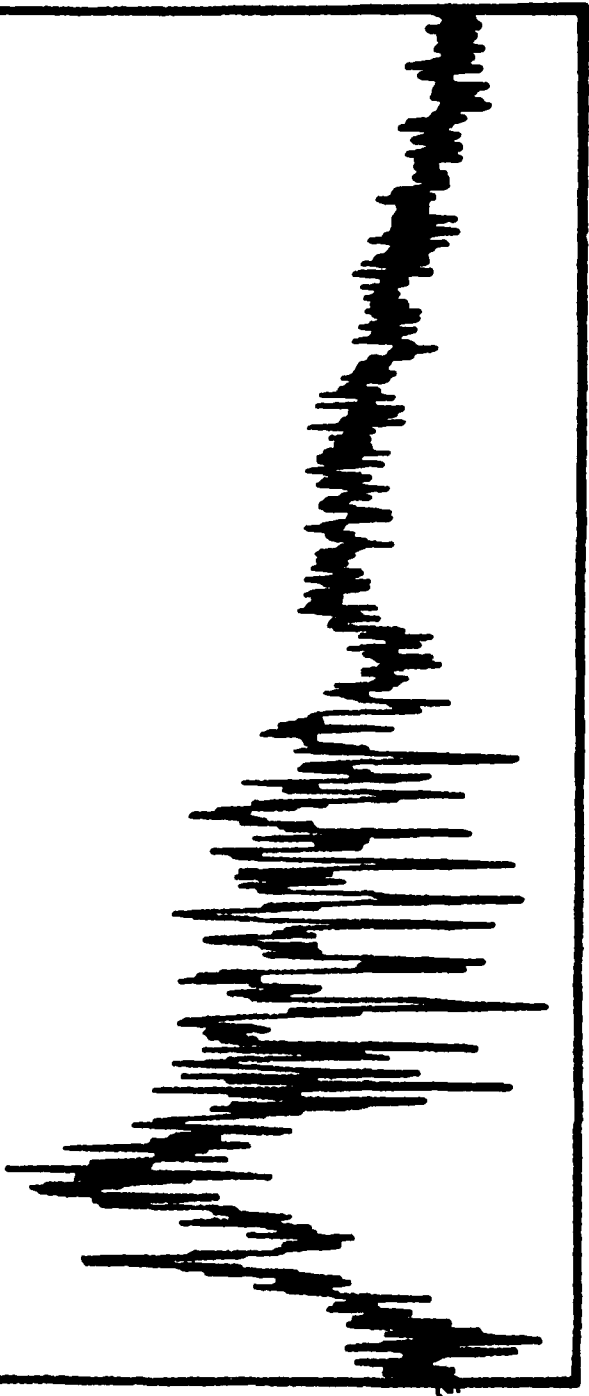


Fig. 3₄ (a) Spectrum M 500 cm⁻¹ ~ 1000 cm⁻¹

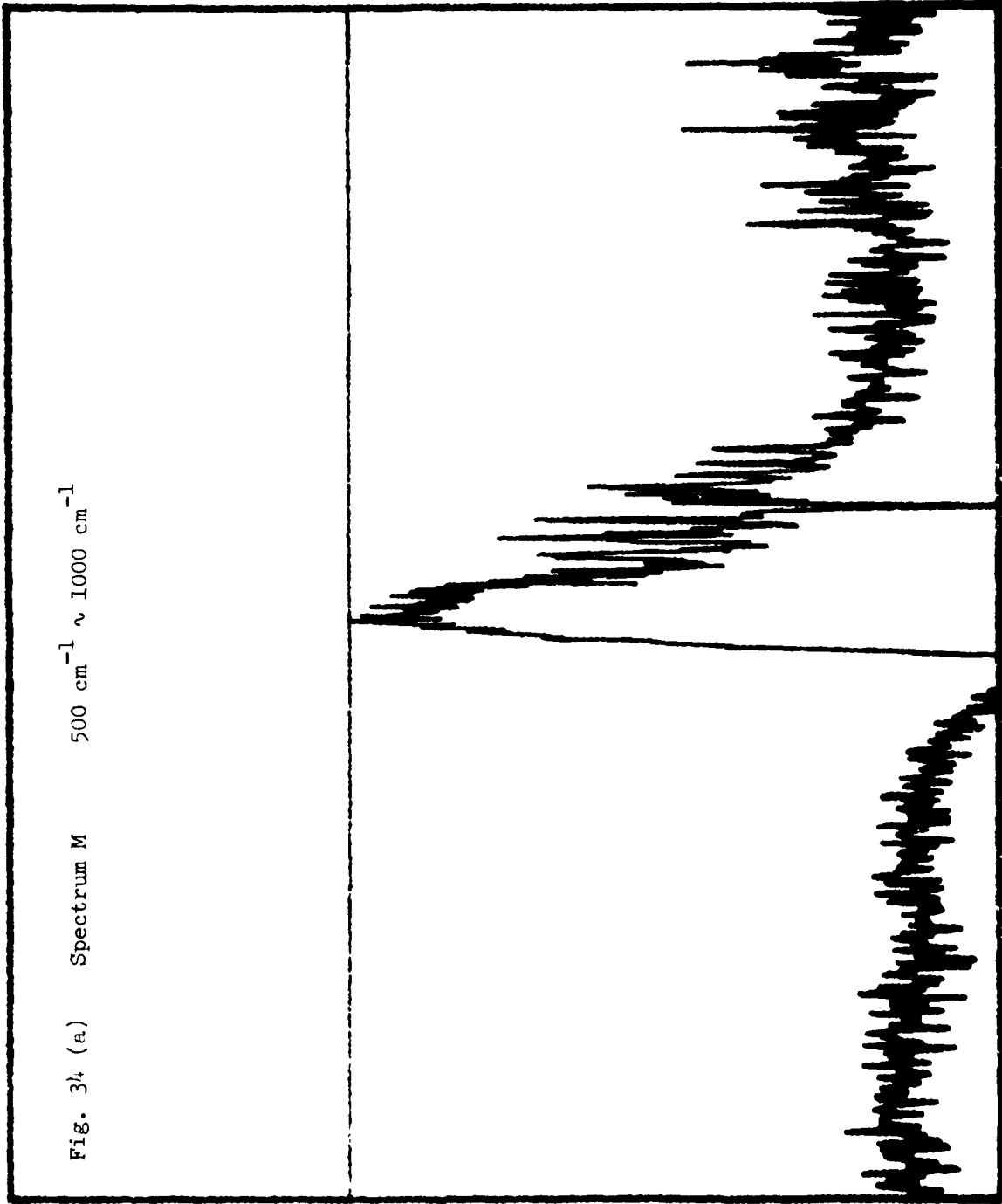


Fig. 34 (b) Spectrum M 1000 cm^{-1} ~ 1500 cm^{-1}

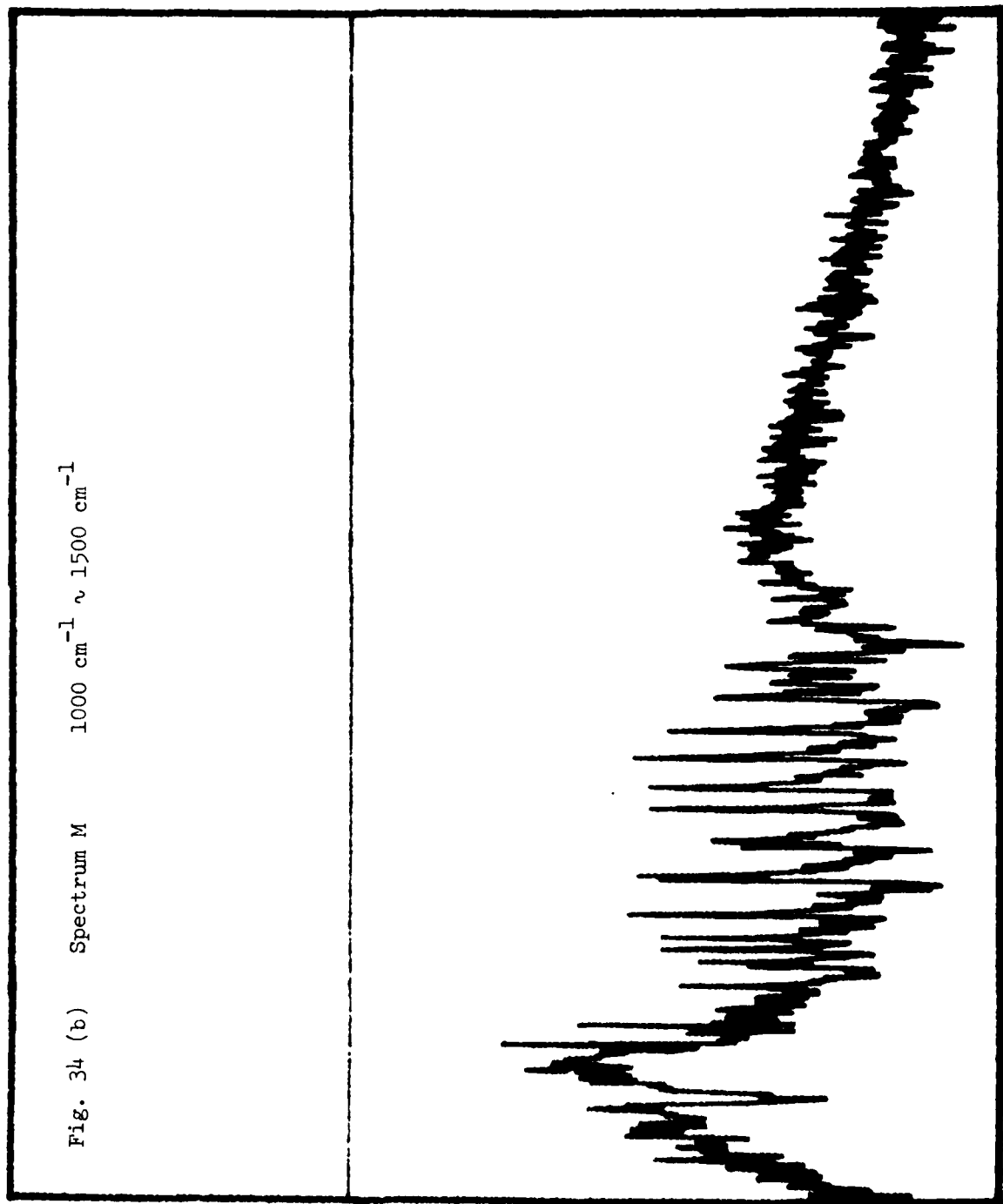


Fig. 35 (a) Spectrum N $500 \text{ cm}^{-1} \sim 1000 \text{ cm}^{-1}$

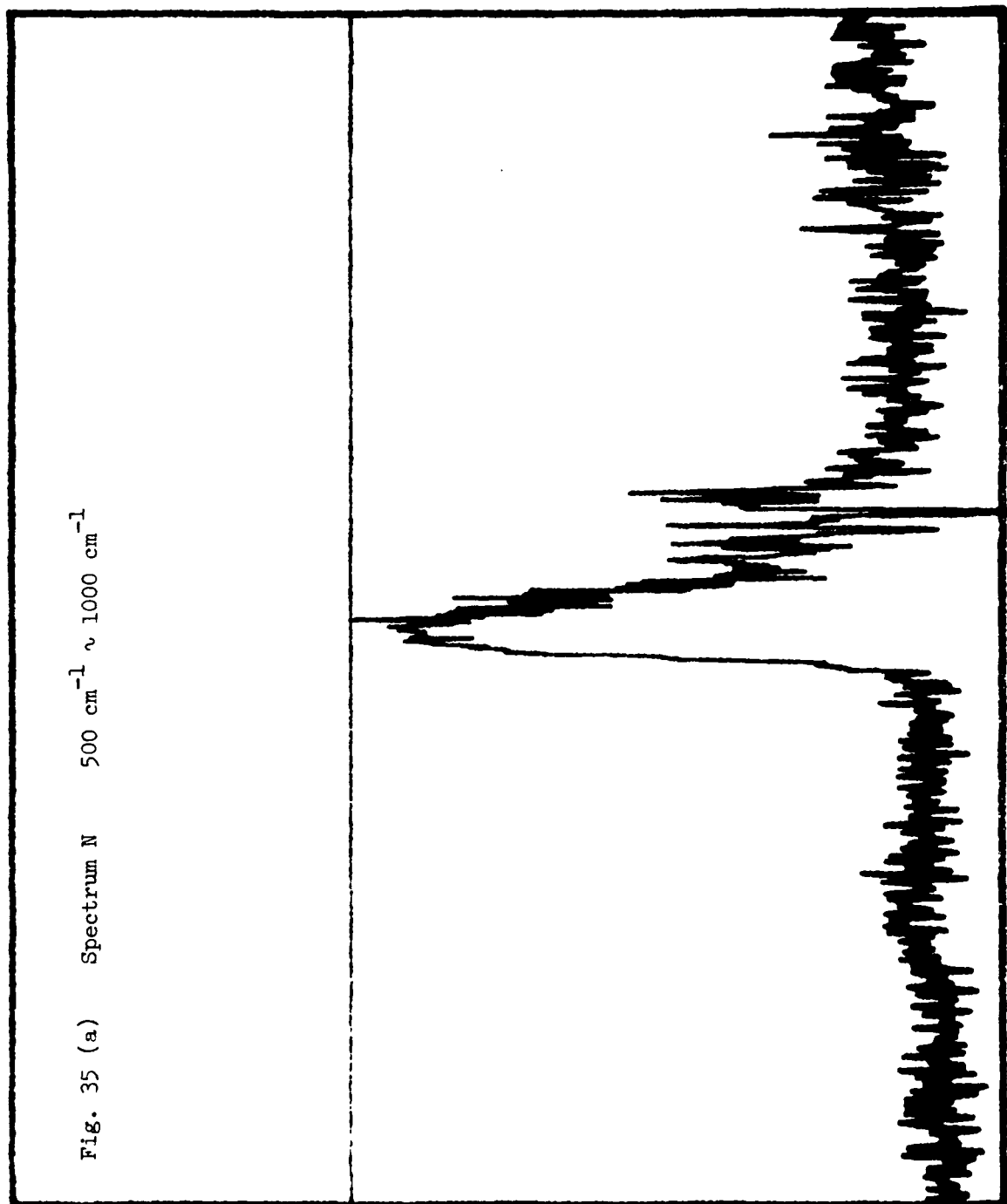


Fig. 35 (b) Spectrum N $1000 \text{ cm}^{-1} \sim 1500 \text{ cm}^{-1}$

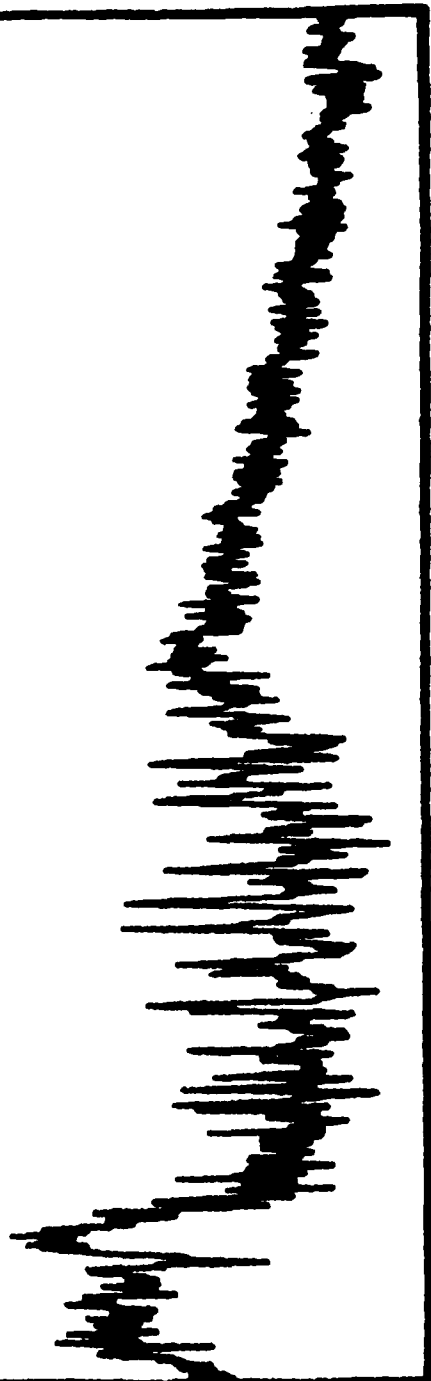


Fig. 36 (a) Spectrum P $500 \text{ cm}^{-1} \sim 1000 \text{ cm}^{-1}$

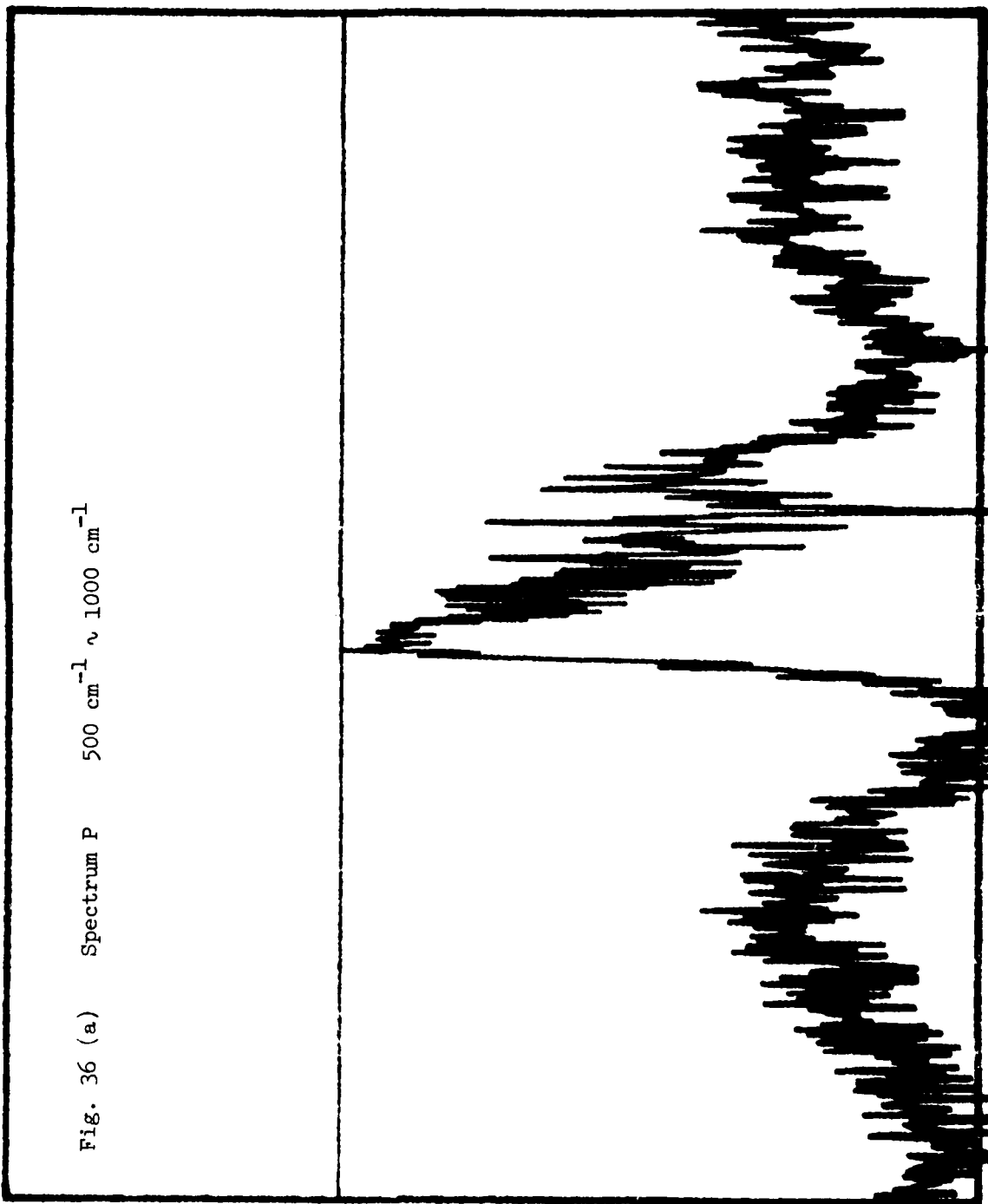


Fig. 36 (b) Spectrum P $1000 \text{ cm}^{-1} \sim 1500 \text{ cm}^{-1}$

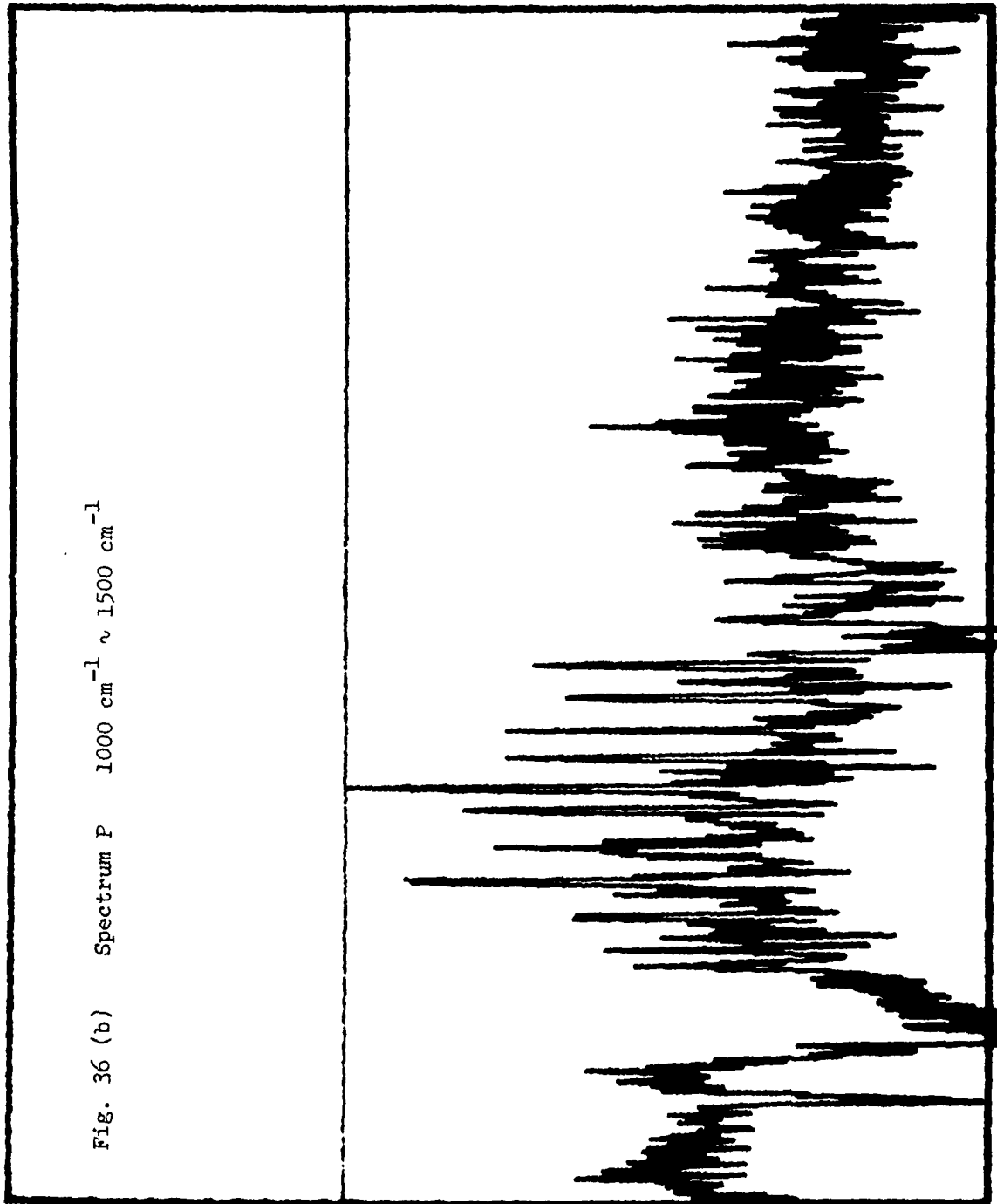


Fig. 37 (a) Spectrum Q $500 \text{ cm}^{-1} \sim 1000 \text{ cm}^{-1}$

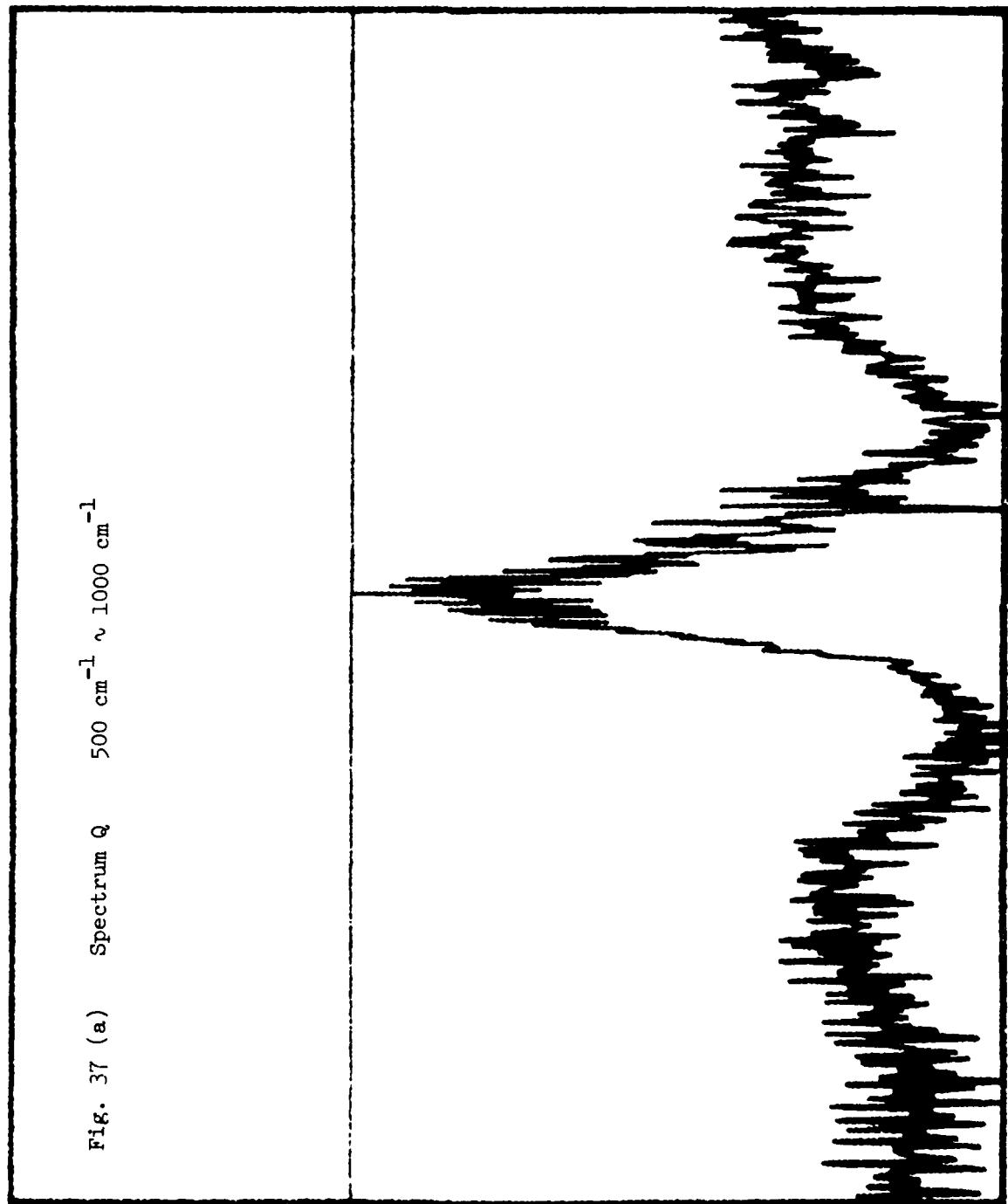


Fig. 37 (b) Spectrum Q 1000 cm^{-1} $\sim 1500 \text{ cm}^{-1}$

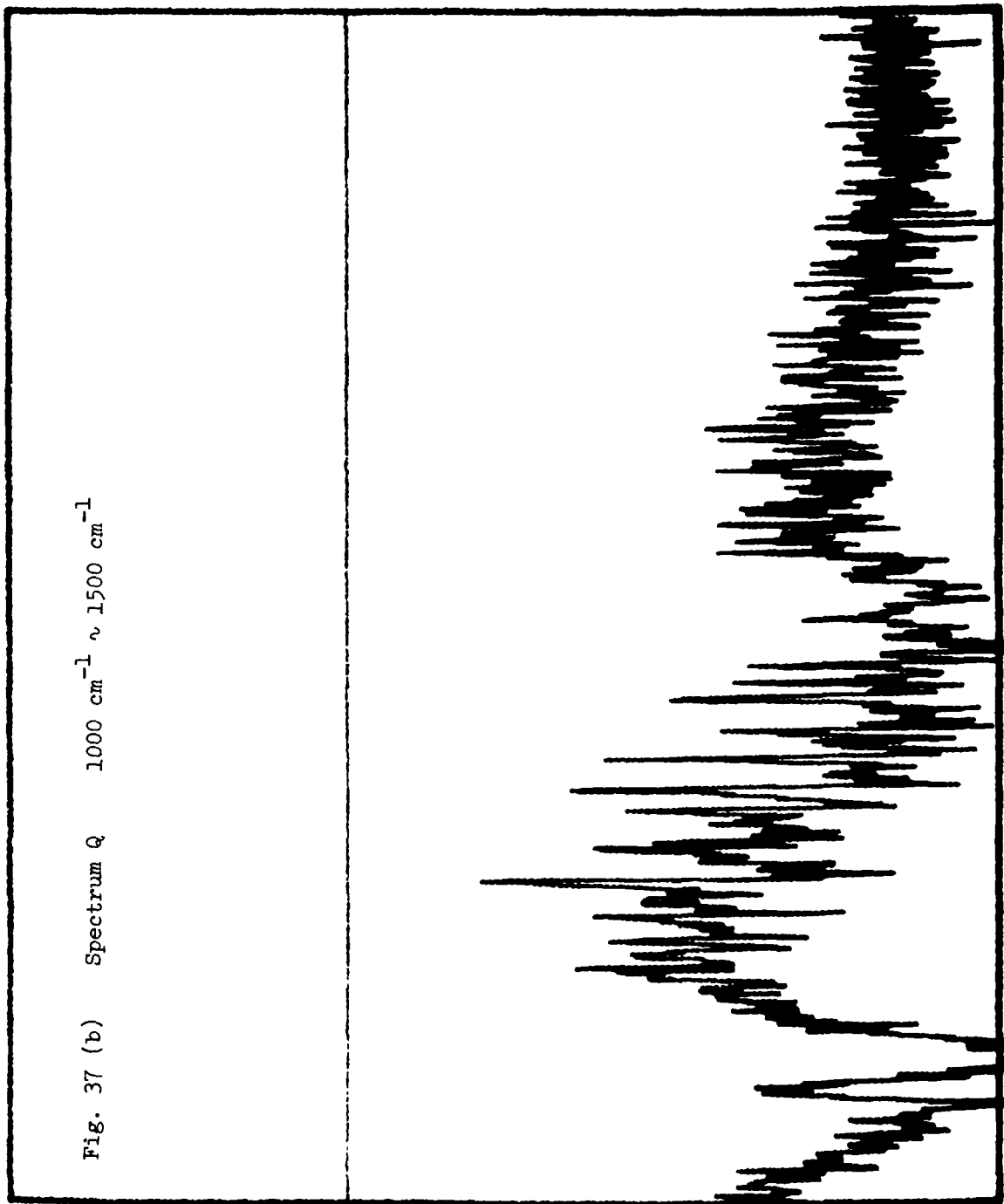


Fig. 38 (a) Spectrum R $500 \text{ cm}^{-1} \sim 1000 \text{ cm}^{-1}$

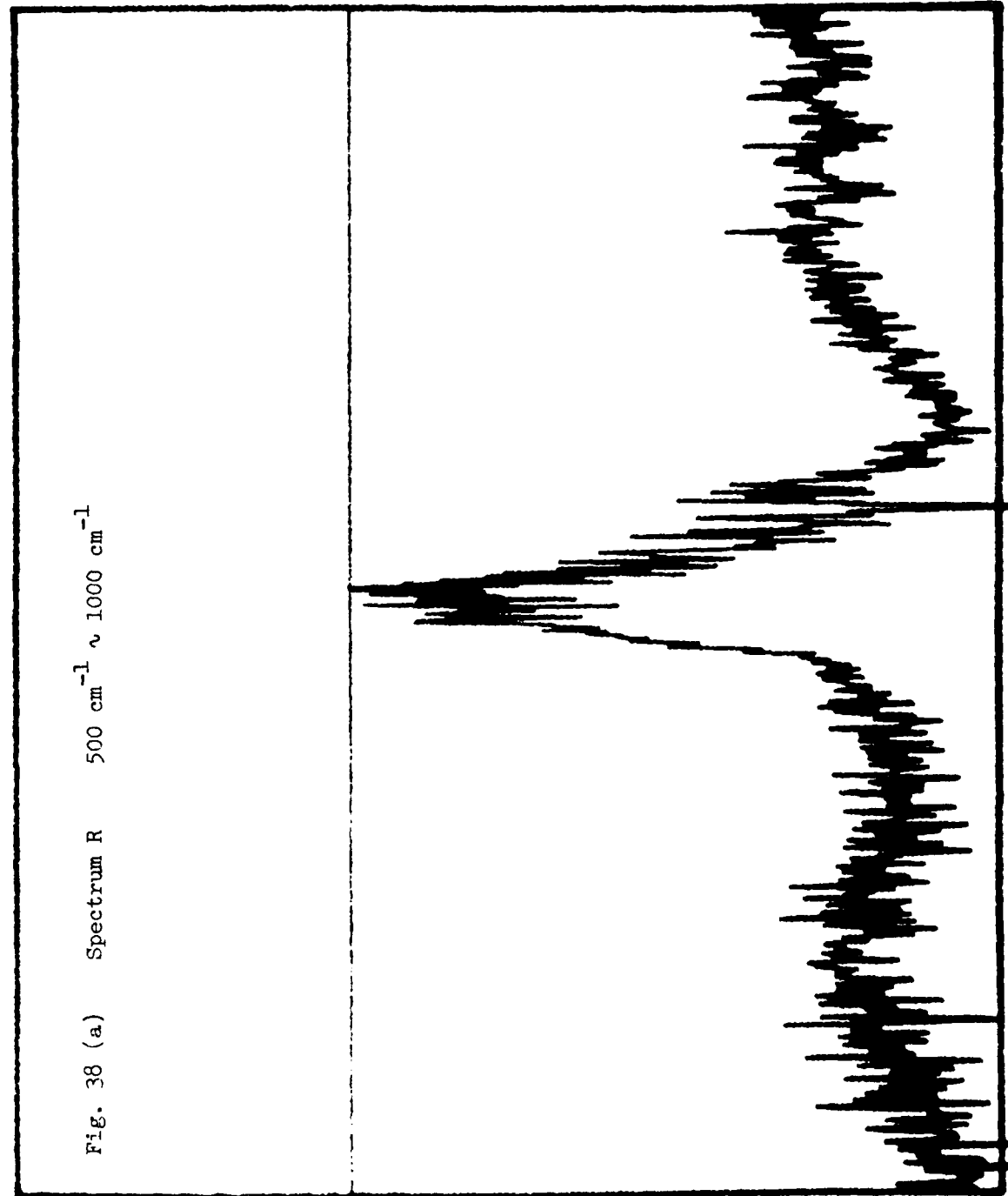


Fig. 38 (b) Spectrum R $1000 \text{ cm}^{-1} \sim 1500 \text{ cm}^{-1}$



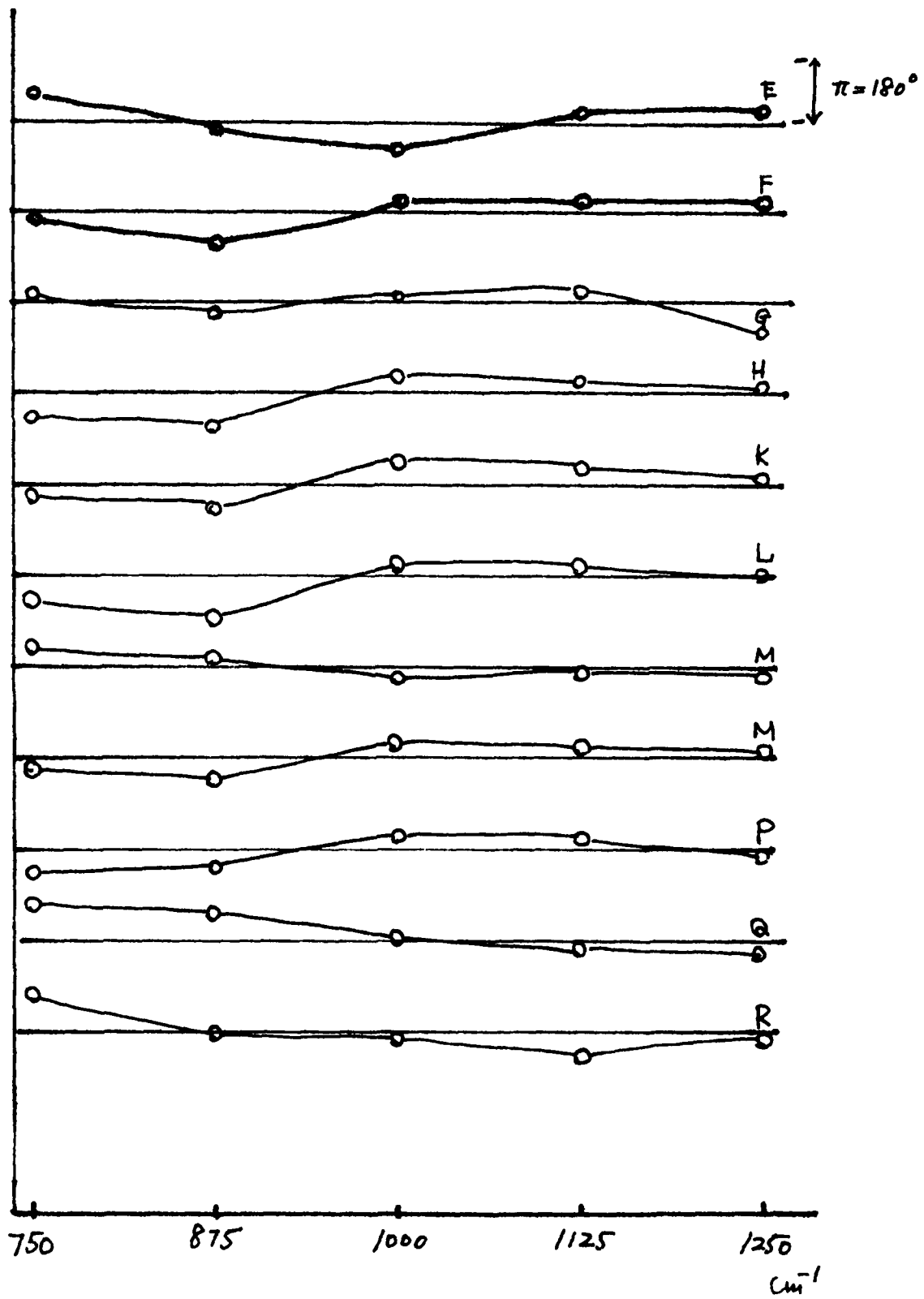


Fig. 39 The phase curves, spectra E through R.

Spectral Data #N

Figure 40 shows the spectrum recovered from the data N with a resolution of 0.12 cm^{-1} . The interferometer was not calibrated for its spectral output as a function of the wavenumber. Thus the radiance value of the detected emission feature is remained undetermined. The detector used in this flight was a Ge:Hg operated at a liquid He temperature. A sharp drop in the spectral feature observed below 750 cm^{-1} was caused by the detector's sensitivity loss at that wavenumber. The spectrum was observed at altitude of approximately 5000 m above sea level. The interferogram was directed about 10° upward with unknown azimuthal orientation. With the observed spectrum, two synthesized spectra, calculated for a single atmospheric layer of 250°K with the column density given in the figure caption, are shown in Figure 40. The observed spectrum shown in the figure is far noisier than what the instrument was designed to produce at the best condition. A quantitative discussion of the spectral radiance level is not applicable for the present case. The emission features are nonetheless easily identifiable by comparing them with the synthetic spectra.

There are three major peculiarities noticed in the observed spectrum. Since insufficient amount of spectral data were collected, we wish to draw no conclusion regarding a validity of their observation. Nonetheless, they are described below.

The H_2O line feature in $800 \sim 900 \text{ cm}^{-1}$ is mysteriously weak in the observed data. The beamsplitter should not be held responsible for the unusual feature in this spectral range, because the atmospheric absorption spectrum measured with a globar source prior to the launching showed no peculiarity. The Q branch of the 800 cm^{-1} CO_2 band (12201-10002 of

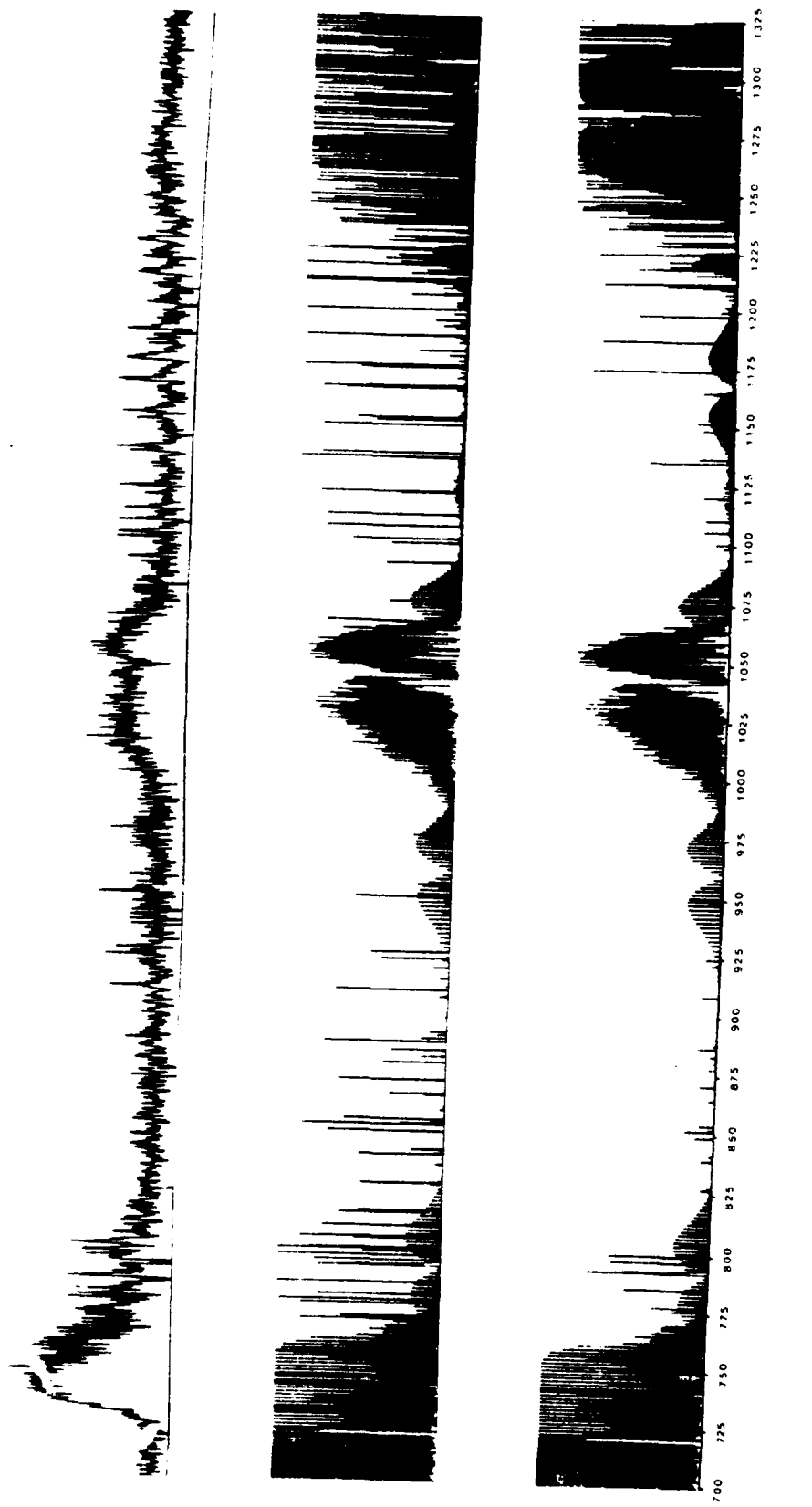


Fig. 40 Spectra observed and synthesized for a resolution of 0.12 cm^{-1} .

Top: Observed at altitude of 5000 m.

Middle: Synthesized assuming a single layer at $T = 250^\circ\text{K}$. Total molecular concentration:
 $\text{H}_2\text{O} = .23 \times 10^{24}; \text{CO}_2 = .52 \times 10^{23}; \text{N}_2\text{O} = .18 \times 10^{19}; \text{O}_3 = .41 \times 10^{20}$.

Bottom: Synthesized assuming a single layer at $T = 250^\circ\text{K}$. Total molecular concentration:
 $\text{H}_2\text{O} = .23 \times 10^{23}; \text{CO}_2 = .52 \times 10^{23}; \text{N}_2\text{O} = .18 \times 10^{20}; \text{O}_3 = .41 \times 10^{20}$.

$^{12}\text{C}^{16}\text{O}_2$) shows an absorptive feature. The band center at 1040 cm^{-1} of the O_3 band (001-000) is very narrow in the observed while the synthetic shows a well defined band center.

A semi-quantitative estimate for the column density of detected atmospheric molecules was tried by generating various synthetic spectra which are shown in Figures 41 and 42. All spectra are, as those shown with the observed spectrum, plotted in the emissivity against the black-body emission at the highest temperature of the synthetic model atmosphere. The figure caption details the atmospheric condition for each synthesis.

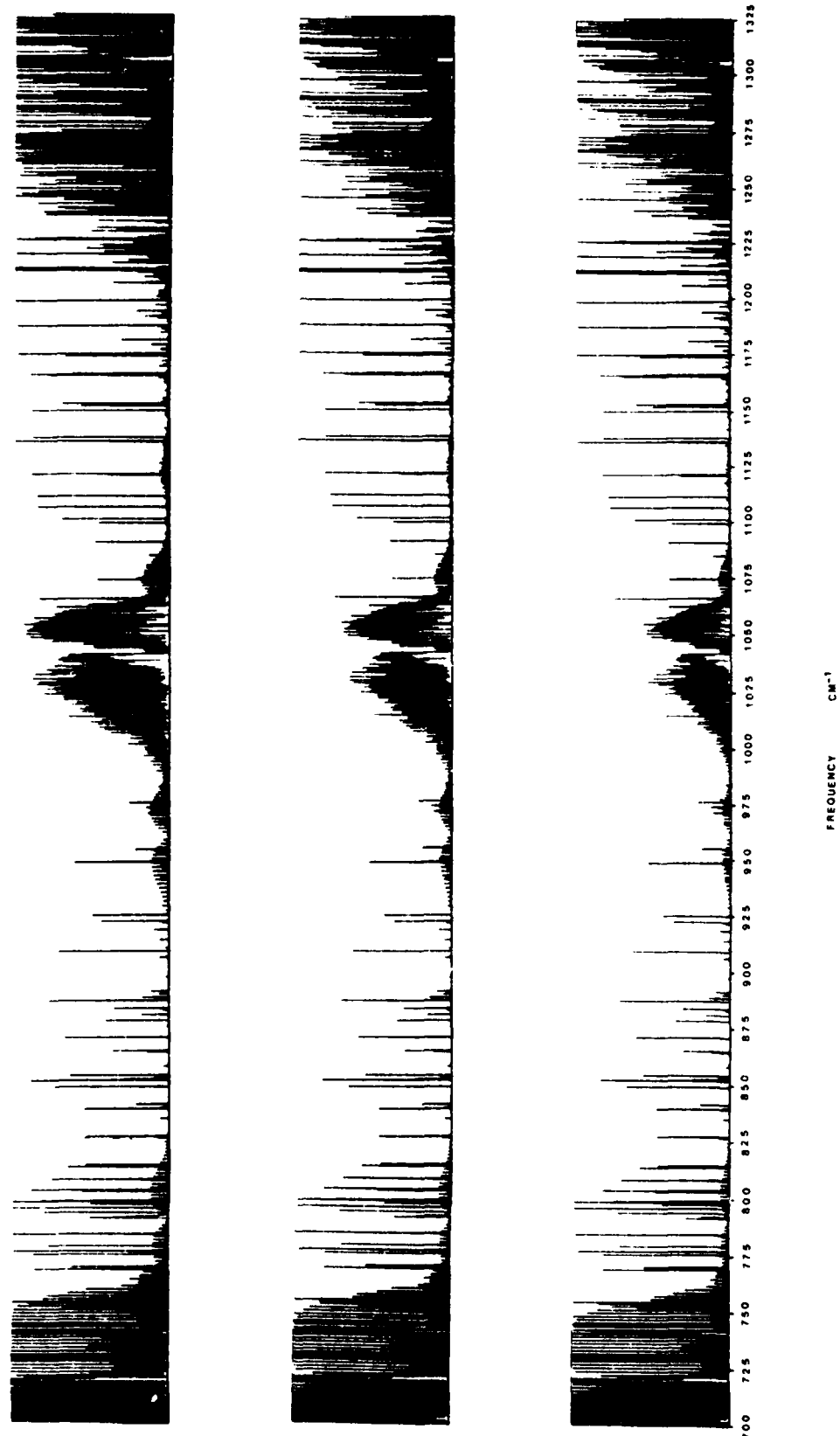


Fig. 4.1

Fig. 41 Caption

Theoretical Spectra

Top: Synthesized assuming a single layer at T = 250°K; total molecular concentration: $H_2O = .23 \times 10^{24}$, $CO_2 = .24 \times 10^{23}$, $O_3 = 1.42 \times 10^{19}$, $N_2O = .24 \times 10^{19}$.

Middle: Synthesized assuming six layers specified below.

Temp.	H_2O	CO_2	O_3	N_2O
1 250	.12 x 10 ²⁴	.4 x 10 ²²	.2 x 10 ¹⁹	.4 x 10 ¹⁸
2 245	.06 x 10 ²⁴	.4 x 10 ²²	.2 x 10 ¹⁹	.4 x 10 ¹⁸
3 240	.05 x 10 ²⁴	.4 x 10 ²²	.5 x 10 ¹⁹	.4 x 10 ¹⁸
4 230	0	.4 x 10 ²²	.5 x 10 ¹⁹	.4 x 10 ¹⁸
5 240	0	.4 x 10 ²²	.01 x 10 ¹⁹	.4 x 10 ¹⁸
6 250	0	.4 x 10 ²²	.01 x 10 ¹⁹	.4 x 10 ¹⁸

Bottom: Synthesized assuming six layers specified below.

Temp.	H_2O	CO_2	O_3	N_2O
1 250	.12 x 10 ²⁴	.4 x 10 ²²	.2 x 10 ¹⁹	.4 x 10 ¹⁸
2 245	.06 x 10 ²⁴	.4 x 10 ²²	.2 x 10 ¹⁹	.4 x 10 ¹⁸
3 240	.06 x 10 ²⁴	.4 x 10 ²²	.5 x 10 ¹⁹	.4 x 10 ¹⁸
4 230	0	.4 x 10 ²²	.5 x 10 ¹⁹	.4 x 10 ¹⁸
5 220	0	.4 x 10 ²²	.01 x 10 ¹⁹	.4 x 10 ¹⁸
6 220	0	.4 x 10 ²²	.01 x 10 ¹⁹	.4 x 10 ¹⁸

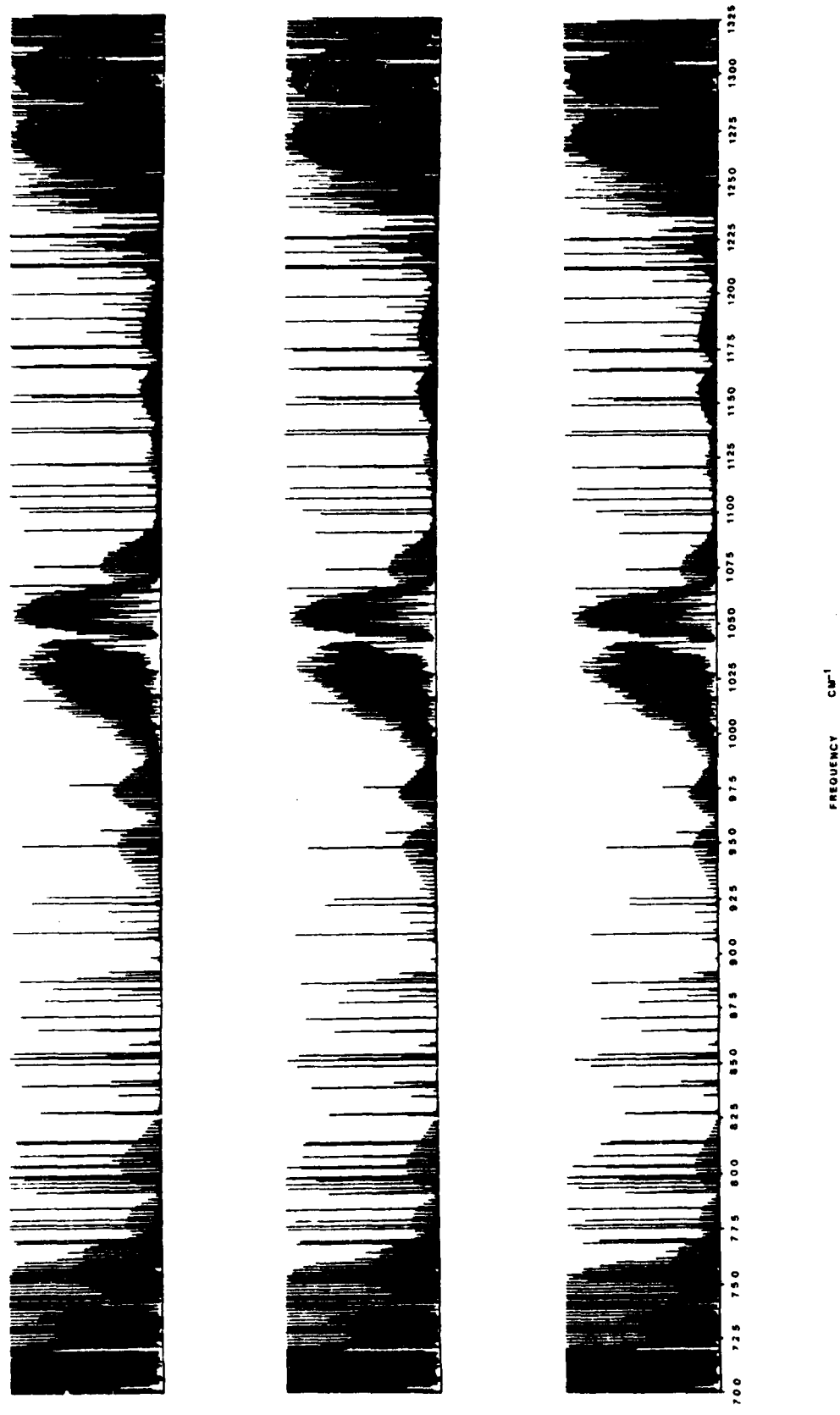


Fig. 2. Theoretical spectra synthesized assuming a single layer with various temperatures. Total molecular concentration: $H_2O = .23 \times 10^{24}$; $CO_2 = .24 \times 10^{23}$; $O_3 = 1.42 \times 10^{19}$; $N_2O = .1 \times 10^{19}$. Top: temperature = 280. Middle: temperature = 270. Bottom: temperature = 260.

Conclusion and Recommendations For Future Flights

The October 1980 flight provided a valuable test for the basic concept of the SCRIBE program. It established a validity of the experiment. The cryogenic interferometer was shown to be very effective for measuring the atmospheric emission. The principal problem which contributed to a degradation of the result was the unstable turn-around behavior in the interferometer scanning. We expect that the problem will be solved in a satisfactory degree by the next flight. With the interferometer scanning problem being solved, several problems related to it will be cured automatically. There are several modifications which we would like to recommend:

- (1) Elimination of the gain-adjusting scheme. The radiance level of the emission is known. An on-board calibration scheme for the radiance level is necessary, and it would determine the gain of the detector electronics.
- (2) Interferogram sampling interval to be a single laser fringe distance. The present sampling interval of twice the fringe distance could invite more problems.
- (3) Improvement of the electronics which generates the 4-bit interferogram status word. The last flight data indicated a poor reliability of the scheme.

Appendix A

```
.TITLE DR11B TO RK1
.CSECT DUMPAL
.GLBL BASE8, HNDLRS

.MCALL ..V2...REGDEF,.PRINT,.EXIT,.CSIGEN
.MCALL .READC,.WRITW,.CLOSE,.SRESET,.ENTER

..V2..
.REGDEF

BLKSIZ = 40 ; # BLOCKS @ RECORD
RECSIZ = < BLKSIZ * 400 > ; # WORDS @ RECORD
FRAMSZ = RECSIZ ; # DATA WORDS

ERRWD = 52 ; MONITOR ERROR CODES

DRVEC = 124 ; ADDRESS OF DR INT VECTOR
DRPSW = 340 ; INTERRUPT PRIORITY BR7

DRWC = 172410
DRBA = DRWC + 2
DRST = DRWC + 4
DRDA = DRWC + 6

TKS = 177560 ; TT HARDWARE REGISTERS
TKB = TKS + 2

SWR = 177570
EOTBIT = 2000 ; MT EOT STATUS BIT
CNTRLC = 203 ; ASCII ~C

; * * * * * * * * *

START: JSR PC,INIT
        JSR PC,BELL
        JSR PC,PCMIN
        JSR PC,RKOUT
        JSR PC,TRACE ; BUFFER LOAD

        .PRINT #DONE
        JSR PC,BELL
        JSR PC,CLOSER
        .EXIT

DONE:  .ASCIZ / DONE/
        .EVEN
        ; * * * * * * * * *

; INITIALIZE DEVICES, OPEN FILES, PRESET
; PROGRAM VARIABLES, AND SET INT. VECTOR

INIT:  MOV #TKS,TSTEMP
        CLR #TKS
```

```

        CLR      FRAME
        CLR      BLKNUM

        .ENTER #AREA,$0,$DEV,$-1
        BCS      BADENT
        MOV      #DRINT,$@DRVEC
        MOV      #DRPSW,$@DRVEC+2
        RTS      PC

        DEV:    .RAD50 /RK1/
                .RAD50 /PCM/
                .RAD50 /RK1/
                .RAD50 /DAT/

        AREA:   .BLKW  10
        BADENT: .PRINT #EMSG
                .EXIT
        BADWR:  .PRINT #WMSG
                .EXIT

        EMSG:   .ASCIZ /BAD ENTER/
        WMSG:   .ASCIZ /BAD WRITE/
                .EVEN

; * * * * * * * * * *
; RING BELL ON TERMINAL
;

        BELL:   .PRINT #BELMSG
                RTS     PC

        BELMSG: .BYTE  7,7,7,7,7,0
                .EVEN

; * * * * * * * * * *
; START DR11B WITH INTERRUPT ENABLED
; ( VECTOR POINTS TO "DRINT" )

        PCMIN: CLR      DRFLG
                MOV      #30,BCOUNT
        LOOPA:  BIT      $1,$@SWR
                BEQ      LOOPA          ; LOOP UNTIL "READY"

                MOV      #-FRAMSZ,$@DRWC
                MOV      #B0,$@DRBA
                CLR      $@DRST           ; STROBES DRST REGISTER
                MOV      $@177570,$@DRST  ; SW REG
                RTS     PC

; * * * * * * * * * *
; RK1 WRITE
;

        RNDOUT: MOV      #B1,B
        AGAIN:  MOV      #B0,BUF
        AA:     BIT      $1,DRFLG
                BEQ      AA
                MOV      #B0,B
                WRITW  #AREA,B0,BUF,$20000,BLKNUM
                BCS      BADWR
                ADD      #40,BLKNUM
                MOV      #B1,BUF
                BIT      $1,DRFLG
                RNE      AA
                MOV      #B1,B

```

```

.WRITW *AREA,$0,BUF,$20000,BLKNUM
BCS BADWR
ADD $40,BLKNUM
DEC BCOUNT
BNE AGAIN
RTS PC

DRFLG: .WORD 0
BCOUNT: .WORD 30
BUF: .WORD 0

* * * * *
; DR11 INTERRUPT HANDLER
; TRAP & REPORT ERRORS,
; START MAGTAPE WRITE.

DRINT: MOV B,@#DRBA
       MOV #-FRAMSZ,@#DRWC
       MOV @#SWR,@#DRST
       INC DRFLG

DRDONE: RTI

* * * * * * * * *

; DUMPS DR11B REGISTERS

DRDUMP: MOV R0,-(SP)
         MOV R1,-(SP)

         MOV @#DRWC,R0
         MOV #DRWCM,R1
         JSR PC,BASE8

         MOV @#DRBA,R0
         MOV #DRBAM,R1
         JSR PC,BASE8

         MOV @#DRST,R0
         MOV #DRSTM,R1
         JSR PC,BASE8

         MOV @#DRDA,R0
         MOV #DRDAM,R1
         JSR PC,BASE8

         PRINT #DRDMSG
         MOV (SP)+,R1
         MOV (SP)+,R0
         RTS PC

DRDMSG: .ASCII / DR DUMP/
        .BYTE 12+ 15

        .ASCII / WC /
DRWCM:  .BLKB 6

        .ASCII / BA /
URBAM:  .BLKB 6

        .ASCII / ST /

```

```

DRSTM: .BLKB 6
        .ASCII / DA /
DRDAM: .BLKB 6
        .BYTE 0
        .EVEN

; * * * * * * * * *

;
; DISPLAYS CURRENT FRAME NUMBER IF
; TTY KEY IS PRESSED. ALSO STOPS
; PROGRAM ON ^C

TRACE: TSTB @TKS
       BEQ TRACND

       .PRINT #TRIDUMP
       MOV R1,-(SP)
       MOV @TKB,-(SP)

       MOV BCOUNT,R0
       MOV #FRMNUM,R1
       JSR PC,BASE8

       .PRINT #TRACEM
       MOV (SP)+,R0
       CMPB #CNTRL0,R0
       BNE TRACNM

       .PRINT #TRACEX
       MOV TSTEMP,@TKS
       JSR PC,CLOSER
       .EXIT

TRACNM: MOV (SP)+,R1

TRACND: RTS PC

TRIDUMP: .ASCIIZ / TR DUMP /
TRACEM: .ASCIIZ / FRAME # /
FRMNUM: .BLKB 6
        .BYTE 0
TRACEX: .ASCIIZ / ABORT/
        .EVEN

; * * * * * * * * *

;
; REPORT ERRORS & ABORTS PROGRAM

ERRORS: MOV ERRNUM,R0
        MOV #ERRSUR,R1
        JSR PC,BASE8

        MOV ERRWD,R0
        MOV #ERRWRD,R1
        JSR PC,BASE8

        .PRINT #ERRMSG
        JSR PC,CLOSER
        .EXIT

ERRMSG: .ASCII / ERROR: SUB /

```

```
ERRSUB: .BLKB 6
        .ASCII /, CODE /
ERRWRD: .BLKB 6
        .BYTE 0
        .EVEN

; * * * * * * * * *

;                               CLOSE FILES, RESET SYSTEM

CLOSER: .CLOSE $0
        .CLOSE $3
        .CLOSE $4
        .SRESET
        RTS    PC

; * * * * * * * * *

; STATUS BLOCK

STATUS = .
FRAME:      0
BLKNUM:     0
ERRNUM:     0
RK1FLG:     0
SPTEMP:     0
TSTEMP:     0
EMT1:      .BLKW 5
EMT2:      .BLKW 5
EMT3:      .BLKW 5
EMT4:      .BLKW 5

ENDBUF: . = STATUS+1000          ; 400 WORDS

B0:      .BLKW RECSIZ
B1:      .BLKW RECSIZ
B:       .WORD 0

.END     START
*
```

```

DIMENSION IDATA(4096),IBUFF(4096),NAME1(4),NAME2(4),NAME3(1)
DATA NAME1/3RRK1,3RPCM,3RRK1,3RDAT/
DATA NAME2/3RDTO,3RPCM,3RDAT,3RDAT/
DATA NAME3/3RDTO/
DO 70 I=1,4096
IDATA(I)=0.
CONTINUE
70
C
C READ FROM RK1
C
JSIZE=4096
IC=IGETC()
IF(LOOKUP(IC,NAME1).LT.0)STOP 'BAD LOOK UP'
JC=IGETC()
IF (IFETCH(NAME3).NE.0)STOP 'FATAL ERROR FETCHING HANDLER'
IC1=IENTER(JC,NAME2,0,0)
IF (IC1.EQ.-1)STOP 'ENTER FAILURE NO CHANNEL'
IF (IC1.EQ.-2)STOP 'NO SPACE'
ISTART=1
IEND=0
INDEX=0
NB=0
IAA=4096
ICOUNT=18
INB=1
10 CALL IREADW (4096, IDATA, NB, IC)
ICODE=IREADW (4096, IDATA, NB, IC)
IF (ICODE.EQ.-1) GO TO 100
NB=NB+16
CALL SLECT (IDATA, IBUFF, JSIZE, ISTART, IEND)
IF (IEND.LT.IAA)GO TO 10
K=1
DO 20 I=ISTART,IAA
IBUFF(I)=IDATA(K)
K=K+1
20
CONTINUE
IF (ICOUNT.NE.1) GO TO 25
DO 22 I=2049+4096
IBUFF(I)=0
22
CONTINUE
25 CALL IWRITW(4096,IBUFF,INB,JC)
INB=INB+16
J=1
KEND=IEND-ISTART
DO 30 I=K,KEND
IBUFF(J)=IDATA(I)
J=J+1
30
CONTINUE
IEND=J-1
ICOUNT=ICOUNT-1
IF (ICOUNT.NE.0) GO TO 10
100 CALL IFREEC(1C)
CALL CLOSEC(JC)
CALL IFREEC(JC)
CALL EXIT
STOP
END
*
```

```

SUBROUTINE SLECT (IDATA,IBUFF,JSIZE,ISTART,IEND)
DIMENSION IDATA(1),IBUFF(1)
DATA ITEST /5/
INDEX=1
ISTART=IEND+1
J=1
DO 10 I=1,JSIZE
IX=IDATA(I).AND.ITEST
IF (IX.NE.5) GO TO 10
CALL ZEROUT (IDATA(I),INDEX)
IF (INDEX.EQ.0) GO TO 10
IDATA(J)=IDATA(I)
J=J+1
10    CONTINUE
J=J-1
IEND=ISTART+J-1
IF (IEND.GT.4096)GO TO 30
J=1
DO 20 I=ISTART,IEND
IBUFF(I)=IDATA(J)
J=J+1
20    CONTINUE
30    RETURN
END
*
;TAKE ZERO DATA OFF THE TAPE (DATA,INDEX)
.MCALL ..V2...REGDEF
..V2..
.REGDEF
.GLOBL ZEROUT
ZEROUT: TST    (RS)+  

        MOV    @ (RS)+,R2  

        MOV    $1,@ (RS)  

        ;  

        BIC    #17,R2  

        ROR    R2  

        ROR    R2  

        ROR    R2  

        ROR    R2  

        TST    R2  

        BNE    OUT  

        CLR    @ (RS)  

;  

OUT:   RTS    PC
;  

.END    ZEROUT
*
```

Appendix B

```

PROGRAM TREAID(TAPE9,TAPE1,TAPE6)
DIMENSION ID(256),IE(512)
100 FORMAT(3(1X,08))
101 FORMAT(3(2X,08))
N=104
10 CONTINUE
70 50 I=1,256
ID(I)=0.
50 CONTINUE
BUFFER IN(9,1)(ID(1),ID(N))
IF(UNIT(9)) 11,21,31
11 CONTINUE
CALL TPOCODE(ID,IE)
WRITE(6,100)(IE(I),I=1,256)
GO TO 10
21 CONTINUE
31 CONTINUE
CALL EXIT
STOP
END

```

```

SUBROUTINE TFDPCODE (ID,IE)
DIMENSION ID(2),IE(2),IA(6),IB(5),IC(4)
DATA (IA(I),I=1,6)/77777770000000000008,77777770000B,7777B,
177770000000000J00000JB,77777777000000C8,77777778/
DATA (IC(I),I=1,4)/17B,17003,1700008,1700000B/
L=1
J=1
DO 11 I=1,51
IX=ID(L).AND.IA(1)
IB(1)=SHIFT(IX,-36)
IX=ID(L).AND.IA(2)
IB(2)=SHIFT(IX,-12)
IX=ID(L).AND.IA(3)
IY=ID(L+1).AND.IA(4)
IZ=SHIFT(IY,-48)
IZ=SHIFT(IX,12)
IR(3)=IZZ+IZ
IX=ID(L+1).AND.IA(5)
IB(4)=SHIFT(IX,-24)
IB(5)=ID(L+1).AND.IA(6)
L=L+2
DO 12 K=1,5
IX=IB(K).AND.IC(4)
IY=IB(K).AND.IC(3)
IZ=IR(K).AND.IC(2)
IZZ=IP(K).AND.IC(1)
IF(J)=SHIFT(IY,-12)+SHIFT(IZ,-2)+SHIFT(IZZ,8)+IX
J=J+2
CONTINUE
1 CONTINUE
IX=ID(L).AND.IA(1)
IB(1)=SHIFT(IX,-36)
IX=IB(1).AND.IC(4)
IY=IB(1).AND.IC(3)
IZ=IB(1).AND.IC(2)
IZZ=IB(1).AND.IC(1)
IE(J)=SHIFT(IY,-12)+SHIFT(IZ,-2)+SHIFT(IZZ,8)+IX
RETURN
END

```

PRINT(6,1) TAPE1,TAPE2,OUTPUT,TAPES
 DIMENSION TAPE(4096)
 100 FORMAT(16F7.2)
 101 FORMAT(16F4.0)
 102 FORMAT(6I6)
 READ(6,102),JUNK
 READ(6,102),JUNK
 READ(6,102),JUNK
 READ(6,101)(TAC(I),I=1,4096)
 TAVER1=0
 TAVER2=0
 J=4096
 DO 10 I=1,4096
 TAVER1=TAVER1+TAC(I)
 TAVER2=TAVER2+TAC(I)
 J=J-1
 10 CONTINUE
 TAVER1=TAVER1/256
 TAVER2=TAVER2/256
 PRINT 100,TAVER1-TAVER2
 TDIF=(TAVER2-TAVER1)/2
 DO 15 I=1,1024
 TAC(I)=TAC(I)-TAVER1
 TAC(I)=TAC(I)-TDIF GO TO 16
 15 CONTINUE
 16 CONTINUE
 PRINT 100, I
 I=I+15
 I=I+15
 PRINT 100,(TAC(I),I=1,I,I,I)
 IK=I-1
 DO 19 K=1,IK
 A=FLOAT(TAC(K))/4096.
 TAC(K)=TAC(K)/A
 19 CONTINUE
 IK=IK+1
 TAC(IK)=TAC(IK)-TAVER1
 TRK=TRK+1
 DO 21 K=IK,4096
 TAC(K)=TAC(K)-TAVER2
 21 CONTINUE
 WRITE(1,100)(TAC(I),I=1,4096)
 DO 22 K=1,8
 READ(6,101)(TAC(I),I=1,4096)
 DO 23 I=1,4096
 TAC(I)=TAC(I)-TAVER2
 23 CONTINUE
 WRITE(1,100)(TAC(I),I=1,4096)
 27 CONTINUE
 CALL EXIT
 STOP
 END

Appendix C